Dissertation
submitted to the
Combined Faculties for the Natural Sciences and for Mathematics
of the Ruperto-Carola University of Heidelberg, Germany
for the degree of
Doctor of Natural Sciences

presented by
M.Sc. Valentino Konjik
born in: Osijek, Croatia
Oral examination: _____

RosB from *Streptomyces davawensis* is the key enzyme of roseoflavin biosynthesis

Referees: Prof. Dr. Michael Lanzer

Prof. Dr. Matthias Mack

Abstract

The antibiotic roseoflavin (RoF) is the only known natural riboflavin (vitamin B_2) analogue and is active against gram-positive bacteria. RoF is produced by *Streptomyces cinnabarinus* (*S. cinnabarinus*) and *Streptomyces davawensis* (*S. davawensis*) and can be considered to be an "antivitamin". In RoF biosynthesis one of the methyl groups of the predicted precursor riboflavin undergoes a site-specific replacement by a dimethyl amino group whereby 8-demethyl-8-amino-riboflavin (AF) was postulated to be an intermediate. The first discovered enzyme of roseoflavin biosynthesis was the S-adenosyl methionine (SAM) dependent dimethyltransferase RosA which converts AF to RoF. Subsequent systematic gene deletion experiments carried out in the RoF-producer *S. davawensis* suggested that a single enzyme (RosB) is responsible for the formation of AF. However, when recombinant RosB was tested in an assay mixture containing riboflavin-5'-phosphate (RP) the formation of the predicted final reaction product AF was not observed. Instead the compound 8-demethyl-8-formyl-riboflavin-5'-phosphate (HOC-RP) was detected, probably an intermediate of the RosB reaction. How the formyl-group of HOC-RP was replaced by an amino group to give AF or 8-demethyl-8-amino-riboflavin-5'-phosphate (AFP) remained unclear.

The present work was initiated to investigate the predicted oxidation of HOC-RP to 8-demethyl-8-carboxyl-riboflavin-5'-phosphate (HOOC-RP), to identify the amino group donor of the RosB reaction and to shed light on the reaction mechanism of the multi-step enzyme RosB. It was found that RosB accepts only RP as a substrate and not riboflavin (RF). RosB activity depends on the presence of O_2, thiamine and the amino group donor glutamate. HOOC-RP was found to be an (additional) intermediate of the RosB reaction. The crystal structure of RosB was solved with bound AFP (1.7 Å) and HOC-RP (2.0 Å). RosB is composed of four flavodoxin-like subunits which have been upgraded with specific extensions and a unique C-terminal arm. Structure-based active site analysis was complemented by mutational and isotope-based mass-spectrometric data to propose an enzymatic mechanism. The present work also shows that the RoF biosynthetic pathway still has not been completely resolved. RosB releases AFP, yet the substrate for the subsequent RosA reaction is AF. Consequently, a phosphatase must be present which has not yet been identified.

Zusammenfassung

Roseoflavin ist das einzig bekannte Vitamin B_2-Analogon, welches eine antibiotische Wirkung gegen grampositive Bakterien aufweist. Es wird von *Streptomyces cinnabarinus* und *Streptomyces davawensis* (*S. davawensis*) produziert und kann als „Antivitamin“ betrachtet werden. Im Verlauf der Roseoflavinbiosynthese wird spezifisch eine der beiden Methylgruppen des wahrscheinlichen Vorläufermoleküls Riboflavin durch eine Dimethylaminogruppe substituiert. Es wurde angenommen, dass 8-Demethyl-8-amino-riboflavin (AF) ein Zwischenprodukt dieser Synthese sei. Als erstes Enzym der Roseoflavinbiosynthese wurde RosA beschrieben, eine Dimethyltransferase, welche mithilfe von S-Adenosylmethionin (SAM) aus AF RoF bildet. Die Ergebnisse der systematischen Gendeletionsexperimente im RoF-Produzenten *S. davawensis* zeigten, dass sehr wahrscheinlich nur ein Enzym (RosB) für die AF-Bildung verantwortlich ist. Als jedoch RosB mit Riboflavin-5‘-Phosphat (RP) in vitro getestet wurde, konnte die Synthese von AF nicht beobachtet werden. Anstelle von AF wurde 8-Demethyl-8-formyl-riboflavin-5’-phosphat (HOC-RP) gefunden, eine wahrscheinliche Zwischenstufe der RosB-Reaktion. Wie die Formylgruppe von HOC-RP gegen eine Aminogruppe ausgetauscht wird um AF (oder 8-Demethyl-8-amino-riboflavin-5’-phosphat, AFP) zu bilden blieb unklar.

Die vorliegende Arbeit wurde initiiert, um die wahrscheinliche Oxidation von HOC-RP zu 8-Demethyl-8-carboxy-riboflavin-5’-phosphat (HOOC-RP) zu untersuchen, den Amino-gruppendonor der RosB-Reaktion zu identifizieren und den Reaktionsmechanismus des mehrstufigen Enzyms RosB zu analysieren. RosB akzeptiert nur RP als Substrat und nicht RF. RosB benötigt Sauerstoff, den Aminogruppendonor Glutamat und Thiamin, um den Austausch der Methylgruppe gegen eine Aminogruppe zu katalysieren. HOOC-RP wurde als weiteres Intermediat der RosB-Reaktion identifiziert. Die Kristallstruktur von RosB gebunden an die Flavine AFP (1,7 Å) und HOC-RP (2,0 Å) wurde gelöst. RosB besteht aus vier flavodoxinähnlichen Untereinheiten die mit spezifischen Domänen und einem einzigartigen C-terminalem Arm ausgestattet worden sind. Die strukturelle Analyse des aktiven Zentrums von RosB wurde durch Mutagenesestudien und isotopenbasierten massenspektrometrischen Untersuchungen ergänzt. Auf Grundlage dieser Ergebnisse wurde ein Reaktionsmechanismus erarbeitet. Die vorliegende Studie zeigt auch, dass die Roseoflavinbiosynthese noch nicht vollständig verstanden wird. RosB setzt AFP frei, jedoch ist das Substrat für die nachfolgende Reaktion von RosA AF. Demnach muss eine (noch unbekannte) Phosphataseaktivität in *S. davawensis* vorhanden sein, die die Dephosphorylierung von AFP zu AF katalysiert.

Table of Content

1. Introduction

1.1. *Streptomyces davawensis*

The genus *Streptomyces* belongs to the phylum of the actinobacteria. *Streptomyces* species can be isolated from the soil and the rhizosphere, their life cycle starts with the germination of the semi-dormant spores forming a vegetative hyphal mass, which progresses and divides only at the tip. When reaching the surface or when nutrients are scarce Streptomycetes form hydrophobic aerial hyphae ending with a semi-dormant spore.[1,2] These spores are able to survive long periods of drought and/or lack of nutrients.

Known *Streptomyces* species have large genomes (8-12 Mbp) with a G+C content of more than 70 %. Additionally, they carry one or multiple plasmids.[3] The housekeeping genes for proliferation and growth appear to be located in the core of the genome whereas the flanking regions (up to 2.3 Mbp) often encode genes which are responsible for the synthesis of a large number of biologically active secondary metabolites, such as antibiotics and pigments.[4] Interestingly, these flanking regions appear to interact with plasmids and phages, which also aids to the adaption to challenging and quickly changing environments, such as the soil.

Ecologically speaking, Streptomycetes contribute heavily to the composting cycle of complex organic material by secreting a large variety of hydrolytically active enzymes.[5] A prominent side product in this process is the volatile compound geosmin which is released in several degradation processes and is responsible for the typical smell of a wet forest.

There are only a few human pathogenic *Streptomyces* known. For instance, *S. somaliensis* causes the disease actinomycosis in human.[6]

S. davawensis was first mentioned in 1974 by Otani et al. where it was discovered in a screening program for antibiotic producing organisms[7]. In more detail, *S. davawensis* was isolated from a Philippines soil sample and a red pigment (RoF) of the supernatant showed antibiotic behavior against gram-positive bacteria.

1.2. Riboflavin biosynthesis and its properties

RF was first isolated from milk in 1872 by A. Wynter Blyth. The complete structural analysis of this yellow pigment took 63 years and was accomplished by Euler and co-workers in 1935.[8] RF is a vitamin also called vitamin B_2 and is synthesized by plants, fungi and most microorganisms, but not by humans and animals. The major sources for RF are milk products, cereals, grains and green parts of vegetables.

The RF pathway is well studied and differs only slightly between organisms (see Figure 1). Guanosine-5'-triphosphate (GTP) is one of the starting points of RF synthesis. Eubacteria hydrolyse GTP in a single step forming 2,5-diamino-6-(5-phospho-D-ribosylamino)-pyrimidin-4(3*H*)-one (1), formate and pyrophosphate. On the other hand, Archaea have two enzymes catalysing this reaction; the first one catalyses the oxidation of C(8) of GTP to formate and the second one the cleavage of the formyl residue. Subsequently, 1 is reduced with NADPH and the red labelled amine group is hydrolysed yielding 5-amino-6-(5'-phospho-D-ribitylamino)-uracil (2). Afterwards, 2 becomes dephosphorylated yielding 5-amino-6-ribitylamino-2,4(1H,3H)-pyrimidinedione (3). Again, depending on the organism either the reduction of the ribosyl side chain or the hydrolysis of the pyrimidine moiety is performed first, whereas the de-phosphorylation is always the last reaction. The second precursor 3,4-dihydroxy-2-butanone-4-phosphate is derived from D-ribulose-5'-phosphate (pentose phosphate pathway), which reacts with 3 affording 6,7-dimethyl-8-ribityllumazine (4). Finally, two equivalents of 4 deliver RF and 3, whereas 3 is cycled back into the RF synthesis pathway. Recently, the elusive phosphatase giving 3 was as well characterized from *Arabidopsis thaliana*[9].

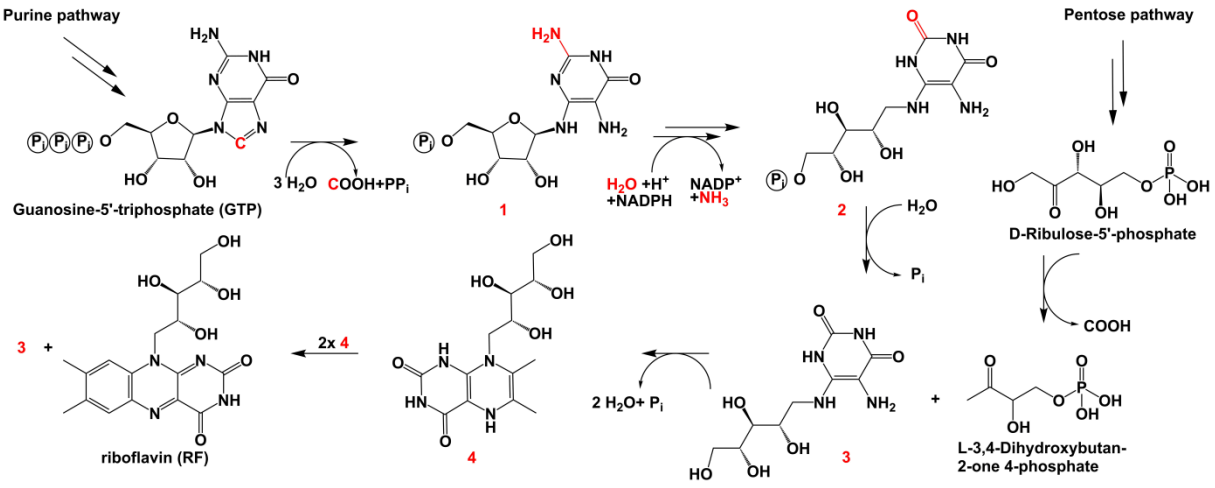

Figure 1: A condensed riboflavin (RF) biosynthesis scheme is illustrated. Guanosine-5'-triphosphate (GTP) is supplied by the purine pathway and D-ribulose-5'-phosphate is delivered by the pentose phosphate pathway. A well-studied multi-step enzyme cascade yields RP through four crucial intermediates.

In general, these enzymes have low kinetic rates in comparison to other pathways, which could indicate a regulatory mechanism, although only little is known about the regulation on the enzymatic level; however the regulation of the gene expression levels is better studied. So called Riboflavin-5'-phosphate riboswitches (RP- or FMN riboswitches) are found in the 5'-untranslated region of bacterial mRNA coding for RF biosynthetic and/or RF transporter genes. If RP reaches a certain concentration it will bind to the RP riboswitch, causing a conformational change of the mRNA which results into downregulation of the transcription and/or translation[10]. RF is biologically not active, and is therefore metabolized to RP or flavin adenine dinucleotide (FAD), by flavokinases and FAD synthetases.

In physical terms, RP/FAD has an amphipathic character with the aromatic isoalloxazine ring system and the hydrophilic ribityl residue. The most important feature is the reversible reduction to RPH_2/$FADH_2$. Notably, in comparison to other redox involved cofactors, such as NAD(P) it can also receive only one electron forming a semiquinone. Furthermore, the redox potential of unbound RF at pH 7 is around -200 mV (-219 mV for FAD, -205 mV for RP) and can vary from -400 mV to 60 mV depending on the environment of the enzyme binding pocket[11].

All flavin derivatives are light sensitive but thermostable. In general, flavins show characteristic absorption spectra with absorption maxima at 445, 375, 265 and 220 nm[12]. The precise position of the maxima and the molar absorptivities depend significantly on the environment of the flavin chromophore. Additionally, RP and RF can serve as photosensitizer. Upon light absorption it reaches the triplet excited state, where it is capable of generating singlet oxygen or it interacts directly with the substrate generating radicals[8]. Yet FAD, is a less efficient photosensitizer, due to its low quantum yield.

Nowadays, RF has a world production volume of 3,000 tons/year, whereas 2500 tons/year are produced via fermentation[13]. Besides that, it is used as a component in healthy diets, as a natural coloring agent and as a food supplement in the domestic industry.

1.3. Roseoflavin - biosynthesis and antibiotic properties

First experiments with *S. davawensis* showed that a liquid culture supplemented with [2-^{14}C(U)] guanine or [2-^{14}C] riboflavin incorporated ^{14}C into Rof (see Figure 2, red encircled carbon). However, no [^{14}C] RoF was found with the supplementation of [8-^{14}C] guanine. Possible intermediates, such as 8-demethyl-8-hydroxy riboflavin, 8-demethyl-riboflavin, and 8α-hydroxy riboflavin (all same ^{14}C-labelling) were also tested, however no [^{14}C] RoF was

detected.[14] These experiments led to the conclusion that RF is the precursor of RoF. Furthermore, Matsui et al. postulated that the intermediate AF is formed during synthesis. This hypothesis was support in 1987 by the fact that an *S. davawensis* liquid culture fed with AF showed increased amounts of RoF in the supernatant.[15] In 2011, *rosA* the first gene of the RoF biosynthesis was found, which codes for RosA (EC 2.1.1.B93) an SAM dependent dimethyltransferase.[16] *In vitro* assays showed that the protein RosA (EC 2.1.1.B93) catalyses the di-methylation of the amino group in AF but **not** in AFP (see Figure 2). An inactivation of *rosA* in *S. davawensis* caused an accumulation of AF instead of 8-demethyl-8-methylamino-riboflavin (MAF) and RoF.

Systematic gene deletion experiments led to the identification of *rosB*.[17] When *rosB* was deleted, the corresponding *S. davawensis* strain was not able to generate RoF. Heterologous expression of *rosB* in *S. coelicolor*, resulted into AF synthesis indicating that *rosB* indeed was involved RoF biosynthesis. Yet, the precise function of this enzyme was unknown. Besides that, RosB recognizes only the phosphorylated RP as a substrate but **not** RF. The gene *rosB* is located about 49 kbp upstream of *rosA* and therefore not united in one cluster. The reason for that is still not known.

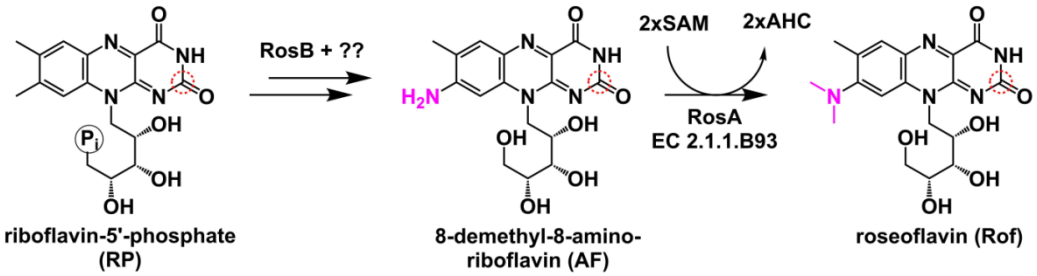

Figure 2: The state of the art concerning the roseoflavin biosynthesis. RosB accepts only RP as substrate and yields potentially 8-demethyl-8-amino-riboflavin (AF), which is then methylated twice by the well-studied RosA.

RoF has a similar structure to RF and is taken up through RF importers of microorganisms (e.g. *Corynebacterium pyogenes*, *Streptococcus pyogenes*, *Listeria monocytogenes*, many lactic acid bacteria, *Mycoplasma* species, spirochetes, rickettsiae and protists)[18] which are not able to synthesize RF and have to scavenge for it (see Figure 3). RoF is phosphorylated by flavokinases yielding roseoflavin-5'-phosphate (Ro-RP). Furthermore, Ro-RP is adenylylated with ATP delivering roseoflavin adenine dinucleotide (Ro-FAD). Ro-RP and Ro-FAD are the analogues to the RP and FAD and act as a Trojan horse.[19] They bind to flavoproteins reducing their enzymatic activity and Ro-RP bind to the RP riboswitch downregulating the RF biosynthesis.

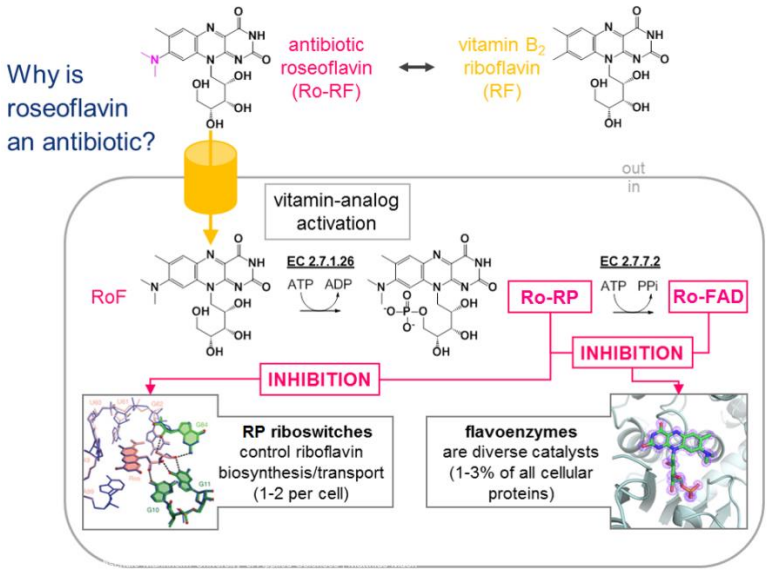

Figure 3 : The postulated mechanism of antibiotic action of roseoflavin. Due to the similar structure compared to RF, it can be actively taken up by riboflavin importers (yellow cylinder). Inside it is metabolized to the active forms Ro-RP and Ro-FAD. In this state, it can bind to RP riboswitches downregulating RF synthesis and it can bind to flavoproteins inhibiting their activity. (M. Mack - personal communication)

Additionally, microorganisms capable of synthesizing RF and also having a RF importer show as well sensitivity against RoF, due to the fact that Ro-RP is capable of binding to the RP riboswitch and makes the cell RF auxotrophic.[20-23] Yet, Ro-RP does not bind to the RP riboswitch of *S. davawensis*, due to a single point mutation.[24] Another possible explanation for the antibiotic ability can be the difference in the redox potential. A coherent experiment showed a redox potential of -222 mV which is 38 mV lower than RFs one[25]. This effect is caused by the dimethyl amine group (stronger electron donor than a methyl group) which makes RoF a less efficient electron carrier than the natural flavin analogue[26]. Additionally, a protonated dimethyl amine moiety can disturb crucial hydrogen bonds between amino acids and/or water molecules in the active site of the enzyme. This can lower the activity of the flavoprotein, which bound Ro-RP or Ro-FAD as a prosthetic group. RoF sensitivity was predominantly shown in gram positive bacteria, such as *Bacillus subtilis*[23], *Listeria monocytogenes*[21], and *Staphylococcus aureus*[25].

1.4. Flavoproteins and flavodoxins

Otto Warburg reported the first isolation of a yellow protein in the early 1930s, which turned out to be a flavin binding protein[27] (also called flavoprotein). In general, flavoproteins bind RP or FAD mostly as a prosthetic group and use them as an electron carrier. Macheroux et al.[28] did a Protein Database (pdb) analysis, which revealed that 90 % of known flavin-depending enzymes are oxidoreductases. The remaining ones show transferase, lyase, isomerase and ligase activity. Important reactions which these enzymes catalyse are for instance the molecular oxygen activation[29] (excitation from singulet to triplet state), other oxidations[29], halogenations[30], reduction of disulfides[31] and also biological sensing mechanisms[32].

It is believed that flavin depending enzymes are present in all living cells with an estimated amount of up to 3.5 % of the total enzymes quantity.[33] 75 % use FAD as cofactor and 25 % use RP.[33] Besides that, 10 % of the resolved protein folds showed a covalently attached flavin via 8α and/or C(6), although this predominantly occurs in FAD binding proteins.[33]

The most abundant folds found in nature are the Rossman fold (binds FAD but not RP) and the $(\alpha\beta)_8$ TIM barrel fold (binds FAD and RP). These ones can be found in all three domains of life and had evolved a great variety of functions, whereas the majority of other folds present only a few functions.[34]

The TIM barrel fold consists of 8 α-helices and 8 β-sheets which alternate regarding its primary sequence. The secondary structure shows an inner barrel of α-helices and an outer barrel of parallel β-sheets (see Figure 4B).

The Rossmann fold consists of up to seven parallel β-strands, which are connected with coils and/or α-helices located on both sides. The ribityl residue usually serves as an identity mark, and is therefore deeply buried inside of the protein (see Figure 4C).

The flavodoxin fold (binds RP but not FAD) is derived from a Rossmann fold and belongs to the bacterial RP binding protein family. Flavodoxins have very often an electron carrier function, such as the nitroreductase from *Clostridium pasteurianum*. Usually, *C. pasteurianum* fixates anaerobically nitrogen with ferredoxins. These enzymes are iron depending. If the organism experiences an iron deficient environment, it synthesizes the mentioned flavin depending nitroreductase, which performs the nitrogen fixation instead.[35]

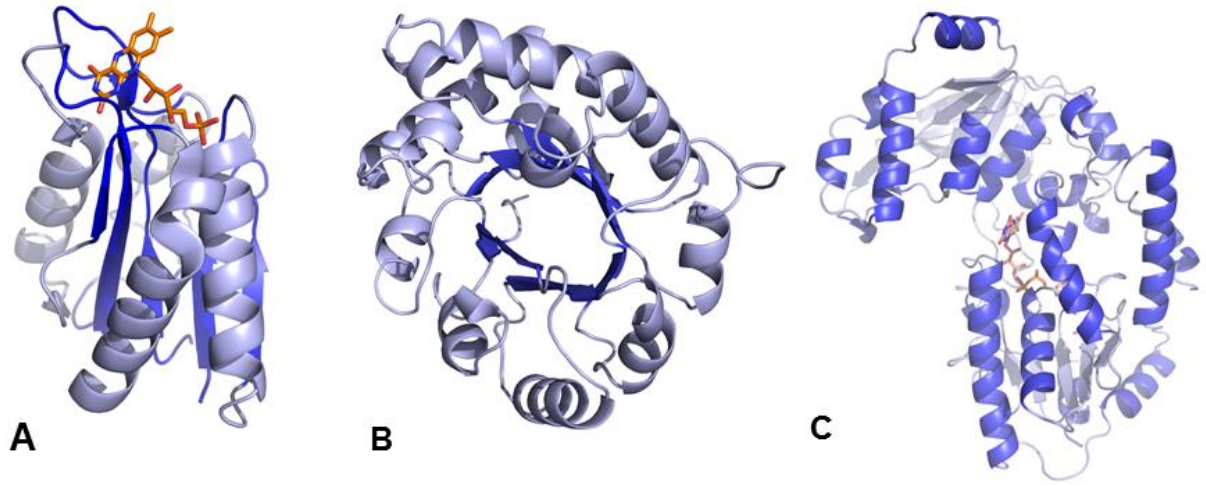

Figure 4: Panel A: An electron transferring flavodoxin from *Desulfovibrio vulgaris* (oligomeric state: monomer). PDB entry: 1FX1. RP (carbon in orange) is located on the β-sheet tips. Panel B: A triose phosphate isomerase from *Gallus gallus* having a TIM barrel fold is shown (monomer shown only, top view). PDB entry: 8TIM. Panel C: An adrenodoxin reductase of mitochondrial P450 systems from *Bos Taurus* is shown having a Rossmann fold (oligomeric state: monomer). FAD (carbon in orange) is located on the β-sheet tips. PDB entry: 1CJC.

The flavodoxin fold consists of an αβ fold with five parallel β-sheets in the center and two and/or three α-helices in the front and back. The first reported flavodoxin crystal structure was published in 1976[36] and was isolated from *Desulfovibrio vulgaris* (see Figure 4, panel A). It has five parallel β-sheets and two α-helices in the front and in the back. RP is located at the β-sheet tips and the ribityl moiety points towards the protein center. Additionally, there are also flavodoxin-like proteins, which form dimers or dimers of a dimer (not shown). Two important binding motifs have to be highlighted: The P-loop or Walker-loop (Sequence: GXXXXGK[TS]) binds the phosphate moiety and can also be found in other enzymes like ATP or GTP binding ones.[37] Secondly, the βαβ fold, also known as the Rossman motif (GXGXXG) binds nucleotides, such as NAD(P) but also the isoalloxazine ring of flavins. Especially, an aspartate being in contact with the O3' of the ribose moiety is highly conserved.

Since today, the amount of resolved flavodoxin crystal structures increased to 135 (pdb database date: 2016 November). The design of parallel β-sheets in the center and α-helices in the front and back is conserved in all of them with alterations in number and extensions in certain loops. This makes the flavodoxin fold a very good identification tool for RP binding proteins.

1.5. Aim of the thesis

In a previous work *rosB* was identified to be a crucial gene[17] for the RoF biosynthesis. It was shown that a *rosB* disrupted *S. davawensis* mutant did not produce any roseoflavin. *In vitro* studies revealed that RosB catalysed the oxidation from RP to HOC-RP. Yet, it was unclear how HOC-RP is converted to AF. This work addresses the need to understand the function of the enzyme RosB in this context and to elucidate the formation of AFP. Besides that, the reaction mechanism and the crystal structure were of interest.

2. Materials & Methods

2.1. Lab equipment

Table 1: List of used lab equipment for standard procedures:

Device	Model	Manufacturer
Autoclave	Varioklav® Dampfsterilisator 75S	H+P Labortechnik, Habermoos, Germany
Bench centrifuge	Eppendorf 5415 R	Eppendorf, Hamburg, Germany
Centrifuge (30k rpm)	Sorvall WX Ultra	Thermo Fischer, Waltham, USA
Centrifuge (6k rpm)	Heraeus Fresco 21	Heraeus, Hanau, Germany
Dialysis membrane	Tubing-Visking size 11	Medicell Int. LTD, London, UK
Electroporation device	Gene Pulser® II	BIO-RAD, Munich, Germany
French Press	Constant Cell Disruption System	Constant System, Daventry, UK
Gel electrophoresis (horizontal)	Mini-Sub Cell GT + Wide, Power Pac 200, Power Pac 300	BIO-RAD, Munich, Germany
Gel Imager	Molecular Imager® GelDoc™ XR, Quantity One 1D-Analysis software	BIO-RAD, Munich, Germany
Heating block	Thermomixer comfort	Eppendorf, Hamburg, Germany
Incubator	15 L NLF22	Bioengineering, Wald, Switzerland
LC/MS-system	1200 Infinity series with DAD/FLD and API-ESI 6130 Quadrupole	Agilent Technologies, Waldbronn, Germany
Optical microscope	BH-2	Olympus Europe, Hamburg, Germany
PCR	C1,000™ Thermal Cycler, dual	BIO-RAD, Munich, Germany
Photometer DNA quantification	NanoVue	GE Healthcare, Little Chalfont, UK
Photometer	Uvikon 933	BioTek Kontron Instruments AG, Neufahrn
Shaking incubator	Certomat® IS	Sartorius Stedim GmbH, Göttingen, Germany
Sterile bench	Variolab Mobilien W 90	Waldner Laboreinrichtungen GmbH & Co KG, Wangen, Germany
Water bath	IKA® HBR4 digital	IKA GmbH, Staufen im Breisgau, Germany

2.2. Chemicals

$H_2{}^{18}O$ was purchased from Euriso-Top (Saint-Aubin Cedex, France), potassium dihydrogen phosphate and di-potassium hydrogen phosphate were bought from Merck (Darmstadt, Germany), KCl, NaCl, ammonium sulfate, glycerol, 99 % for synthesis, isopropyl-β-D-thiogalactopyranoside, BC grade and all used antibiotics were purchased from Applichem GmbH (Darmstadt, Germany). LB broth medium and agar-agar were bought from Carl Roth GmbH & Co. KG (Karlsruhe, Germany). Restriction endonucleases were purchased from Fermentas (Heidelberg, Germany). All other chemicals were bought from Sigma Aldrich GmbH (Taufkirchen, Germany), unless described differently. The HPLC organic solvents were MS grade and bought from Applichem GmbH (Darmstadt, Germany).

$^{18}O_2$ had a purity of 98 %. Riboflavin 5′-monophosphate, synthetic, ≥70 % was used for assay experiments Riboflavin 5′-monophosphate, >95 % was used for the column calibration. Roseoflavin was obtained from Chemos (Regenstauf, Germany) and 8-demethyl-8-amino riboflavin (AF) was prepared synthetically and was a gift from Peter Macheroux (Dept. of Biochemistry, Graz University of Technology, Austria). 8-demethyl-8-carboxyl-riboflavin (HOOC-RF) was prepared synthetically and was a gift from Tadhg Begley (Texas A&M University, USA). 8-demethyl-8-aminoriboflavin-5'-phosphate (AFP) and HOOC-RP were prepared as described in chapter 2.6.6. Dihydroresorufin was bought from Biomol GmbH (Hamburg, Germany).

2.3. Media and medium additives

All media were prepared in 1 L beakers and autoclaved. Agar plates were prepared by adding 2 $\frac{w}{V}$% agar-agar. Antibiotics were sterile filtered by employing a 0.2 μm cellulose acetate filter and were supplemented after autoclaving under sterile conditions at ~50 °C.

GYT medium

Tryptone	2.5 g
Yeast extract	12.5 g
Glycerol 50 $\frac{w}{V}$%	100 mL

Adjust pH to 7.0.

LB medium[38]

Tryptone	10 g
Yeast extract	5 g
NaCl	5 g
H_2O	1,000 mL

M9 medium[39]

Na_2HPO_4	8 g
KH_2PO_4	4 g
NaCl	0.5 g
NH_4Cl	0.5 g
Glucose 20 $\frac{w}{v}$ %	20 mL
*$MgSO_4$ 1 M	1 mL
*$CaCl_2$ 1 M	0.3 mL
*Trace element solution 10x	10 mL
H_2O	fill up till 1,000 mL

Mannitol-soy flour medium (MS medium)[40]

Soya flour	20 g
D-mannitol	20 g
Tap water	1,000 mL

Adjust pH to 7.0.

SOC medium[40]

Tryptone	20 g
Yeast extract	5 g
NaCl	0.6 g
KCl	0.2 g
H_2O	1,000 mL
*$MgCl_2$	1 g

*$MgSO_4$	2.5 g
*D(+)-glucose	3.6 g

TAE-buffer (50x) (for DNA gel electrophoresis)[38]

Tris-base	242 g
Acetic acid	57.1 mL
EDTA 0.5 M	100 mL
H_2O	1,000 mL

Trace element solution 100x

EDTA	5 g
$FeCl_3$ x 6 H_2O	0.83 g
$ZnCl_2$	84 mg
$CuCl_2$ x 2 H_2O	13 mg
$CoCl_2$ x 6 H_2O	10 mg
H_3BO_3	10 mg
$MnCl_2$ x 6 H_2O	1.6 mg
H_2O	1,000 mL

First EDTA dissolved and pH adjusted to 7.5. Sterile filtrated.

Tryptone soya broth (TSB)[2]

Pepton from casein	17 g
Pepton from soy flour	3 g
D(+)-glucose	2.5 g
NaCl	5 g
KH_2PO_4	2.5 g
H_2O	1,000 mL

YS medium

Potato starch	10 g
Yeast extract	2 g
H_2O	1,000 mL

! = Adjust pH to 7.0.

2 x YT medium

Tryptone	16 g
Yeast extract	10 g
NaCl	5 g
H_2O	1,000 mL

„*“ = sterile filtered with a 0.2 μm cellulose acetate filter and supplemented after autoclaving under sterile conditions.

2.4. Microbiological methods

2.4.1. Bacterial strains and growth conditions

Streptomyces strains were grown in baffled Erlenmeyer flasks at 30 °C and 150 rpm. Note, that the flask size was always 10x of the culture volume, in order to guarantee sufficient oxygen supply. The cultures were inoculated with 0.01-0.03 $\frac{V}{V}$% spore suspension. TSB, YS or M9 medium were used, unless stated otherwise. YS cultures were never supplied with antibiotics.

E. coli strains were grown in LB or M9 in baffled Erlenmeyer flasks at 37 °C and 150 rpm, if not mentioned differently. Cultures were inoculated with a pre-culture incubated in a test tube at 37 °C and 250 rpm.

2.4.2. Preservation of *E. coli* strains in the strain database

Single clones were picked and grown in LB (including antibiotics if necessary) in test tubes at 37 °C and 250 rpm until stationary phase was reached. Sterile glycerol was added to a final concentration of 30 $\frac{w}{V}$% and stored at – 80 °C.

2.4.3. Preparation and preservation of spore suspensions

The strain was grown in TSB medium for 2-3 days. Afterwards, 1 mL mycelia containing cell culture was pipetted on one MS plate (5-10 plates in total). The plates were dried in the sterile bench and incubated for 96 h at 30 °C or until the plate was fully covered with spores (white/grey cover). Each plate was treated with 5 mL sterile Tween 20 solution (0.1 $\frac{V}{V}$%). The spores were scratched off with a cell scraper and transferred to a 50 mL sterile plastic tube. Note that the tube and every following step had to be cooled on ice, in order to prevent germination. Spore chains were scattered by a vortex step and separated from residual mycelium and solid medium/ agar by filtration with sterile cotton wool. The filtrate was centrifuged for 5 min at 4,000 rpm and 4 °C. Afterwards, the supernatant was removed and the remaining spores were treated with 1 mL sterile glycerol solution (20 $\frac{w}{V}$%), aliquoted and stored at -80 °C.

2.4.4. Measurement of *E.coli* cell densities

A cell culture sample was diluted and transferred to a semi-micro cuvette. Optical densities were measured in a photometer at λ=600 nm against a blank with the cell-free culture medium. The value should not exceed 0.8.

2.4.5. Preparation and preservation of chemically competent cells[38]

Standard cloning procedures were done with *E. coli* TOP10 cells. Antibiotics were freshly added, if necessary. A culture of 50 mL LB were inoculated with a pre-culture to an OD_{600} of 0.03 and incubated at 37 °C and 150 rpm. When the culture reached a cell density of 0.4, it was centrifuged at 3,000 rpm and 4 °C for 10 min. Note that all following steps and used solutions were ice-cold used/done. The supernatant was discarded and the cell pellet was re-suspended in 20 mL 0.1 M $CaCl_2$. The cell suspension was incubated for 20 min on ice, and later centrifuged at 3,000 rpm and 4 °C for 10 min. The supernatant was discarded and the cell pellet re-suspended in 2 mL 0.1 M $CaCl_2$. Finally, the cell suspension was treated with 0.66 mL glycerol solution (60 $\frac{V}{V}$%), aliquoted, immediately frozen in liquid nitrogen and stored at -80 °C.

2.4.6. Preparation and preservation of electro-competent cells

A 50 mL pre-culture of the desired *E. coli* strain was incubated at 37 °C and 150 rpm. Antibiotics were freshly added, if necessary. The pre-culture was distributed to 4x250 mL LB including antibiotics and further incubated at 37 °C and 150 rpm. After reaching an OD_{600} of 0.35-0.4, the cells were centrifuged at 2500 rpm and 4°C for 20 min. Note that all the following centrifugation steps had the same parameters. Additionally, all following steps were done on ice and all used solutions were pre-cooled. The supernatant was discarded and the cell pellet was re-suspended in 500 mL H_2O. Afterwards, the cell suspension was centrifuged, the supernatant discarded and the cell pellet re-suspended in 250 mL glycerol (10 $\frac{w}{V}$%). Again, the cell suspension was centrifuged, the supernatant discarded and the cell pellet re-suspended in 10 mL glycerol (10 $\frac{w}{V}$%). Finally, the cell suspension was centrifuged, the supernatant discarded and the cell pellet re-suspended in 1 mL GYT medium. The cell density of a 1:100 dilution sample was measured and the volume adjusted to reach a theoretical OD_{600}=1. Aliquots were immediately frozen in liquid nitrogen and stored at -80 °C.

2.4.7. Disruption of *rosB* in *Streptomyces davawensis*

Gust et al.[4] developed a technique which allows the deletion of genes in *Streptomyces coelicolor* via conjugation. In our group, this technique was modified to be able to disrupt a gene in *Streptomyces davawensis*. A cluster database of *S. davawensis* was bought from Bio S&T. In more detail, the database contained *E. coli* DH10b strains which were carrying each a pESAC13 cosmid containing a random 100 kbp long subgenomic DNA fragment (ESAC = *E. coli – Streptomyces* Artificial Chromosome). Note that pESAC is a pPAC-S1 derivative[41] which has an additional *oriT* from the RK2 replicon[42], it replicates autonomously in *E.coli* and it has a Kana resistance.

E. coli DH10b strains were prepared to be electro-competent and transformed with a thermosensitive pIJ 790 plasmid containing λ RED system – *gam, bet, exo*. Note that after transformation, the incubation temperature must not be higher than 30 °C. The λ RED System gives the option to modify the pESAC13 cosmid via homologue recombination. For this, an apramycin coding (Apra) cassette flanked by extensions had to be designed. To sum up the design, the Flp recombination system recognizes FRT sites (19 nt each) which have to flank the Apra cassette. To locate *rosB*, the FRT sites have to be extended with homologue sequences neighboring *rosB* (39 nt on both sides). The homologue ends enable the homologue recombination of *rosB* and the apramycin cassette, delivering an apramycin resistance.[17] The

needed fragment was kindly provided by Julia Schwartz and was only amplified with PCR (PCR method Knock3, primers = for/rev iFD7989). Figure 5 shows the subgenomic DNA of the *E. coli* DH10b-pESAC120 clones, which carried the pESAC13 cosmid ($Kana^+$).

Electro-competent DH10b-pESAC120 cells were transformed with the pIJ 790 plasmid (Cm^+) and selected for Kana and Chloramphenicol (Cm) resistances on LB plates at 30 °C. A positive clone was picked and made electro-competent as well. Then, competent *E. coli* DH10b-pESAC120 pIJ-790 cells were transformed with the FLP recombinase-ready apramycin cassette. Positive clones were picked and streaked on fresh LB-agar plates at 37 °C (only kana and apra!), in order to remove the thermosensitive pIJ 790 plasmid. Cm sensitive clones were picked and used for the conjugation.

S. davawensis degrades methylated DNA, therefore a tri-parental mating had to be done between *E. coli* DH5αpR9406 (contains *tra*-genes for infection, $Carb^+$), *E. coli* GM2163 (methyl sensitive strain, Cm^+) and *E. coli* DH10b-pESAC120 (cosmid; $rosB^-$::$Apra^+$, $Kana^+$). Each strain was inoculated in 10 mL LB (including antibiotics if possible) and cultivated overnight at 37 °C and 250 rpm. The next day, a 30 mL LB culture including antibiotics was inoculated to an OD_{600} of 0.05. At OD600=0.4-0.6 the cells were centrifuged and washed with LB three times. The cell pellets were re-suspended in the remaining liquid and pooled together. Finally, 30 μL drops were pipetted on LB agar plates. After drying, the plates were incubated at 37 °C overnight. Cell colonies were streaked on LB agar plates containing Kana, Apra, Carb and Cm. Only a completely infected *E.coli* GM2163 is able to grow under this condition. One positive *E. coli* GM2163 clone was picked and again inoculated to an OD_{600} of 0.05. After reaching OD600=0.4-0.6 the cells were centrifuged, washed three times with LB and finally re-suspended in 500 μL LB.

S. davawensis spores were thawed and centrifuged to remove as much liquid as possible. The spores were re-suspended in 1.5 mL 2x YT medium and heat-shocked for 10 min at 50 °C. 500 μL spores and 500 μL *E.coli* GM2163 suspensions were gently mixed, centrifuged, the supernatant removed and re-suspended in the remaining liquid. 30 μl drops were pipetted onto MS+10 mM $MgCl_2$ plates at 30 °C, overnight. After roughly 16 hours, the plates were covered with 1 mL of nalidixic acid 0.5 $\frac{mg}{mL}$ and Apra 1.25 $\frac{mg}{mL}$ to inhibit *E.coli* growth and to select for positive mutants, respectively. Furthermore, the plates had to be dry to continue the incubation at 30 °C for additional 4-8 days. Grown colonies were picked and streaked on fresh MS plates containing Apra. To exclude single cross-overs each picked clone was also streaked on MS plates containing Apra and kanamycin. A double cross-over is a disruption with only the Apra cassette and a single one with the whole pESAC cosmid. Therefore, *S. davawensis*

mutants with double cross-overs have to be kanamycin sensitive. After the second picking round, spores were only picked to streak on fresh plates. Several picking and sporulation rounds were needed to gain a contaminant-free *S. davawensis* mutant. To exclude contamination, the spores were inoculated in 30 mL YS medium and incubated at 30 °C and 150 rpm for three days. A sample was taken and analysed under the microscope to exclude any contamination.

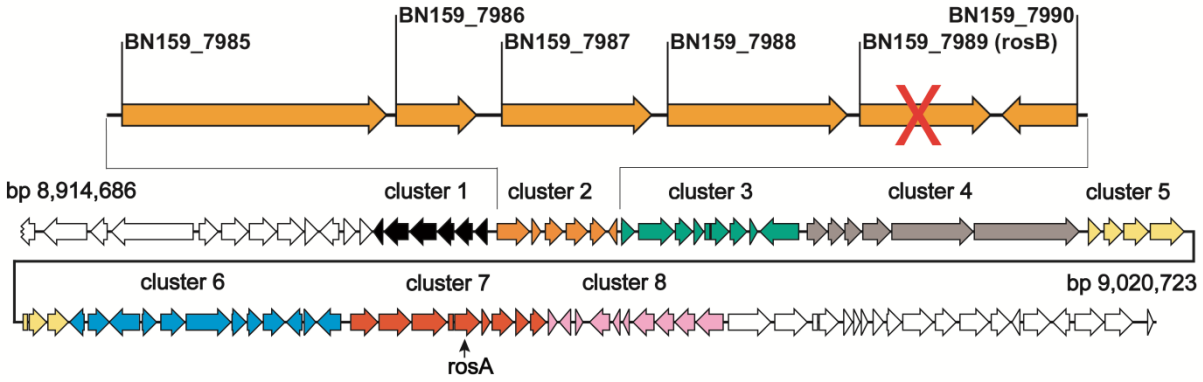

Figure 5: The subgenomic sequence of the pESAC13 cosmid carried by the *E.coli* DH10B-pESAC120 is shown. After the disruption of *rosB*, no roseoflavin can be found in the supernatant of a stationary *S. davawensis* culture, but an Apra resistance is present.

2.4.8. RosB production in *E.coli* Rosetta 2 (DE3)

Protein production was done with *E. coli* Rosetta 2 (DE3) from Merck (Darmstadt, Germany) which contained pET24a(*rosB)* or pET24a($rosB^{TAA}$). 4x250 mL LB were inoculated with 10 mL pre-culture and incubated at 37 °C and 150 rpm until an OD_{600}=1.0 was reached. Note that, any used LB contained 50 $\frac{\mu g}{mL}$ kanamycin and 35 $\frac{\mu g}{mL}$ Cm. 200 μM IPTG was added and further incubated overnight. The cell cultures were centrifuged at 6,000 rpm, 4 °C for 5 min. The supernatant was discarded and the cell pellet was re-suspended in 250 mL PBS (pH=8). The cell suspension was centrifuged at 6,000 rpm, 4 °C and 5 min. Finally, the supernatant was discarded and the cell pellet stored at -20 °C.

RosB is highly-expressed and has very low limitations regarding expression parameters. It can be expressed at 37 °C and 20 °C combined with either 1 mM IPTG for 2 hours or 200 μM IPTG overnight.

2.4.9. RosB expression in *E.coli* BL834

Protein expression was done with *E. coli* BL834 using the EMBL protocol.[39] The starting volume was 4x250 mL. Additionally, the starvation time was four hours and the expression time was set to ten hours with 1 mM IPTG. The incubation parameters were always 37 °C and 150 rpm.

2.5. Molecular biological methods

2.5.1. Isolation of genomic DNA and plasmid DNA

Genomic DNA from *S. davawensis* was isolated with the Genomic DNA Extraction Kit from Fermentas (Heidelberg, Germany), following the standard protocol. Plasmid DNA was isolated with the GeneJET Plasmid Miniprep Kit from Thermo Fisher Scientific (Dreieich, Germany), following the standard protocol.

2.5.2. PCR methods

All PCR reactions were performed with the KAPA HiFi HotStart PCR Kit from KAPABIOSYSTEMS. The PCR master mix was always prepared as described in the manufacture´s protocol. Following amplification methods were used:

knock3			
step	**time**	**temperature**	
initial denaturation	2 min	95 °C	
denaturation	45 s	98 °C	
primer annealing	45 s	50 °C	} 10 cycles
elongation	45 s	72 °C	
denaturation	45 s	98 °C	
primer annealing	45 s	55 °C	} 15 cycles
elongation	45 s	72 °C	
final elongation	5 min	72 °C	
cool down	∞	10 °C	

DGTGR			
step	**time**	**temperature**	
initial denaturation	5 min	95 °C	
denaturation	20 s	98 °C	} 30 cycles
primer annealing	15 s	65 °C	
elongation	30 s	72 °C	
final elongation	2 min	72 °C	
cool down	∞	10 °C	

Brampkap			
step	**time**	**temperature**	
initial denaturation	3 min	95 °C	
denaturation	20 s	98 °C	} 20 cycles
primer annealing	30 s	62 °C	
elongation	20 s	72 °C	
final elongation	1 min	72 °C	
cool down	∞	10 °C	

2.5.3. Purification of DNA fragments

DNA fragments originated from PCR reactions or digestion by restriction endonucleases were either directly purified with the GeneJET PCR Purification Kit from Fermentas (Heidelberg, Germany), following the standard protocol or by pre-purifying it on an agarose gel electrophoresis (chapter 2.5.10) followed by gel extraction using the GeneJET PCR Gel Extraction Kit from Thermo Fisher Scientific (Dreieich, Germany), following the manufacture's manuals.

2.5.4. Digestion of DNA

Digestion by restriction endonucleases was either done for plasmid analysis which was then separated by agarose gel electrophoresis (chapter 2.5.10) or the preparation of linear plasmid DNA for ligation. Note that the digestion of the plasmid preparation contained always alkaline phosphatase, in order to prevent re-ligation. The experiment was performed as demanded by the standard protocol and the reaction was purified via gel extraction. PCR products were purified with GeneJET PCR Purification Kit.

2.5.5. Ligation

Ligation was done with the T4 DNA Ligase from Fermentas (Heidelberg, Germany) as the standard protocol suggested.

2.5.6. DNA sequencing

Sequencing of dsDNA was performed by EuRoFins MWG Operon (Ebersberg, Germany).

2.5.7. Transformation of chemical competent cells

A frozen aliquot of chemically competent cells was thawed on ice and either mixed with 100 ng DNA or 5 μL ligation reaction. The cell/DNA suspension was slightly tapped and incubated on ice for 30 minutes. Afterwards, cells were heat-shocked at 42 °C for 45 s and immediately let rest on ice for 5 min. The transformed cells were fused with 0.25 mL ambient tempered SOC medium. Furthermore, the cell suspension was incubated at 37 °C and 230 rpm for 1 h. A dilution series was streaked on LB-agar plates (including necessary antibiotics) and each plate was incubated at 37 °C overnight. Single colonies were picked and analysed via plasmid preparation followed by DNA sequencing.

2.5.8. Transformation of electro-competent cells[38]

A frozen aliquot of electro-competent cells was thawed on ice and either mixed with 1 μL ligation product or 20 ng purified plasmid DNA. The mixture was slightly tapped and incubated on ice for 30 min. Afterwards, the cell suspension was transferred to a pre-cooled electroporation cuvette. The electroporation was performed at 200 Ω, 25 μF and 2.5 kV. The transformation was fused with 500 μL pre-cooled SOC medium and gently mixed. Afterwards, the cell suspension was incubated at 37 °C and 230 rpm for 1 h. A dilution series was streaked on LB agar plates (including necessary antibiotics) and each plate was incubated at 37 °C overnight. Single colonies were picked and analysed via plasmid preparation followed by DNA sequencing.

2.5.9. Construction of plasmids and strains used for protein expression

Standard cloning procedures were done with *E. coli* TOP10 cells. Antibiotics were freshly added, if necessary. pET24a(*rosB)* and pIJ790 were constructed earlier[17]. pRARE2-pACYC184-plasmid was isolated from Rosetta 2 (DE3) *E. coli*.

The pET24a($rosB^{TAA}$) plasmid was constructed amplifying rosB from pET24a(*rosB)* using the primers Bramp_rev_*Bam*HI+Stop and Bramppetfor (PCR method=Brampkap). The reversed primer contains the codon TAA, therefore the translation stops before the His_6-Tag can be translated. The generated PCR fragment and pET24a(+) were digested with *Nde*I and *Bam*HI, purified via gel extraction and ligated (see chapter 2.5.2-5). Finally, chemical competent *E. coli* Rosetta 2 (DE3) was transformed with the ligation product.

Chemically competent *E. coli* BL834 (methionine auxotroph) was transformed with pRARE2-pACYC184-derived plasmid to enhance protein expression originated from GC-rich DNA. Furthermore, this strain was made chemically competent and transformed with pET24a(*rosB)*. Methionine auxotroph was tested by streaking the generated mutant on a M9 plate containing the necessary antibiotics and on a M9 plate containing the necessary antibiotics and 1 mM methionine (control).

2.5.10. Agarose gel electrophoresis

PCR products and plasmids were loaded with 6x DNA loading dye and separated on a 1 $\frac{w}{V}$% agarose gel with 90 V for 30-60 min. The processed gel was stained with an ethidium bromide bath and a picture taken according to standard protocols[38].

2.6. Biochemical methods

2.6.1. Preparation of crude extract from *E. coli*

The cell pellet was thawed and re-suspended in an appropriate buffer containing one tablet of "cOmplete™, EDTA-free Protease Inhibitor Cocktail" from Roche (Mannheim, Germany). The cell suspension was passed through the French Press three times with a pressure of 2 kbar. Subsequently, the cell suspension was centrifuged at 30,000 rpm, 4 °C for 30 min. The supernatant was used for further protein purification steps. Note that the cell suspension was always kept on ice.

2.6.2. SDS-PAGE[43]

Protein samples were diluted 1:1 with 2x reducing SDS sample buffer and heated for 15 min at 95 °C. The denatured samples were loaded into pre-cast "Any kD™ Mini PROTEAN® TGX Stain-Free™" Protein Gels (10 well, 30 μl) from BioRad Laboratories GmbH (Munich, Germany). Each pocket was loaded with 8 μg total protein and one pocket was loaded with 5 μL "PageRuler Prestained Protein Ladder Plus" from Thermo Fisher Scientific GmbH (Dreieich, Germany). The protein samples were focused at 100 V for 10 min and separated for 30-45 min at 200 V. Afterwards, the gel was washed with water and stained with "Coomassie Brilliant Blue R-250 Staining Solution" from BioRad (Dreieich, Germany) for 2 h. Finally, the gel was de-stained multiple times with water and finally digitized.

2.6.3. Protein concentration determination via Bradford[44]

Protein concentrations were measured by the Bradford method, using BSA as standard.

2.6.4. High Pressure Liquid Chromatography-Mass Spectrometry

Each HPLC sample was treated with 10 $\frac{V}{V}$% acid. For diode array detector- fluorescence light detector (DAD-FLD) measurements a 50 $\frac{w}{V}$% TCA solution was used and for DAD-MS measurements 98 % formic acid was used. After acidifying, the sample rested for 5-10 min on ice. Afterwards, it was centrifuged at 14,000 rpm for 2 min, filtered with a cellulose acetate filter (0.2 μm) and placed in the auto sampler which was held at 14 °C. All measurements were done under aerobic conditions.

Method - Reprosil C_{18} column

An 1260 Agilent system was used containing a 1260 DAD, followed by an 1260 FLD using a Reprosil C_{18} column, 5 μm 10x2 mm column (Dr. Maisch GmbH, Ammerbuch-Entringen). The column was equilibrated with 15 $\frac{V}{V}$% buffer B methanol and buffer A (10 mM formic acid and 10 mM ammonium formate, pH=3.7). Samples were eluted with an isocratic gradient of 70 % A, at a flow rate of 0.5 $\frac{mL}{min}$. Note, the initial gradient was isocratic 40 $\frac{V}{V}$% buffer B. The column was heated to 50 °C and 15 μl (10% of maximum sample volume) aliquots were injected. Furthermore, product ion spectra were recorded from the gradient with a step size of

0.1 and the sums were taken for each identified peak. The capillary voltage was set to 3 kV and the fragmentor to 165 V with a mass range from 222 to 800. The source and desolvation temperatures were kept at 350 °C. The desolvation gas was delivered at 12 $\frac{l}{h}$ with a maximum of 13 $\frac{l}{h}$ and the nebulizer pressure was set to 35 psig with a maximum at 65 psig. The shutter opened at 3.2 min. The data was processed with the software LC/MSD Chemstation (Rev.B.04.03[16]).

Method – Kinetex Biphenyl column

An 1260 Agilent system was used containing a 1260 diode array detector (DAD), followed by an ESI-Single Quadrupol Mass spectrometer using a Kinetex Biphenyl, 2.6 μm, 150x2.1 mm (Phenomenex, Aschaffenburg). The column was equilibrated with buffer 15 $\frac{V}{V}$% B methanol, buffer A (10 mM formic acid, 10 mM ammonium formate, pH=3.7) and samples were eluted with the gradient profile summarized in Table 2, at a flow rate of 0.2 $\frac{mL}{min}$. The column was heated to 50 °C and 2 μl (10% of the maximum sample volume) aliquots were injected, if not mentioned differently. Furthermore, product ion spectra were recorded from the gradient with a step size of 0.1 and the sums were taken for each identified peak. The capillary voltage was set to 3 kV and the fragmentor to 133 V with a mass range from 155 to 1,000. The source and desolvation temperatures were kept at 350 °C. The desolvation gas was delivered at 12 $\frac{l}{h}$ with a maximum of 13 $\frac{l}{h}$ and the nebulizer pressure was set to 35 psig with a maximum at 65 psig. The shutter opened at 3.2 min. The data was processed with the software LC/MSD Chemstation (Rev.B.04.03[16]).

Table 2: The gradient profile for the Kinetex Biphenyl 2.6 µm, 150x2.1 mm is shown (this work).

time [min]	solvent A [%]	solvent B [%]	comment
0	85	15	gradient
3	77	23	
3.1	73	27	
5	70	30	
6.5	68	32	
13.5	68	32	
20	5	95	
20.1	0	100	wash
24.1	0	100	
24.5	100	0	
29.5	100	0	
30	85	15	re-equilibration

Additionally, the method was calibrated with an injection volume of 2 μL for the substances AFP, AF, RP, RF, FAD and RoF in the range between 0.5 μM and 50 μM (8-10 data points).

Method - ACQUITY UPLC® BEH C_{18} 1.7 μm column

Mass fragmentation pattern analysis was performed by our collaborative partner R. Sandhoff with UPLC-ESI-MS^2. A "triple quadrupole type" Xevo TQ-S tandem mass spectrometer system was used, coupled to an automated Aquity I Class UPLC system using an ACQUITY UPLC® BEH C18 1.7 μm column (length 50 mm, diameter 2.1 mm) (Waters Corporation, Eschborn, Germany). The column was equilibrated with buffer (10 $\frac{V}{V}$% methanol, 0.1 $\frac{V}{V}$% formic acid, and 10 mM ammonium formate) and eluted with an increasing amount of buffer B (95 $\frac{V}{V}$% methanol, 0.1 $\frac{V}{V}$% formic acid, and 10 mM ammonium formate) at a flow rate of 0.45 $\frac{mL}{min}$.

For this system, methanol was added to a final concentration of 10 $\frac{V}{V}$% to the sample and the treated sample was placed directly into the auto sampler held at 15 °C. The column was heated to 40 °C and 10 μl (100% of injection needle capacity) aliquots were injected. Furthermore, product ion spectra were recorded from the gradient with a dwell time of 0.16 s and the sums were taken for each identified peak. The capillary voltage was set to 2.5 kV, whereas the cone and the source offset were fixed at 50 V. The source and desolvation temperatures were maintained at 90 °C and 300 °C, respectively. The desolvation gas was delivered at 800 l/h, while the cone gas was delivered at 150 $\frac{l}{h}$ and the collision gas flow was fixed to 0.15 ml/min. Samples were injected and processed using MassLynx (v 4.1 SCN 843) from Waters Corporation, unless mentioned differently.

2.6.5. Fast Protein Liquid Chromatography

All chromatographic steps were performed using the ÄKTApurifier™ system (GE Healthcare, Munich, Germany). All columns were purchased from GE Healthcare (Munich, Germany). The data was processed with the software Unicorn 5.1. The crude extract was prepared as described in chapter 2.6.1. RosB was stored at -20 °C until usage.

Affinity-SEC (desalting) RosB purification

The affinity purification was performed using a HisTrap™ HP 5 mL column from (GE Healthcare, Little Chalfont UK) at a flow rate of 2 $\frac{mL}{min}$. The buffers used in this protocol are summarized in Table 3:

Table 3: The binding buffer A, elution buffer B for the affinity purification and the desalting buffer are shown.

binding buffer A		**elution buffer B**		**SEC buffer**	
component	**concentration [mM]**	**component**	**concentration [mM]**	**component**	**concentration [mM]**
K_2HPO_4	16.4	**K_2HPO_4**	16.4	**K_2HPO_4**	16.4
KH_2PO_4	3.6	**KH_2PO_4**	3.6	**KH_2PO_4**	3.6
KCl	300	**KCl**	300	**KCl**	300
imidazole	10	**imidazole**	500	**pH**	8
pH	8	**pH**	8		

Crude extract was loaded onto the column and bound protein was washed with buffer A until the UV signal had reached its initial intensity. Impurities were eluted with 20 %B. RosB elution was initiated with 80 %B. The eluted protein was directly transferred onto a HiPrep™ 26/10 desalting column (GE Healthcare, Little Chalfont UK) at a flow rate of 8 $\frac{mL}{min}$. The eluted RosB was treated with glycerol (60 $\frac{w}{V}$%) yielding a final concentration of 30 $\frac{w}{V}$%. Finally, RosB was concentrated with a Vivaspin 6 column with a molecular weight cut-off (MWCO) of 10 kDa (Sartorius, Göttingen) at 10 °C and 6,000 rpm.

Affinity-HIC-SEC RosB purification

The affinity purification was performed using a HisTrap™ HP 5 mL column at a flow rate of 2 $\frac{mL}{min}$. The buffers A and B are summarized in Table 3. The bound protein was washed with buffer A until the UV signal had reached its initial intensity. Impurities were eluted with 20 %B. This level was hold no longer than 5 CV, because RosB could leach off the column with time. The elution of high AFP charged RosB was initiated with 35 %B and hold for 15-20 CV. Then, a gradient of 1.6 $\frac{\%B}{min}$ was used to elute low AFP charged RosB. The eluted RosB was treated with 35 $\frac{V}{V}$% 2 M ammonium sulfate solution. Note that the ammonium sulfate solution was added dropwise to prevent any protein precipitation. Afterwards, the sample was loaded onto a HIC Phenyl 5 mL HP at a flow rate of 2 $\frac{mL}{min}$. The used buffers for the HIC purification are summarized in Table 4.

Table 4: The binding buffer A and elution buffer B for the hydrophobic interaction purification are shown.

binding buffer A		elution buffer B	
component	**concentration [mM]**	**component**	**concentration [mM]**
BTP	50	**BTP**	50
$(NH_4)_2SO_4$	1,000	**$(NH_4)_2SO_4$**	0
pH	8	**pH**	8

The bound protein was washed for 10 CV with 0 %B and protein elution was initiated with a 6.67 $\frac{\%B}{min}$ gradient. The second half of the protein signal was pooled and concentrated with a Vivaspin 6 column with a MWCO of 10 kDa (Sartorius, Göttingen) at 10 °C and 6,000 rpm. The concentrated sample was loaded onto a 16/600 Superdex 200 at a flow rate of 1 $\frac{mL}{min}$. The buffer for the SEC purification was 50 mM Bis-tris-propane (BTP) (pH=8) and 300 mM KCl. Only the first half of the elute signal was collected and treated with glycerol 60 $\frac{w}{V}$% yielding a final concentration of 30 $\frac{w}{V}$%. Finally, RosB was concentrated with a Vivaspin 6 column with a MWCO of 10 kDa (Sartorius, Göttingen) at 10 °C and 6,000 rpm.

Affinity-Dialysis-AEX RosB purification

The affinity purification was performed using a HisTrap™ HP 5 mL column at a flow rate of 2 $\frac{mL}{min}$. The buffer A and B compositions are listed in Table 5:

Table 5: The binding buffer A and elution buffer B for the affinity purification are shown. If seleno-methionine labelled RosB was purified 2 mM 1,4-dithio-D-threitol (DTT) was added in each buffer.

binding buffer A		elution buffer B	
component	**concentration [mM]**	**component**	**concentration [mM]**
K_2HPO_4	16.4	**K_2HPO_4**	16.4
KH_2PO_4	3.6	**KH_2PO_4**	3.6
KCl	300	**KCl**	300
imidazole	10	**imidazole**	500
pH	8	**pH**	8

The bound protein was washed with buffer A until the UV signal had reached its initial intensity. Impurities were eluted with 20 %B. This level was hold no longer than 5 CV, because RosB could leach off the column with longer time. The elution of RosB was initiated with a gradient of 2 $\frac{\%B}{min}$. The collected RosB was transferred into a dialysis tube with a MWCO 8-12 kDa. The tube was placed in 1 L AEX binding buffer A and gently stirred at 4 °C. The conductivity was checked every 30 minutes until a constant value was reached. This step was

repeated 1-2 times until the initial conductivity value did not alter. The dialyzed sample was loaded onto a Fractogel TMAE M 5 mL column (Merck, Darmstadt) at a flow rate of 1 $\frac{mL}{min}$. Buffer A and B are summarized in Table 6:

Table 6: The binding buffer A and elution buffer B for the anion exchange purification are shown. If seleno-methionine labelled RosB was purified 2 mM DTT was added to each buffer.

binding buffer A		**elution buffer B**	
component	**concentration [mM]**	**component**	**concentration [mM]**
K_2HPO_4	8.2	**K_2HPO_4**	8.2
KH_2PO_4	1.8	**KH_2PO_4**	1.8
KCl	4	**KCl**	1,000
pH	7.7	**pH**	6.5

The bound protein was washed with 10-15 CV binding buffer and then eluted with 100 %B. The eluted RosB was treated with glycerol 60 $\frac{w}{V}$% yielding a final concentration of 30 $\frac{w}{V}$%. Finally, RosB was concentrated with a Vivaspin 6 column with a MWCO of 10 kDa (Sartorius, Göttingen) at 10 °C and 6,000 rpm. Note that DTT is crucial for seleno-methionine labelled RosB and was added in every buffer, in order to prevent metal oxidation.

2.6.6. HOOC-RP preparation from HOOC-RF and human Flavokinase

Flavokinase assays were performed in 50 mM PBS (pH=7.5), containing 0.3 mM flavin, 1 mM ATP, 6 mM NaF, 12 mM $MgCl_2$ and 24 mM sodium dithionite ($Na_2S_2O_4$). The mixture was pre-incubated at 37 °C for 5 minutes and then fused with the enzyme followed by an incubation time of 48 h. The reaction was stopped with 10 $\frac{V}{V}$% TCA and chilled on ice for 5 min. Afterwards, it was centrifuged at 7,500 rpm and 4 °C for 10 min. The supernatant was filtered with a 0.2 μm cellulose acetate filter and diluted until a total ion concentration of <0.1 M was reached (app. 1:100). The dilution was loaded under vacuum on a strong anion exchanger gravity flow 1 mL column from Sigma-Aldrich GmbH (Taufkirchen, Germany). The bound flavin was washed with 3 mL H_2O and eluted with 0.5 M PBS (pH=8). The eluted flavin was analysed via HPLC-MS Method – Kinetex Biphenyl column and stored at -20 °C.

2.6.7. Preparation of protein-free crude extract of *S. davawensis.*

S. davawensis was incubated in 5x100 mL M9 medium for several days (until visual confirmation of RoF production) at 30 °C and 150 rpm. To achieve a homogenous mycelia

size the cultures were inoculated from a pre-culture which had been incubated for three days. The cultures were centrifuged at 6,000 rpm for 3 minutes at 4 °C and washed three times with 50 mM PBS (pH=7.5). Afterwards the cell pellet was frozen at -20 °C. The frozen cell pellet was mortared in order to further homogenize and to reduce mycelia size. The cell paste was taken up in 10-30 mL 50 mM PBS (pH=7.5) and the cell wall disrupted with a Constant Cell Disruption System (Constant System, Daventry, UK) with sequential increase of the pressure by 400 bar, 800 bar, 1400 bar and 2,000 bar. Notice that the last pressure step had to be done at least twice. The crude extract was transferred into a round-bottom flask and shock-frozen in liquid nitrogen. Afterwards, the frozen crude extract was lyophilized to dryness with a Lyovac-GT2 (Leybold-Heraeus, Köln) for several days under high vacuum. Be aware that the crude extract has to be solid at any time and protected from light. The dry powder was taken up in a minimum amount of distilled water and centrifuged with Vivaspin columns (Sartorius, Göttingen DE) with MWCOs of 50 kDa, 30 kDa, 10 kDa, and 3 kDa, starting with the highest MWCO, collecting the flow-through and transferring it to the Vivaspin column with the smaller MWCO. The centrifuge steps were done at 10 °C with the highest possible rpm, suggested by the supplier. Finally, the flow-through of the 3 kDa Vivaspin column was collected and stored at -20 °C until usage.

2.7. Protein crystallization

2.7.1. X-ray structure determination[45]

The X-ray structure determination was done by our collaboration partners at the Max-Planck-Institute in Frankfurt.

The AFP loaded RosB complex was crystallized via vapour diffusion methods using the CrystalMation robotic system (Rigaku Europe, Kent, UK) and commercially available crystallization kits. Crystallographic data were gathered at the PXII beamline of the Swiss Light Source (SLS, Villigen, Switzerland) and processed with XDS. The SeMet-RosB multi wavelength anomalous dispersion experiment was done using Se K-Edge (0.9795 Å). Heavy atom sites were localized performing SHELXD and phases were subsequently determined by SHARP. Furthermore, the phases were improved by two-fold in average using DM. The majority of the model was automatically constructed using Buccaneer; the more flexible regions were built within COOT. This preliminary model was the base searching model for the search for AFP-RosB dataset based on a better diffracting crystal form. Molecular replacement (MR) was performed using Phaser-MR followed by a refinement step using Refmac5 including

non-crystallographic symmetry options. Afterwards, the model was manually corrected within COOT. The HOC-RP-RosB structure was determined by MR using the RosB-AFP structure as search model and Phaser-MR for calculation. The structure was refined using Refmac5 and manually evaluated by COOT. Structural data are available in the Protein Data Bank under accession number 4D7K. The best crystallization set-ups for the best diffracting crystals are given in Table 7.

Table 7: The crystallographic data of RosB crystals are summarized.

	RosB SeMet[a]	**RosB-AFP**[b]	**RosB-OCH-RP**[c]
crystallization conditions			
	0.3 M sodium formate, 0.2 M NDSB[d]-211, 19 % (v/v) PEG[e] 3350	0.3 M sodium formate, 0.1 M potassium chloride, 17 % (v/v) PEG 3350	0.3 M sodium formate, 25 % (v/v) Silver Bullet 49, 17 % (v/v) PEG 3350
data collection			
space group	*P* 2 2 2	*C* 2	*I* 4 2 2
wavelength [Å]	0.9795	1.,0000	1.,0000
resolution range [Å]	50.0-2.5 (2.6-2.5)	50.0-1.7 (1.8-1.7)	50.0-2.0 (2.1-2.0)
unit cell *a*; *b; c* [Å]	68.8; 113.4; 256.3	131.5; 71.1; 214.8	108.5; 108.5; 178.2
redundancy	4.9 (5.4)	10.6 (5.5)	10.7 (11.3)
completeness [%]	99.7 (99.6)	92.9 (70.8)	99.9 (99.9)
R_{sym} **[%]**	13.5 (86.1)	10.6 (103.3)	10.3 (212.5)
$I/\sigma(I)$	11.3 (2.28)	15.36 (1.96)	15.5 (1.3)
$CC_{1/2}$	99.5 (79.3)	99.8 (72.0)	99.9 (74.1)
refinement statistics			
Mol. asym. unit		8	1
No. residues, cofactors, water molecules		2016, 8, 2129	252, 1, 217
$R_{working}$, R_{free} **(%)**		17.6, 21.05	17.52, 19.51
$B_{average}$ **(Å²) polypeptide, cofactor water**		24.4, 19.5, 42.3	45.9, 38.3, 58.5
R.m.s. deviation bond lengths (Å), bond angles (°)		0.018, 1.93	0.011, 1.25
Ramachandran Plot favored, outliers (%)		97.4, 0.3	98.4, 0.4

2.8. Enzyme assay

2.8.1. RosB assay

Several different RosB assays were employed during this work and were improved with regard to enzyme activity. The following protocol provides a detailed description of the assay. Notably, all incubation steps were performed in a Thermomixer Comfort (Eppendorf, Germany), unless mentioned differently.

RosB protocol

All solutions were prepared on ice. Note that flavin containing solutions had to be kept in brown tubes, to prevent light-induced degradation and that each assay component was prepared as 10x stock solution which was stored at -20 °C. A master mix of 100 μM RP, 20 μM $CaCl_2$, 100 mM bis-tris-propane (BTP) (pH=8.8), 10 mM thiamine, 5 mM and glutamic acid were freshly prepared on ice, aliquoted and 39 μM RosB added to each aliquot. Each prepared batch was 100 μL in total volume; it was slightly tapped and centrifuged for a few seconds. The experiments were performed at 39 °C. The reactions were stopped with the addition of acid as described in chapter 2.6.4.

Oxygen dependency assay protocol

The oxygen depending assay refers to the aerobic/anaerobic test which investigated the participation of oxygen in each single oxidation step of RP. It consisted of three time steps; an oxic incubation step, a resting step on ice to remove oxygen and an anoxic step. The master-mix of the first step is summarized in Table 8.

Table 8: The recipe for the oxic step stopping at HOC-RP, HOOC-RP and AFP is illustrated. The negative control contained equal amounts of water instead of protein solution. The concentrations refer to a total volume of 150 µL with a pH=8.

reaction until HOC-RP		reaction until HOOC-RP		reaction until AFP	
component	**concentration [µM]**	**component**	**concentration [µM]**	**component**	**concentration [µM]**
RosB	/	**RosB**	190	**RosB**	190
BTP	100.,000	**BTP**	100.,000	**BTP**	100.,000
$CaCl_2$	20	**$CaCl_2$**	20	**$CaCl_2$**	20
RP	266	**RP**	266	**RP**	266
thiamine	/	**thiamine**	/	**thiamine**	666
glutamic acid	/	**glutamic acid**	/	**glutamic acid**	/

In the oxic step the assay was allowed to react until the pre-intermediate of the oxidation step which was analysed. In the case of HOC-RP the substrate was incubated without any RosB, in the case of HOOC-RP the reaction could precede until HOC-RP and in the case of AFP the reaction proceeded until HOOC-RP. The aerobic incubation was done at 39 °C for 2 hours. Afterwards, the assays were transferred into a nitrogen tent and incubated on ice with an open lid for three hours (second step). Simultaneously, the supplement mix was prepared on ice and also incubated with an open lid for three hours. The supplement mix and assay were fused and incubated anoxic for another 3 h at 39 °C (third step). The supplement mix is summarized in Table 9.

Table 9: The recipe for the supplement mix is summarized for the oxidation step stopping at HOC-RP, HOOC-RP and AFP. The supplement mix volume was 25 µL for each experiment which yielded a total volume of 175 µL for each experiment. Note that the negative controls were supplied with water instead of protein solution. The concentrations refer to a total volume of 150 µL.

reaction until HOC-RP		**reaction until HOOC-RP**		**reaction until AFP**	
component	**concentration [µM]**	**component**	**concentration [µM]**	**component**	**concentration [µM]**
RosB	290	**RosB**	additional 100	**RosB**	additional 100
thiamine	/	**thiamine**	666	**thiamine**	/
glutamic acid	/	**glutamic acid**	/	**glutamic acid**	333

The reaction until HOOC-RP and AFP received additional fresh RosB (see table) in order to neglect possible inactive RosB generated by the temperature changes. Each reaction was stopped with 10 $\frac{V}{V}$% acid as described in chapter 2.6.4.

$^{18}O_2$ assay protocol

A master mix of 100 μM RP, 20 μM $CaCl_2$ and 10 mM thiamine in BTP buffered solution (pH=8.8) was prepared and flushed with gas for 15 min (1 bubble per second). Afterwards, the mix was centrifuged, aliquoted and 39 μM RosB were added. The assay was incubated for 90 min at 39 °C.

Dihydroresorufin assay protocol

Resorufin is a highly sensitive fluorescence (Abs=571 nm, Em=585 nm) which is formed by the selective reaction of Dihydresorufin (AmplexRed) with hydrogen peroxide and horse radish peroxidase as catalyst.

A master mix of 100 μM RP, 20 μM $CaCl_2$ and 100 mM bis-tris-propane (BTP) (pH=7), was freshly prepared on ice, aliquoted and 39 μM RosB were added to each aliquot. The assay was incubated for 12 h at 39 °C in a total volume of 100 μL. The RosB assay had to be pre-incubated, because the dihydroresorufin interferes with the RosB reaction. 50 μL of the RosB assay was mixed with 50 μL hydrogen peroxide detection mix containing 2 units horse radish peroxidase and 50 μM dihydroresorufin (total concentration). The combined assay was further incubated for 30 min at RT. The reaction was stopped with 10 $\frac{V}{V}$% acid as described in chapter 2.6.4.

A positive control was performed with the hydrogen peroxide detection mix by adding 1 mM hydrogen peroxide. Note that the positive control turned immediately red. Figure 6 shows dihydroresorufin (black chromatogram) and the oxidized resorufin (red chromatogram).

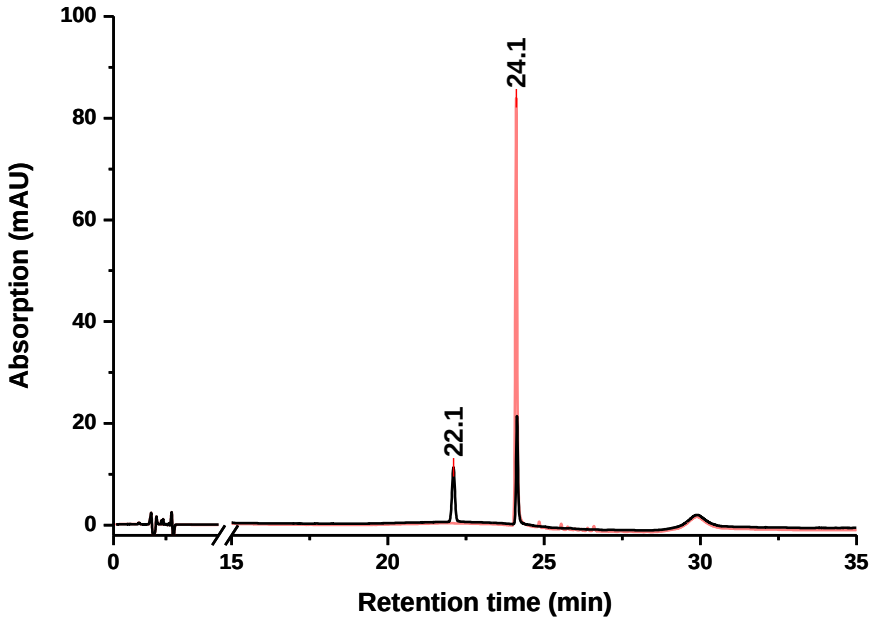

Figure 6: The UV-VIS chromatogram of Dihydroresorufin (black chromatogram) and hydroresorufin (red chromatogram) is shown. 10 µM Dihydroresorufin is immediately oxidized on ice in the presence of 1 mM hydrogen peroxide and two units horse radish peroxidase. The signal at 22.1 min is only present in the reduced dihydroresorufin.

3. Results

3.1. HPLC method development for the analysis of phosphorylated flavin derivatives

To have a high resolution for all possible RP oxidation states, a new HPLC method had to be developed. Besides that, the used RP is chemically synthesized. More precisely, the phosphorylation does not happen selectively at the terminal hydroxyl group of the ribityl residue. The intensity distribution of the RP isomers is dictated by the steric accessibility of the targeted alcohol residue. A more accessible alcohol residue has a higher yield than a less one (3'<4'<5' with regard to signal intensity).

The chromatogram (480 nm) of the initial HPLC method measured on the Reprosil C18 column (5 μm, 10x2 mm) is depicted in Figure 7 top lane.

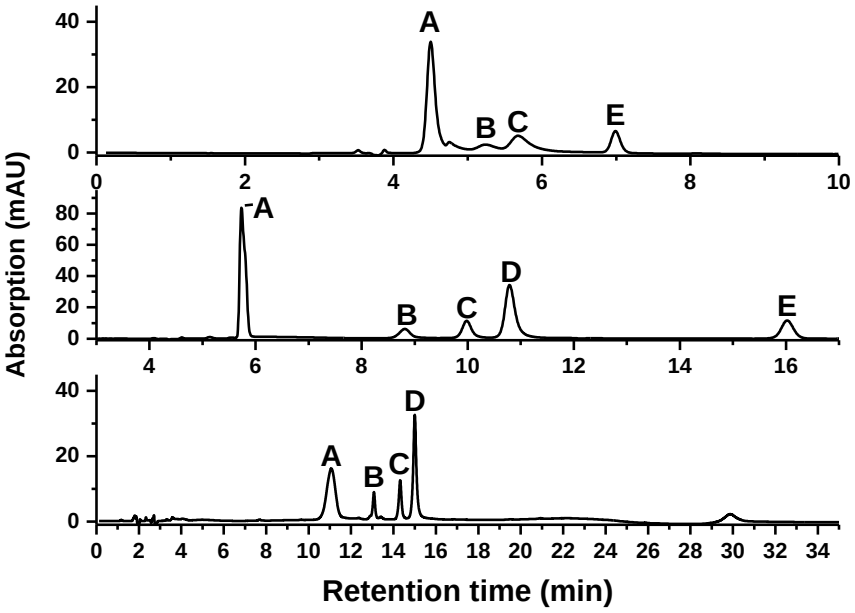

Figure 7: Separation of the flavins depending on the used method is shown (measured at 480 nm). A RosB assay was performed with 100 µM RP and 39 µM RosB in phosphate buffered solution (pH = 8.0) for 2 hours at 30 °C. The assay was stopped and analysed via HPLC as described in chapter 2.6.4. Top panel: Initial Method - Reprosil C18 column, Mid panel: Method - Reprosil C18 column, Bottom panel: Method – Kinetex Biphenyl column. The biphenyl column has the highest peak resolution with a run-time of 35 min and the C18 column with the improved method a moderate resolution with a run-time of 17 min. The C_{18} column with the initial method shows an insufficient RP isomer separation and a run-time of 10 min. Peak assignment: A = HOC-RP, B,C and D = RP isomers, E = RF.

The HOC-RP signal (A) and two RP isomers (B and C) can be observed, although with a strong tailing and poor peak resolution. Consequently, the gradient profile was altered until a sufficient resolution was obtained. The improved results are illustrated in Figure 7, centred lane. Indeed, the RP signal split into three signals with a moderate resolution and the run-

time was 17 min. The signals can be assigned to HOC-RP (A), riboflavin-3'- (B), riboflavin-4'- (C) and riboflavin-5'-phosphate (D). The AFP signal overlaps with the HOC-RP peak and HOOC-RP elutes within the dead volume (see Figure 22). To meet the need of a high resolution for phosphorylated and non-phosphorylated flavins the Phenomenex Kinetex Biphenyl (2.6 μm 150x2.1 mm) column was tested and the gradient profile developed. Figure 7 bottom panel illustrates the results. The signals show a high resolution with a run-time of 35 min. The signals can be assigned to HOC-RP (A), riboflavin-3'- (B), riboflavin-4'- (C) and riboflavin-5'-phosphat (D). The RF signal (E) is an impurity, which can occur during light exposure of the RP stock solution (de-phosphorylation of RP).

Above that, the MS data shows better signal-noise ratios compared to the measurements with the C_{18} column (see Figure 8). Notice, the lower background of 50,000 hits compared to 200,000 hits and the well resolved signals.

To sum up, the higher resolution and lower MS background united in one column met the crucial needs for future studies. Since the improvement of the resolution had been a continuous progress, measurements with the C_{18} column and biphenyl column are presented in this work.

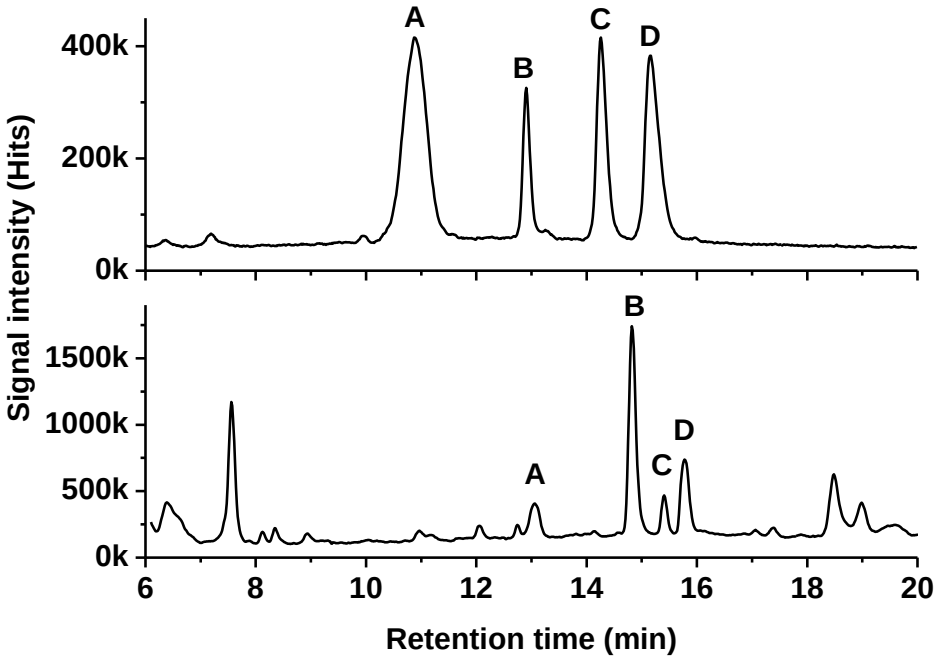

Figure 8: The MS measurement of a RosB assay with 100 µM RP in 100 mM BTP solution (pH = 8.8) at 30 °C and 2 h is shown. Top panel: Measurement on a Kinetex Biphenyl column. Bottom panel: measurement on a Reprosil C_{18} column. The bottom measurement shows more background signals and a lower signal-to-noise ratio. A = HOC-RP, B = riboflavin-3'-phosphate, C = riboflavin-4'-phosphate and D = riboflavin-5'-phosphate.

3.2. RosB properties

RosB catalyses a challenging reaction; therefore a summary of all physical parameters was gathered as a starting point of the RosB evaluation.

RosB is composed of 257 amino acids and has a molecular weight of 28.86 $\frac{kg}{mol}$. An ExPASy calculation revealed a theoretical IEP of 5.24 (Note: RosB-His_6 M_w= 29.93 $\frac{kg}{mol}$, IEP = 5.61). Previous work identified a tetrameric oligomer.[17] It is stable in various buffers, such as phosphate, tri-ethanol amine and 1,3-bis(tris(hydroxymethyl)methylamino)propane (BTP), whereas it is not active in tris(hydroxymethyl)aminomethane (Tris). To simplify matters, in this work RosB His_6 is abbreviated to RosB, if not mentioned differently. It is not active under reductive condition (data not shown). Long-term storage revealed that RosB sustains activity and does not precipitate even after six months. Besides that, RosB has a total activity of 0.44 $\frac{nmol}{min \times mg(Protein)} \pm 0.01$ (n=6) and an estimated Km for RP of $<20\,\mu$m (data not shown).

3.2.1. Analysis of co-eluted cofactors bound to RosB-His_6

Flavodoxins bind flavins mostly as a prosthetic group; therefore these proteins are often isolated yellow colored. However, RosB is orange colored indicating a different kind of flavin bound to it (see Figure 9 top right). This demanded a HPLC analysis of the co-eluted cofactors.

RosB was overexpressed in *E. coli* employing a strong bacteriophage T7 promoter (30% of the total protein was RosB) (see chapter 2.4.7). Interestingly, even the cells are orange colored compared to non-induced expression ones (see Figure 9 bottom right), which indicates an oxidized state of the bound flavin *in vivo*. This effect is even clearer when grown on M9 minimal medium. After IPTG supplementation the shaking culture turns orange, which is originated by the cells and not the supernatant (data not shown). UV-VIS analysis of RosB revealed a similar absorption spectrum as free AFP, although it is shifted to higher wavelengths compared to AFP (λ=499 nm).

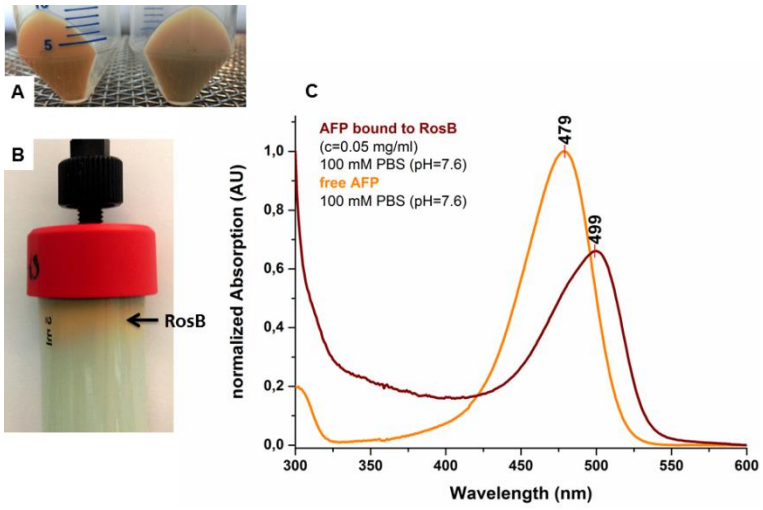

Figure 9: Production and purification of RosB in *E. coli* and UV-VIS comparison of AFP bound to RosB and free AFP. A: left cell pellet= *E.coli* production strain supplemented with IPTG⁺ and washed with PBS. Right cell pellet= *E.coli* production strain without IPTG⁺ but washing with PBS. The cells supplemented with IPTG⁺ appear orange. B: A picture of orange RosB-His_6 bound to a Ni-NTA column (Hi-Trap 5 mL, GE Healthcare) is shown. Bound RosB is highlighted with a black arrow. C: UV-VIS spectrum of RosB overexpressed in *E.coli* Rosetta DE3 (darkbrown) in comparison with 2 µM free AFP (orange) is shown. RosB has an absorption maximum at 499 nm and AFP 479 nm.

RosB was concentrated with a 10k Vivaspin column and precipitated with 10 $\frac{w}{v}$% formic acid while the co-eluted flavins remained in the supernatant. The supernatant was analysed via HPLC (see chapter 2.6.4, Phenomenex).

Figure 10 shows the chromatogram measured at 480 nm (top) and the MS analysis (bottom).

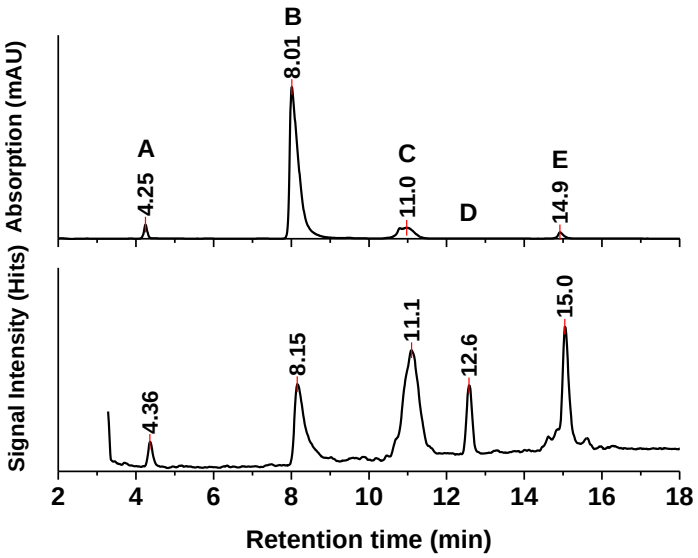

Figure 10: The supernatant of precipitated RosB was analysed via HPLC (see chapter 2.6.5, Kinetex column, 40 µL injection volume. The co-eluted flavins were detected by high performance liquid chromatography coupled to a diode array detector (DAD) and an ESI-Single Quadrupole MS (HPLC/MS). The UV-VIS chromatogram measured at 480 nm (top) and the MS measurement (bottom) are shown. A = HOOC-RP, B = AFP, C = HOC-RP, D = unknown compound and E = RP.

The data revealed four compounds with UV-VIS spectra comparable to flavins (A, B, C and E) and a non-absorbing compound (D). The UV-VIS spectra and MS ones are summarized in Figure 11.

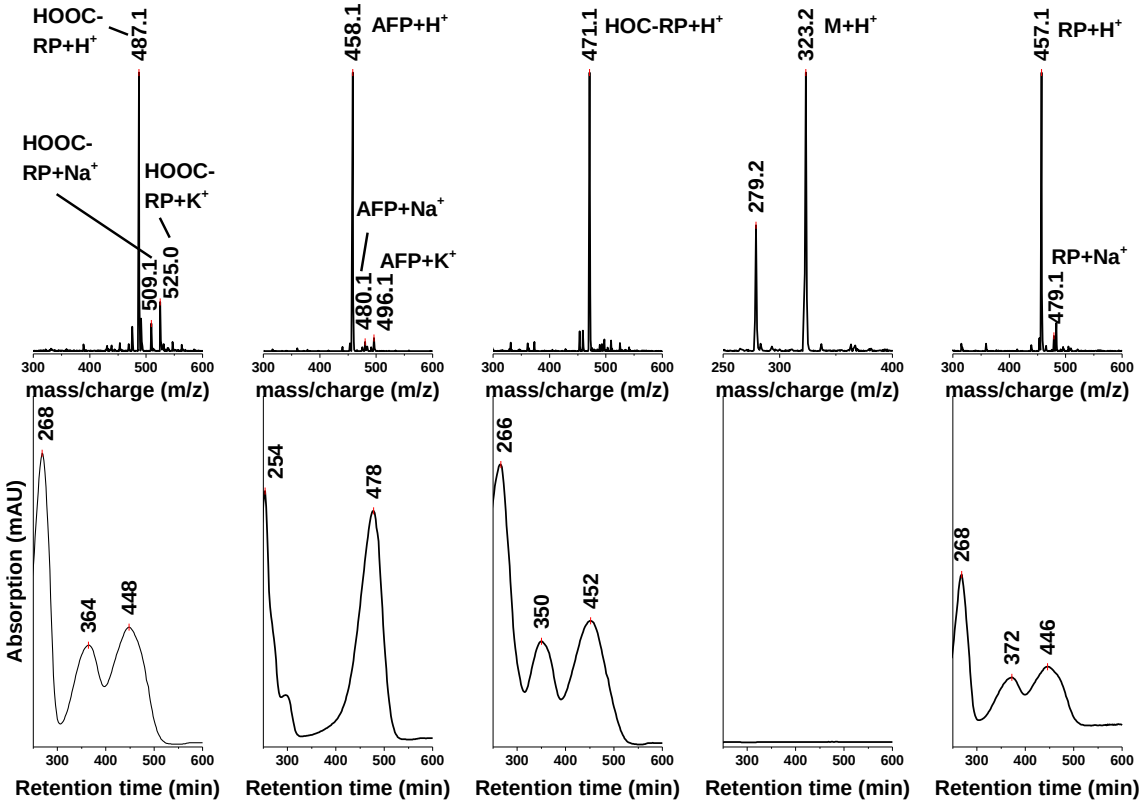

Figure 11: The MS spectra (top) and the UV-VIS spectra (bottom) of the co-eluted RosB flavins are shown. The spectra were extracted with the Chemstation software from the HPLC analysis of Figure 10. From left to right: 1st column: A = HOOC-RP with M+H= 487.1 mz, 2nd column: B = AFP with M+H=458 $\frac{m}{z}$, 3rd column: C = HOC-RP with M+H=471.1 $\frac{m}{z}$, 4th column: D = unknown compound with M+H = 323.2 $\frac{m}{z}$, 5th column: E = RP with M+H = 457.1 $\frac{m}{z}$. The y-axes are concentration independent and do not represent any relationship between the found compounds.

Compound A has a M+H value of 487.1 $\frac{m}{z}$ with absorption maxima of 268 nm, 364 nm and 448 nm. Additionally, the M+Na and M+K signals were identified with $\frac{m}{z}$ values of 509.1 and 525.0, respectively. Compound B has a M+H value of 458.1 $\frac{m}{z}$ with absorption maxima of 254 nm and 478 nm. Furthermore, the M+Na and M+K signals were identified with $\frac{m}{z}$ values of 480.1 and 496.1. Compound C has a M+H value of 471.1 $\frac{m}{z}$ and absorption maxima of 266 nm, 350 nm and 452 nm. Compound D has $\frac{m}{z}$ values of 323.2 $\frac{m}{z}$ and/or 279.2 $\frac{m}{z}$. Besides that, no UV-VIS absorption could be measured. Compound E has M+H and M+Na $\frac{m}{z}$ values of 457.1 and 479.1. The absorption maxima are 268 nm, 372 nm and 446 nm. Comparing the

retention times, $\frac{m}{z}$ values and UV-VIS spectra with standards, we can identify HOOC-RP (compound A), AFP (compound B), HOC-RP (compound C) and RP (compound E) (see Figure 24 in chapter 3.4. for detailed standard data).

3.2.2. Optimization of assay conditions: time, pH, temperature and salts

RosB stops the oxidation of RP at HOC-RP indicating a lack of missing cofactors. To save time and protein quantities, the assay conditions were optimized.

Firstly, the activity had to be determined. For this, triplicates of a 1.5 mL reaction volume were prepared and samples taken at different time points. Figure 12 shows the collected data. RosB activity behaves linear even after 500 min with a conversion of roughly 30 %. The linear manner drops after 1,500 min and seems to converge after 3,000 min at 70 %.

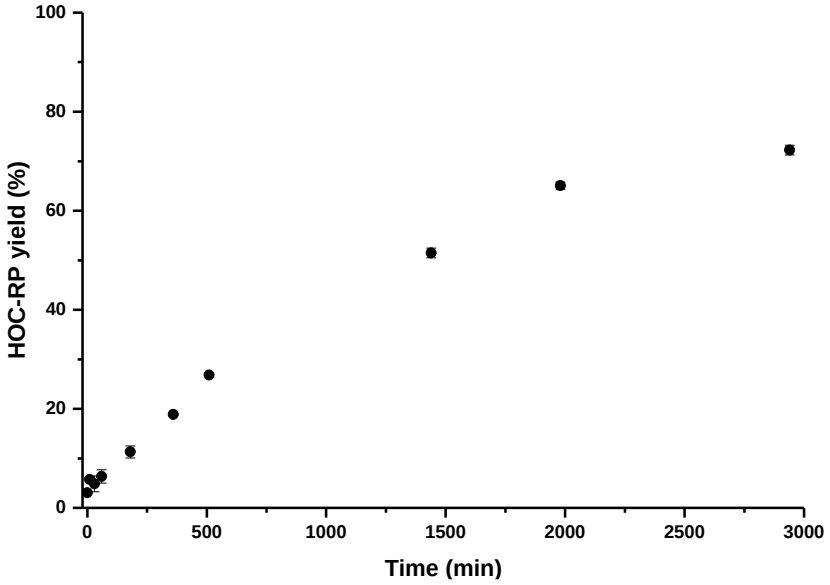

Figure 12: The RosB assay with 100 µM RP in 100 mM phosphate buffered solution (pH = 7.4) at 30 °C was performed. 100 µL samples were taken at certain time points, precipitated and measured via HPLC. The conversion of RP was normalized against a triplicate with t= 0 min. The shown HOC-RP yields are the sum of triplicates with standard deviations.

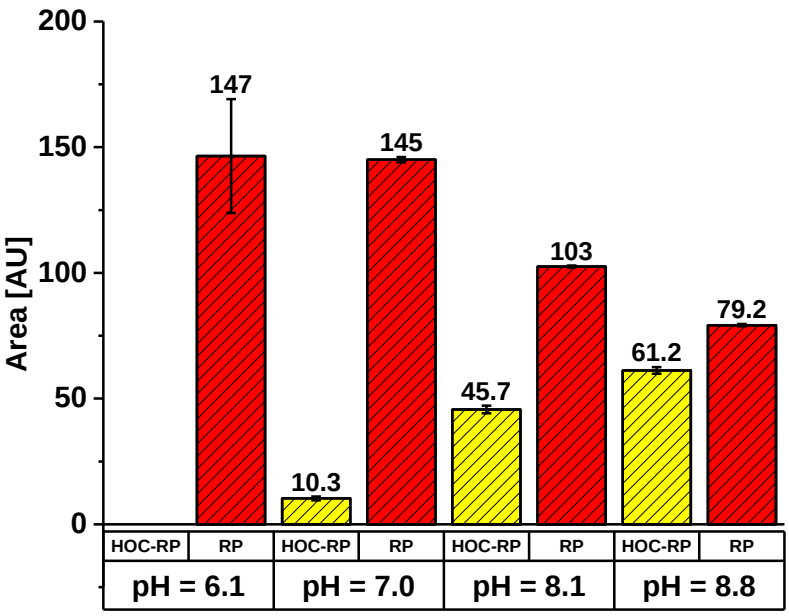

Figure 13: The RosB assay with 100 µM RP in BTP buffer was performed at pH = 6.1, 7.0, 8.1 and 8.8 for 2 hours at 30 °C. The samples were measured as triplicates and analysed via HPLC (see chapter 2.6.5, Kinetex column, 2 µL injection volume). The data suggests a pH optimum >8.8. The shown areas are the peak areas recorded at 480 nm and depicted as the sum of a triplicate with the standard deviation.

Secondly, the buffer pH had to be optimized. Figure 13 shows the summarized triplicates of the experiment. Under acid conditions, no activity was observed, whereas at pH=7.0 activity could be detected. The HOC-RP peak area increased with increased pH from 10.3 to 45.7 and 61.2 AU, respectively. Unfortunately it was not possible to determine the pH optimum, because flavins started to dephosphorylate with pH >9 (data not shown).

Thirdly, the optimum assay temperature was determined as well. Figure 14 illustrates the experiment in triplicates. The HOC-RP peak areas were 144 AU (10 °C), 259 AU (20 °C), 323 AU (30 °C), 458 AU (39 °C) and 354 AU (50 °C). Surprisingly, the data suggests a temperature optimum of 39 °C and not of 50 °C as described previously.[17]

Additionally, bivalent metal chlorides were tested. Co^{2+}, Fe^{2+}, Mg^{2+}, Ca^{2+}, Cu^{2+} and Zn^{2+} chloride salts were added with a final concentration of 20 μM and incubated as described above. Only calcium showed a positive effect on the HOC-RP yield, therefore all following RosB assays were supplemented with 20 μM $CaCl_2$. The results suggest to perform the experiments at 39 °C, pH = 8.8 and t = 2-3 hrs and 20 μM $CaCl_2$.

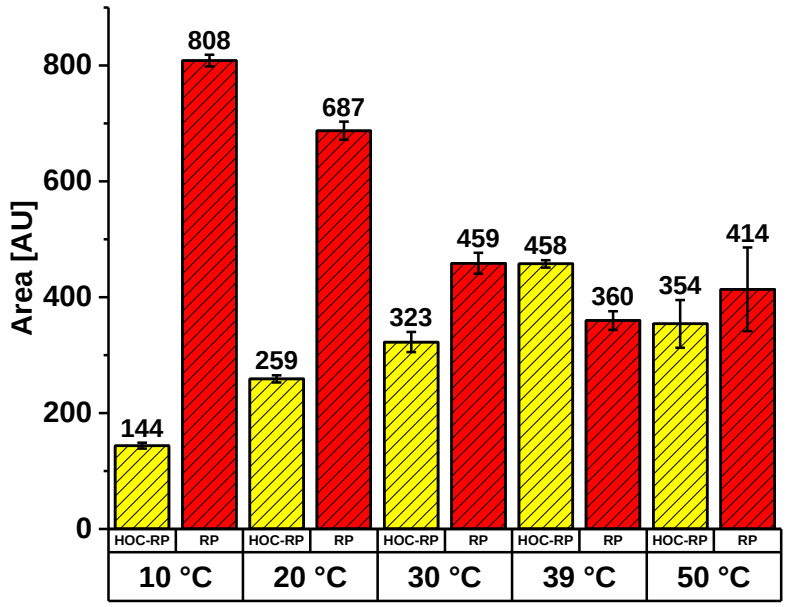

Figure 14: The RosB assay with 100 µM RP in 100 mM BTP solution (pH = 8.8) was performed at 10 °C, 20 °C, 30 °C, 39 °C and 50 °C for 2 hours. The samples were measured as triplicates and analysed via HPLC (see chapter 2.6.5, Kinetex column, 10 µL injection volume). The data suggests a temperature optimum at 39 °C. The shown areas are the peak areas recorded at 480 nm and depicted as the sum of a triplicate with the standard deviation.

3.3. Development of RosB purification protocols

As shown before, RosB is purified with five different co-eluted compounds. This heterogeneous protein makes it difficult to get reproducible data, especially concerning protein crystallization experiments. For this reason, the protein purification protocol was analysed regarding to AFP binding in relation to RosB concentration and elution time (chapter 3.3.1). Furthermore, several purification protocols were developed depending on the purpose.

Firstly, the "High AFP amount RosB purification protocol" is the fastest one and has a high AFP charge. It was the initial protocol and yields up to 100 $\frac{mg}{L}$ RosB. Secondly, the "Low AFP amount RosB purification protocol" yields up to 15 $\frac{mg}{L}$ highly pure RosB with an AFP molar charge less than <5 %. This protocol was necessary to increase the number of empty binding pockets, which are necessary for RosB catalysis. Thirdly, the protocol for the seleno-methionine labelled RosB yielded up to 100 $\frac{mg}{L}$ RosB with a high AFP charge. This protocol showed itself to be the best choice for protein crystallization, even for RosB without seleno-methionine labeling.

3.3.1. AFP amounts bound to RosB vary depending on the purification protocol

AFP co-elutes always as main fraction with RosB and the amount bound to it is heavily depending on the chosen column and setup. Therefore, the AFP charge is in general hardly reproducible and ranges between 40-80 % for the high AFP charge. To gain a better understanding the eluted RosB signal itself was fractionated in order to determine the protein and AFP distribution in relation to each other.

The RosB eluted signals were separated into fractions and concentrated with Vivaspin columns (cutoff: 10 kDa), if necessary. The protein concentration was determined via Bradford (see method section 2.6.3) and the flavin amount via HPLC as described in chapter Method – Kinetex Biphenyl column. Note that the AFP charge is expressed as molar percentage: $\frac{AFP\ mol}{RosB\ mol} \times 100$.

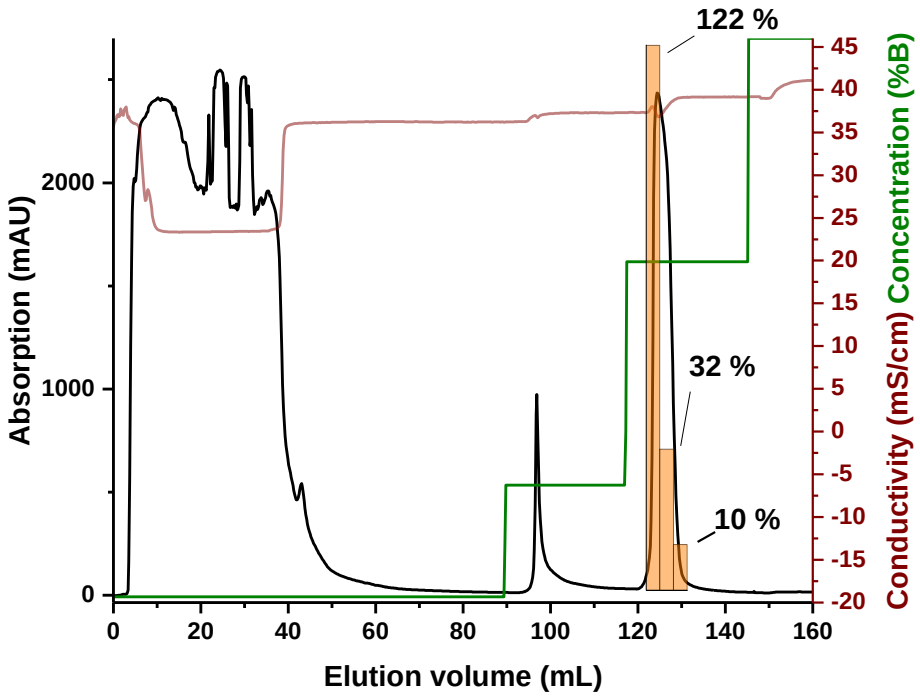

Figure 15: The elution profile of RosB on a Ni-NTA column correlated with the bound AFP amount is shown. Crude extract from an 1 L *E.coli* RosB-pET24a(+) culture was loaded onto a HisTrap™ HP 5 ml (GE Healthcare) with a flow rate of 2 $\frac{mL}{min}$. Impurities were eluted with 20 %B and highly AFP charged RosB (orange column containing signal) was eluted with 60 %B. RosB elution was split into three fractions. The protein concentrations were measured via Bradford. The AFP concentrations were measured via HPLC. Fraction one has 122 % AFP, fraction two 32 % AFP and fraction three 10 % AFP (orange columns).

Figure 15 shows the elution profile of RosB purified from an *E.coli* RosB-pET24a(+) crude extract. The Affinity column (HisTrap™ HP 5 mL) was operated at a flow rate of 2 $\frac{mL}{min}$. The

high initial UV-signal is caused by non-binding proteins, which are typically present in the crude extract. Non-specifically bound proteins were eluted with 20 %B, RosB was eluted with 60 %B and separated into three fractions (orange bar=fraction). It can be seen, that the first fraction contains a charge of 122 % AFP, the second fraction a charge of 32 % and the third one a charge of 10 %. This indicates, that RosB charged with high amounts of AFP eluted earlier than RosB with low AFP amounts. Figure 16 illustrates the elution profile of RosB run on a Phenyl HP 5 mL HIC.

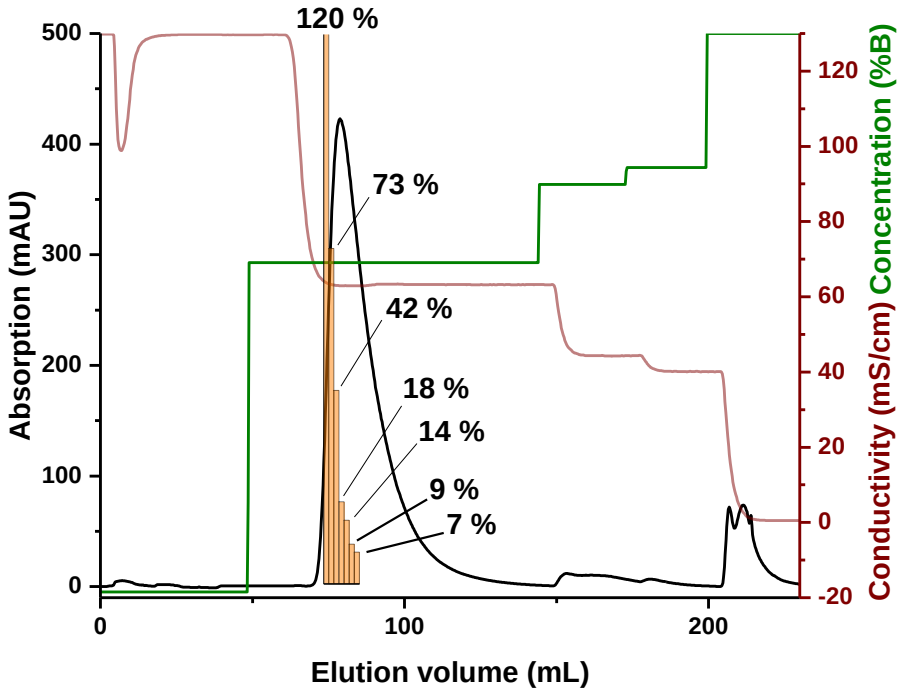

Figure 16: The elution profile of RosB on a HIC column correlated with the bound AFP amount is shown. The eluted AFP-rich RosB from the affinity purification step was loaded onto a Phenyl HP 5 mL HIC at a flow rate of 2 $\frac{mL}{min}$. RosB was washed with 10 CV 0 %B and eluted with 60 %B. RosB was separated into fractions. The protein concentration was measured via Bradford. The AFP concentration was measured via HPLC. Fraction one has 120 % AFP, fraction two 73 % AFP, fraction three 42 % AFP, fraction four 18 % AFP, fraction five 14 % AFP, fraction six 9 % AFP and fraction 7 % (orange columns). The remaining elution volume showed AFP concentration, which were less than the detection limit (<1 %).

The AFP-rich RosB fraction of the affinity purification was loaded at a flow rate of 2 $\frac{mL}{min}$. RosB was washed with 10 CV 0 %B and eluted with 60 %B. The eluted RosB was fractionated and analysed as mentioned above. As in the previous chromatography, the charges show a decrease with elution volume starting with 120 %, 73 %, 42 %, 18 %, 14 %, 9 % and ending with a charge of 7 % AFP. The following RosB fractions were not analysable, because the AFP concentrations were lower than the detection limit of the HPLC (<1 %).

Figure 17 depicts the elution profile of RosB run on a 16/600 Superdex 200 column. An AFP-rich RosB fraction from the HIC elution was loaded at a flow rate of 1 $\frac{mL}{min}$. RosB eluted at 110 mL and showed included a right shoulder.

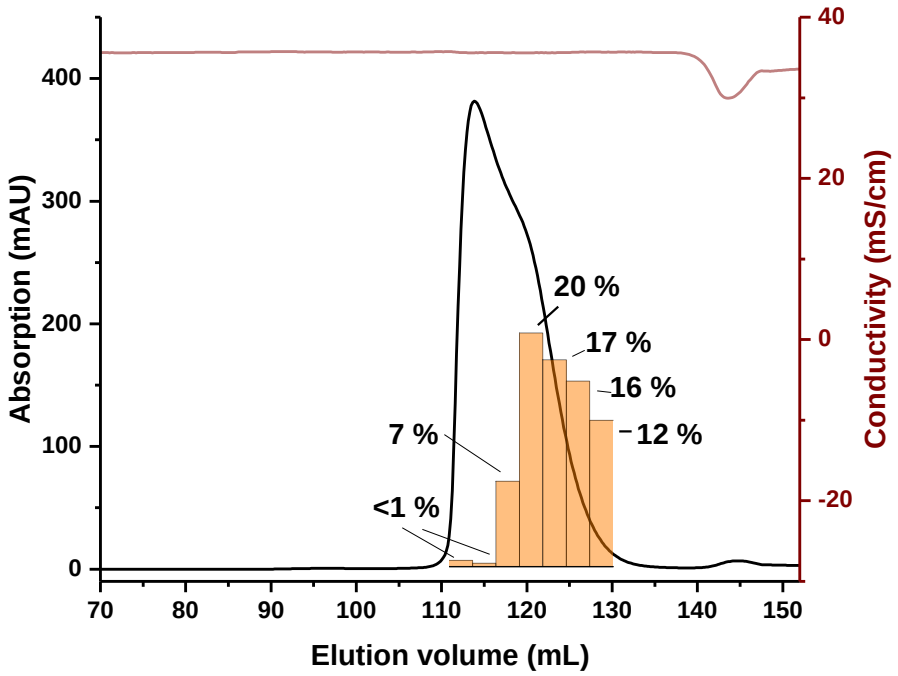

Figure 17: The elution profile of RosB on a Superdex increase column correlated with the bound AFP amount is shown. The eluted RosB from the HIC run was loaded onto a 16/600 Superdex 200 column at a flow rate of 1 $\frac{\mathrm{mL}}{\mathrm{min}}$. RosB eluted at 110 mL. It was separated into seven fractions. The protein concentration was measured via Bradford. The AFP concentration was measured via HPLC. Fraction one and two have <1 % AFP, fraction three has 7 % AFP, fraction four has 20 % AFP, fraction five has 17 % AFP, fraction six has 16 % AFP and fraction seven has 12 % AFP (orange columns).

Surprisingly, the fractions show a reversed picture compared to the other purification steps: The first two fractions contain an AFP charge of <1 %, followed by increasing AFP charges of 7 % and 20 %. Note that the highest AFP charge is aligned to the maximum of the right shoulder of the protein signal. Afterwards, the AFP decreases to 17 %, 16 % and 12 %.

In summary, all chromatographic steps show an inhomogeneous distribution of AFP within the protein signal. Columns which include an interaction between the beads and the protein (affinity column and HIC) let highly charged RosB elute earlier than lower charged RosB. When the protein size is the only separation parameter (SEC) highly charged RosB eluted later than lower charged one.

3.3.2. Low AFP amount purification protocol

The elution profiles of the purification are illustrated in Figure 18. In detail, the left chromatogram illustrates the first elution profile of the Affinity column (HisTrap™ HP 5 mL), the middle one depicts the second elution profile using a HIC (Phenyl HP 5mL) and the right chromatogram shows the elution profile with a SEC (16/600 Superdex 200) column.

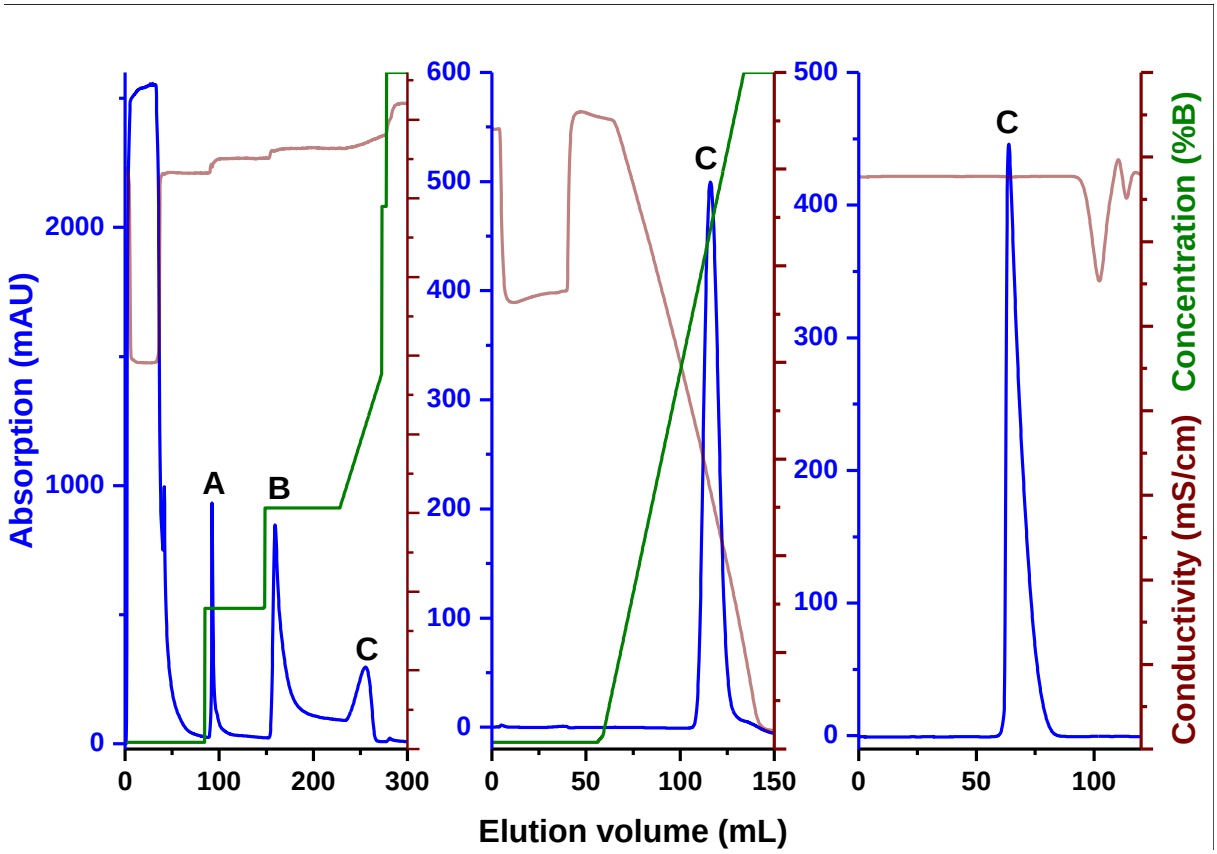

Figure 18: The elution profiles of low charged RosB is shown. Left: Crude extract from 1 L *E. coli* RosB-pET24a(+) culture was loaded onto a HisTrap™ HP 5 ml (GE Healthcare) with a flow rate of 2 $\frac{mL}{min}$. Impurities (Signal A) were eluted with 20 %B and highly AFP charged RosB (Signal B) was eluted with 35 %B. Low AFP charged RosB (Signal C) was eluted with a gradient of 1.6 $\frac{\%B}{min}$. Center: The eluted RosB (Signal C) from the affinity purification step was loaded onto a Phenyl HP 5 mL HIC with a flow rate of 2 $\frac{mL}{min}$. A wash step at 0 %B was held for 10-15 CV followed by a gradient of 1.6 $\frac{\%B}{min}$. RosB (Signal C) was split and only the 2nd half was pooled and used for the last step. Right: The eluted RosB (Signal C, 2nd half) was loaded onto a 16/600 Superdex 200 column with a flow rate of 1 $\frac{mL}{min}$. RosB eluted at roughly 80 mL (Signal C), though only the first half of the signal was pooled. Details are described in method: Affinity-HIC-SEC RosB purification.

RosB containing crude extract was prepared as described in chapter 2.4.7 and loaded onto the first column with a flow rate of 2 $\frac{mL}{min}$ (left chromatogram). The high UV signal is derived by non-binding proteins which are always present in the crude extract. When the UV signal reached the initial signal level, non-specifically bound impurities (Signal A) were eluted with

20 %B. After 5-10 CV, RosB with a high AFP charge (Signal B) was eluted with 35 %B. This step was held for 10-15 CV and replaced by a gradient of 1.6 $\frac{\%B}{min}$. Signal C contained almost colorless RosB, therefore only signal C was pooled and used for the 2nd step. RosB was loaded onto the HIC with a flow rate of 2 $\frac{mL}{min}$ (centered chromatogram). The bound protein was washed with 10-12 CV buffer A, in order to remove AFP from the protein. Afterwards, a gradient of 6.67 $\frac{\%B}{min}$ was applied to elute RosB (Signal C). Note that the signal was split into two halves and only the 2nd half was used for the third column. Finally, the SEC was operated with a flow rate of 1 $\frac{mL}{min}$ (right chromatogram). RosB elutes at roughly 80 mL, although the first half of the signal C was collected only and treated with glycerol.

The purity of RosB was analysed via SDS-PAGE (see Figure 19). The first column shows non-induced crude extract and the second one induced crude extract. A strong expressed RosB signal can be observed at 35 kDa. Column three shows the flow-through of the affinity column and indicates that RosB bound completely to the column. Moreover, column four shows the eluted RosB from the affinity step and column five the eluted RosB from the hydrophobic interaction one. Finally, column six illustrates the final RosB, which was eluted and pooled from the size exclusion step. Note that on column four and five show two bands around 70 kDa and one at 100 kDa. These bands are vanished in column 6.

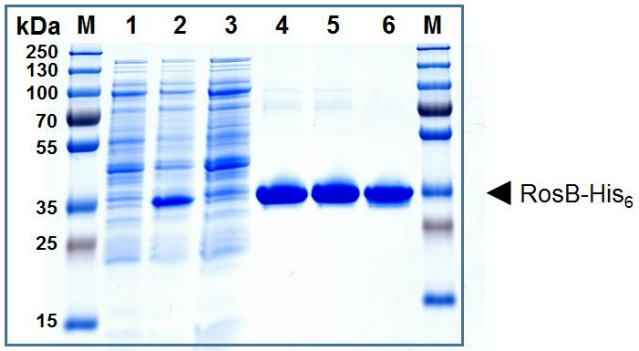

Figure 19: The Comassie stained SDS gel of the RosB purification is shown. The gel was prepared as described in chapter 2.6.2. Each lane was loaded with 8 µg protein. M: molecular weight marker in kilo Dalton (kDa), lane 1: non-induced crude extract, lane 2: induced crude extract, lane 3: flow through affinity column, lane 4: pooled RosB of the affinity purification, lane 5: pooled RosB of the hydrophobic interaction purification and lane 6: pooled RosB of the size exclusion purification. RosB has an apparent molecular mass of about 35 kDa, although the theoretical one is 30 kDa.

3.3.3. High AFP amount purification protocol

The elution profiles of the RosB purification are illustrated in Figure 20. In detail, the left chromatogram depicts the elution profile of the Affinity column (HisTrap™ HP 5 ml) and the right one the elution profile of the desalting column (HiPrep™ 26/10 Desalting).

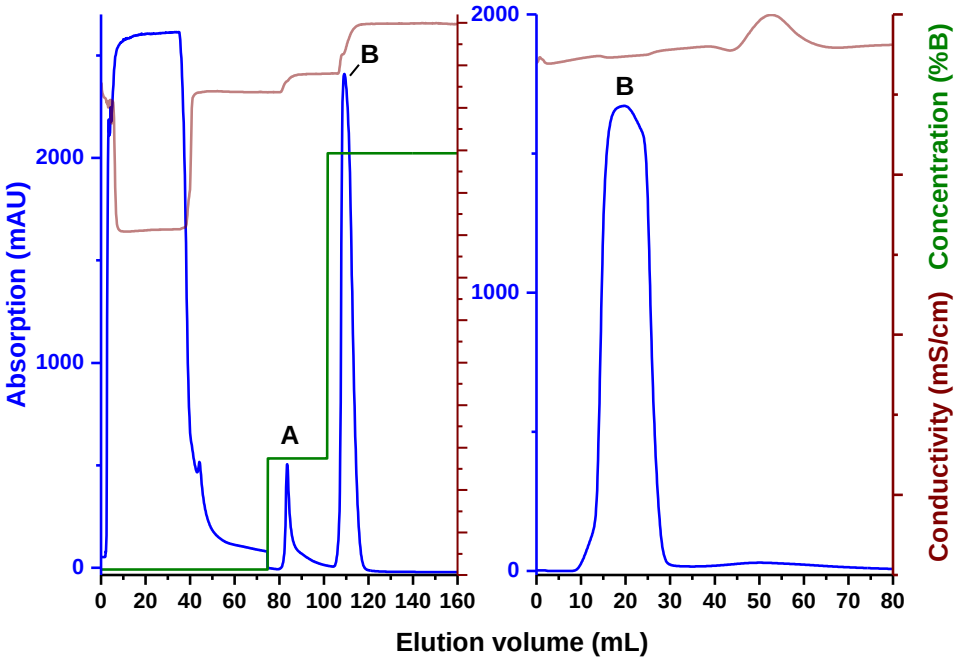

Figure 20: The purification of highly charged RosB is shown. Left: Crude extract of 1 L *E.coli* RosB-pET24a(+) culture was loaded onto a HisTrap™ HP 5 ml (GE Healthcare) with a flow rate of 2 $\frac{mL}{min}$. Impurities (Signal A) were eluted with 20 %B and RosB (Signal B) was eluted with 80 %B. Right: The eluted RosB from the affinity purification step was loaded onto a HiPrep™ 26/10 Desalting with a flow rate of 8 $\frac{mL}{min}$. RosB eluted separately from the salt peak (change in conductivity at ~50 mL). Details are described in method: Affinity-SEC (desalting) RosB purification.

The high UV signal until app. 40 mL is caused by the non-binding proteins present in the crude extract. When the UV signal reached the initial signal level, non-specifically bound impurities (Signal A) were eluted with 20 %B. After 5-10 CV, RosB elution was initiated with 80 %B. The full signal was collected and loaded directly onto the desalting column. RosB elution starts directly after 10 mL and is well separated from the salt peak (change in conductivity at 50 ~mL). The desalting column does not improve the purity of RosB. Therefore the SDS-PAGE analysis (data not shown) is equivalent to column four in Figure 19.

Note, that this method was used to prepare RosB for the cofactor screens described in chapter 3.4.

3.3.4. Generating of seleno-methionine containing RosB purification protocol

RosB was purified with several purification protocols, in order to generate protein crystals reliably. The purification starting with the affinity column, continuing with dialysis and finishing with AEX showed the best results. Figure 21 illustrates the elution profiles of the affinity purification (left) and the AEX step (right):

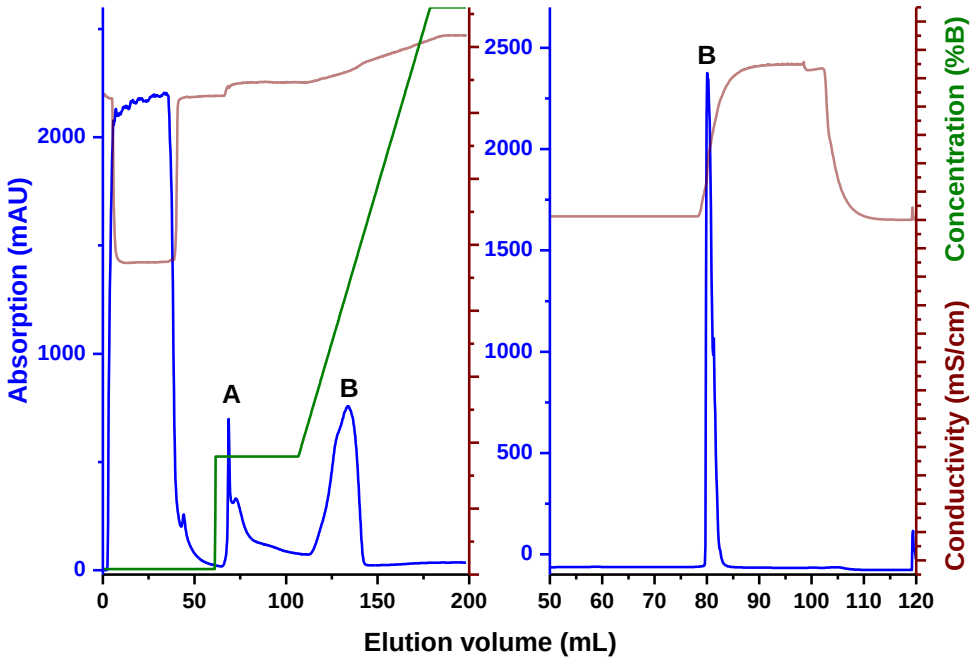

Figure 21: The purification of RosB suitable for crystallization experiments is shown. Left: Crude extract from 1 L *E. coli* RosB-pET24a(+) culture was loaded onto a HisTrap™ HP 5 ml (GE Healthcare) with a flow rate of 2 $\frac{mL}{min}$. Impurities (Signal A) were eluted with 20 %B and RosB (Signal B) was eluted with with a gradient of 1 $\frac{\%B}{mL}$. Right: The eluted RosB from the affinity purification step was dialyzed and loaded onto a Fractogel TMAE 5 mL with a flow rate of 1 $\frac{mL}{min}$. RosB was washed with 10-15 CV and eluted with 100 %B. Details are described in method: Affinity-Dialysis-AEX RosB purification.

RosB containing crude extract was prepared as described in chapter 2.4.9 and loaded onto a HisTrap™ HP 5 ml at flow rate of 2 $\frac{mL}{min}$ (left chromatogram). The high UV signal until 40 mL is caused by the non-binding proteins present in the crude extract. When the UV signal reached the initial signal level, impurities (signal A) were eluted with 20 %B. Afterwards, RosB (signal B) was eluted with a gradient of 1 $\frac{\%B}{mL}$. The eluted protein was poured into a dialysis chamber (MWCO: 12 kDa) and placed in 1 L AEX buffer A. This set-up was gently stirred in a cooling room for two hours. The AEX buffer was renewed 1-2 times until no conductivity change was measurable. Later, the RosB sample was loaded onto a Fractogel TMAE M 5mL at a flow rate of 1 $\frac{mL}{min}$ (right chromatogram). The bound protein was washed

with 10-15 CV buffer A and then eluted with 100 %B (signal B). The purity of RosB was analysed via SDS-PAGE (data not shown) and is identical to lane 5 in Figure 19.

This method showed the best results concerning protein crystallization. This is the reason, why not only the seleno-methionine labelled RosB was prepared in this fashion but also the His_6-tagged RosB. Note that DTT was only supplement for the seleno-methionine labelled RosB.

3.4. *In vitro* Co-factor screen for the RosB catalysed reaction

The product AFP is co-eluted with RosB, which strongly suggests that RosB is performing the AFP synthesis from RP by itself. However, RosB oxidizes RP only to HOC-RP *in vitro*. *S. davawensis* (*rosB::Apra*) is not able to produce any Rof. To prove RosB´s ability of catalysing the oxidation of RP to AFP, a protein-free crude extract from *S. davawensis* (*rosB::Apra*) was prepared and added to the RosB assay. Figure 22 shows the RosB assay in 50 mM PBS (pH=7.5) with 133 μM RP, 20 μM $CaCl_2$, at 39 °C for 12 h.

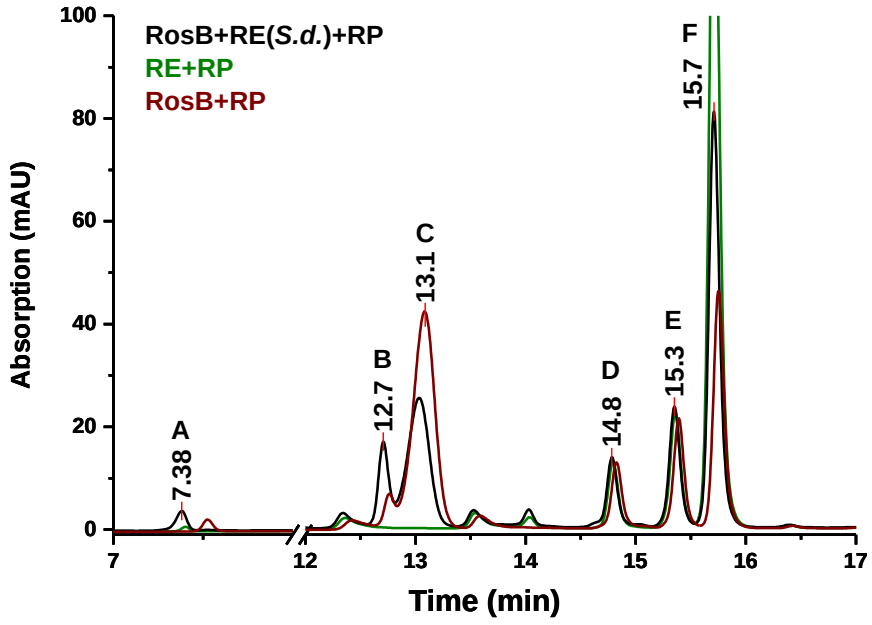

Figure 22: RosB produces AFP from RP in the presence of concentrated and protein-free crude extract from *S. davawensis* (*rosB::Apra*). The RosB assays were incubated at 39 °C in 50 mM PBS (pH = 7.5), 20 µM CaCl2 and 133 µM RP for 12 h and sequentially kept at 5 °C until precipitation and analysis via HPLC (see chapter 2.6.4 Method - Reprosil C18 column, injection volume= 10 µL). The chromatograms measured at 480 nm are shown. A=HOOC-RP, B=AFP, C=HOC-RP, D and E= RP isomers and F=RP (substrate). In the presence of crude extract, an increased amount of HOOC-RP and AFP could be detected. AFP impurity is originated from RosB (brown chromatogram). The negative control (green chromatogram) shows no activity.

On the one hand, the RosB assay (brown chromatogram) shows the typical image. HOC-RP (signal C) is formed, though it consumes only riboflavin-5`-phosphate (signal F) and not the isomer ones (signal D and E). Notice that the AFP signal (signal B) is most likely derived from co-purifed AFP bound to RosB (see chapter 3.2.1).

On the other hand, the assay with crude extract (black chromatogram) shows a lower consumption of RP and lower formation of HOC-RP, but a significantly increased signal B (AFP). The negative control without RosB is depicted in green and shows no RP oxidation at all. The overall retention times are increased by five minutes for an unknown reason.

This result proves RosB`s ability to perform the AFP synthesis by itself. Therefore, a "Kyoto Encyclopedia of Genes and Genomes" (KEGG) database screen for possible co-factors was performed. The database was searched for reactions including oxidases, flavin depending reactions and/or transferases which transfer a formyl-, carboxyl- or amino residue. The tested candidates are summarized in Table 10. Additionally, an amino acid mix of all 20 amino acids was prophylactically added to each experiment to serve as a potential amine donor.

Table 10: The potential cofactors for the RosB reaction are summarized. The candidates were identified by a KEGG database search.

candidate	potential contribution	abbreviation
Pyridoxal 5'-phosphate[46]	amine acceptor	PLP
Pyridoxamine 5'-phosphate[47]	amine donor	PMP
Nicotinamide adenine dinucleotide[48]	electron acceptor	NAD^+
Nicotinamide adenine dinucleotide phosphate[49]	electron acceptor	$NAD(P)^+$
Coenzyme B12[50]	formyl transferring cofactor	CB12
Thiamine[51]	catalysing decarboxylation	Th
Thiamine diphosphate[52]	catalysing decarboxylation	ThPP

As described in the introduction, RosB synthesizes AFP by itself, with the cofactor thiamine or thiamine diphosphate and a yet unknown amino acid as illustrated in Figure 23. Interestingly, the reaction stops at the formation of HOOC-RP (signal A), if the amino acid mixture is absent RosB assay (red chromatogram). Above that, HOOC-RP can be found in low concentration without thiamine (blue chromatogram signal A), which was not detected before, due to insufficient sensitivity levels of the MS. However, this occurs not with shorter incubation times (see chapter 3.5.2 for more details). If the amino acid mix is added (blue chromatogram), the enzymatic reaction ends with the formation of AFP (signal B). As described before, the AFP signal in assay control (brown chromatogram) is originated by the co-purified AFP bound to the enzyme.

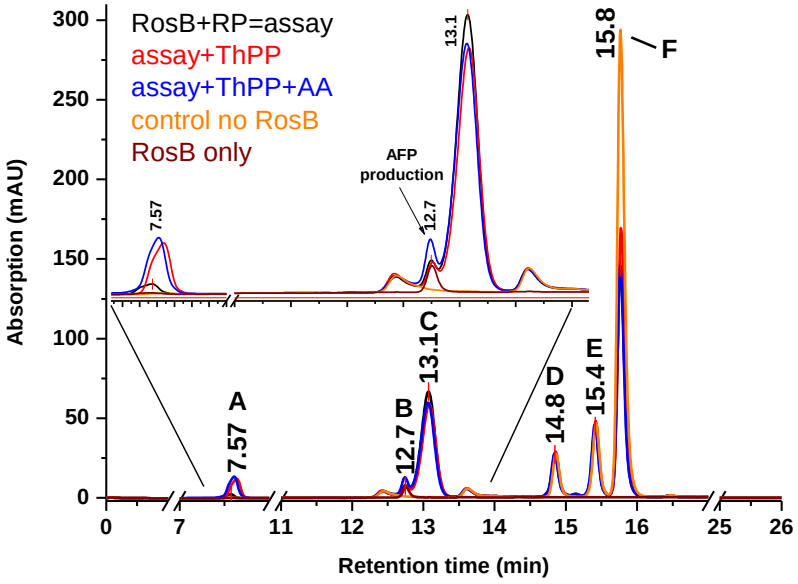

Figure 23: Thiamine diphosphate and a mix of all essential amino acid lead to AFP synthesis in the RosB assay. Black chromatogram: the RosB assay were incubated at 39 °C in 500 mM PBS (pH = 8), 20 µM $CaCl_2$ and 266 µM RP for 12 h and sequentially kept at 5 °C until precipitation and analysis via HPLC (see chapter 2.6.4 Method - Reprosil C18 column, injection volume= 10 µL). Red chromatogram: same as black assay + 666 µM thiamine diphosphate. Blue chromatogram: same as black assay +666 µM thiamine diphosphate and + 133 µM amino acid mix. Orange chromatogram: same as blue assay but RosB excluded and brown chromatogram: 39 µM RosB in 500 mM PBS (pH = 8). The chromatograms measured at 480 nm are shown. A=HOOC-RP, B=AFP, C=HOC-RP, D and E= RP isomers and F=RP (substrate).

To identify the amine donor, each amino acid was tested separately with ThPP, RosB and RP in 50 mM PBS (pH=8). Glutamic acid was identified to be the amine donor. Figure 24 highlights the newly formed flavins HOOC-RP (signal A) and AFP (signal B) in comparison with standards. The HOOC-RP formed in the assay shows the same retention time (3.9 min), identical absorption maxima (268 nm, 364 nm and 448 nm) and an identical $\frac{m}{z}$ value of 487.1 compared to the HOOC-RP standard. Furthermore, the AFP formed in the assay shows the same retention time (7.9 min), same absorption maxima (253 nm, 299 nm and 477 nm) and a very similar $\frac{m}{z}$ value of 458.2, compared to the AFP standard.

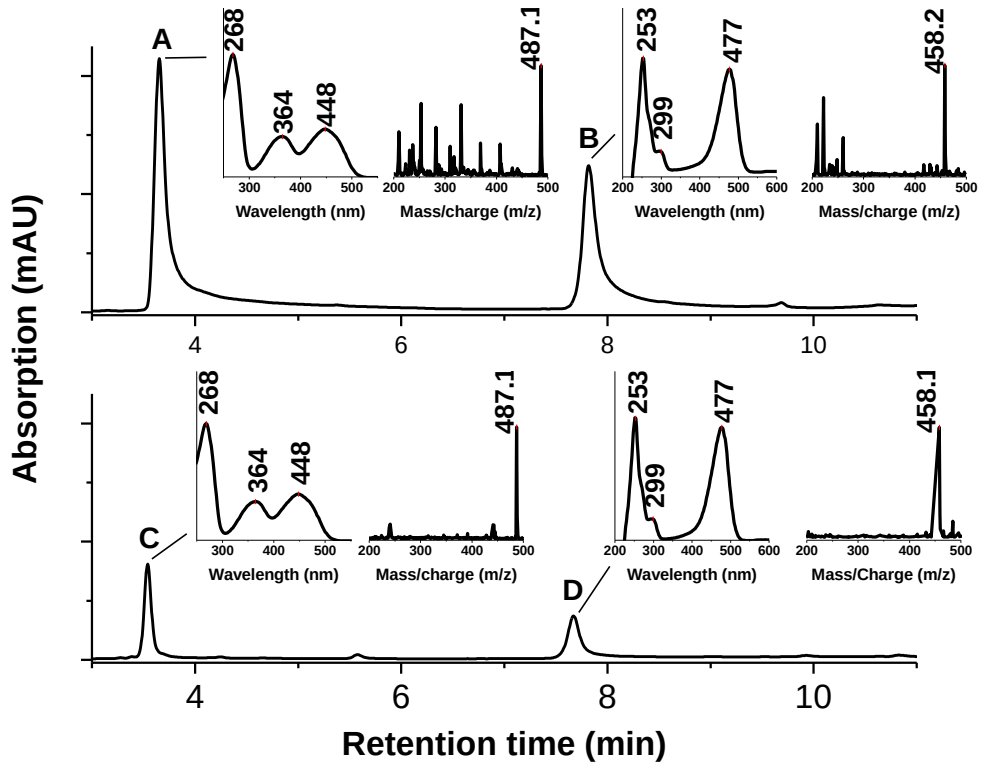

Figure 24: The signals for HOOC-RP and AFP are shown in comparison to suitable standards. Top panel: The RosB assay was performed with 100 µM RP, 5 mM ThPP, 5 mM glutamic acid and 39 µM RosB in BTP solution (pH = 8.8) for 2 hours at 39 °C. Bottom panel: HOOC-RP and AFP standard prepared and analysed as the assay. The assay was stopped and analysed via HPLC as described in chapter 2.6.4 (Method – Kinetex Biphenyl column, injection volume= 10 µL). The chromatograms measured at 480 nm are shown. A=HOOC-RP and B=AFP. The flavin analogues HOOC-RP and AFP elute and have the same properties as their standards.

Another interesting observation was made with the cofactor NAD^+. Figure 25 depicts the positive effect of NAD^+ on the yield of AFP (signal B). Besides that, the RP consumption seems to be increased, whereas the HOC-RP (signal C) formation is kept at the same level. The HOOC-RP (signal A) is slightly reduced. The role of NAD^+ is discussed in more detail in chapter 3.5.1.

To sum up, RosB catalyses AFP synthesis in the presence of thiamine and glutamic acid. NAD^+ seems to be beneficial. HOOC-RP seems to be formed in minor amounts in the absence of thiamine as well; however this is only true for long incubation times, such as 12 hours.

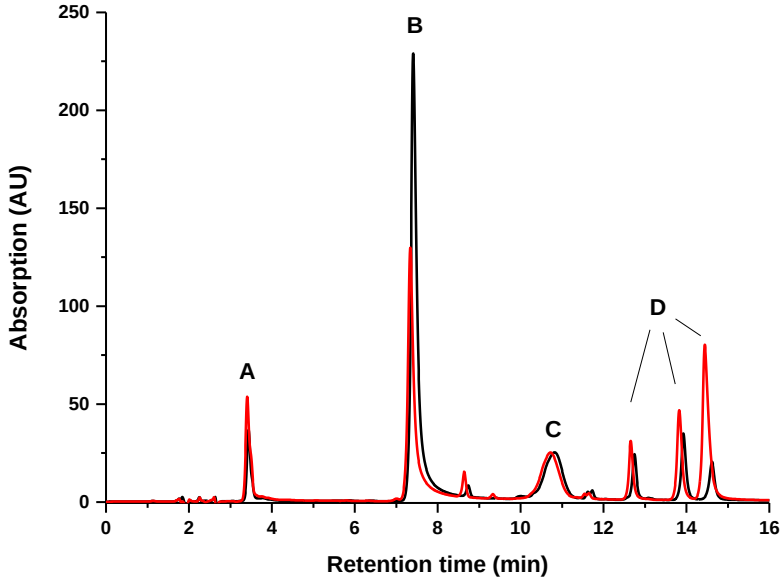

Figure 25: NAD+ enhances AFP yield. Red chromatogram: The RosB assay was performed with 266 µM RP, 5 mM ThPP, 5 mM glutamic acid and 39 µM RosB in BTP solution (pH = 8.8) for 12 hours at 39 °C and sequentially kept at 5°C until precipitation. Black chromatogram: same as red assay+ 5 mM NAD+. The assays were stopped and analysed via HPLC as described in chapter 2.6.4. (Method – Kinetex Biphenyl column, injection volume= 10 µL). HOC-RP yield seems to be the same, although HOOC-RP and AFP yields are increased with NAD+. A=HOOC-RP, B=AFP, C=HOC-RP and D=RP isomers.

3.5. Reaction Mechanism studies of RosB

3.5.1. Role of glutamic acid

Chapter 3.4 showed that glutamic acid acts as nitrogen donor. To further verify this, the RosB assay was performed in 500 mM PBS (pH=8) with 20 μM $CaCl_2$, 233 μM RP, 1 mM thiamine and 2.5 mM ^{15}N(γ)-glutamic acid for 20 h at 39 °C. As control, the assay was also done with ^{14}N(γ)-glutamic acid. If the γ-amine residue of glutamic acid is transferred to the flavin intermediate, a mass shift from 458→459 $\frac{m}{z}$ had to be expected. The samples were separated via HPLC (Method – Kinetex Biphenyl column, Injection volume=10 μL) and analysed with Single Ion Monitoring (SIM). Figure 26 depicts the SIM data for the $\frac{m}{z}$ values 458 and 459 at 70V.

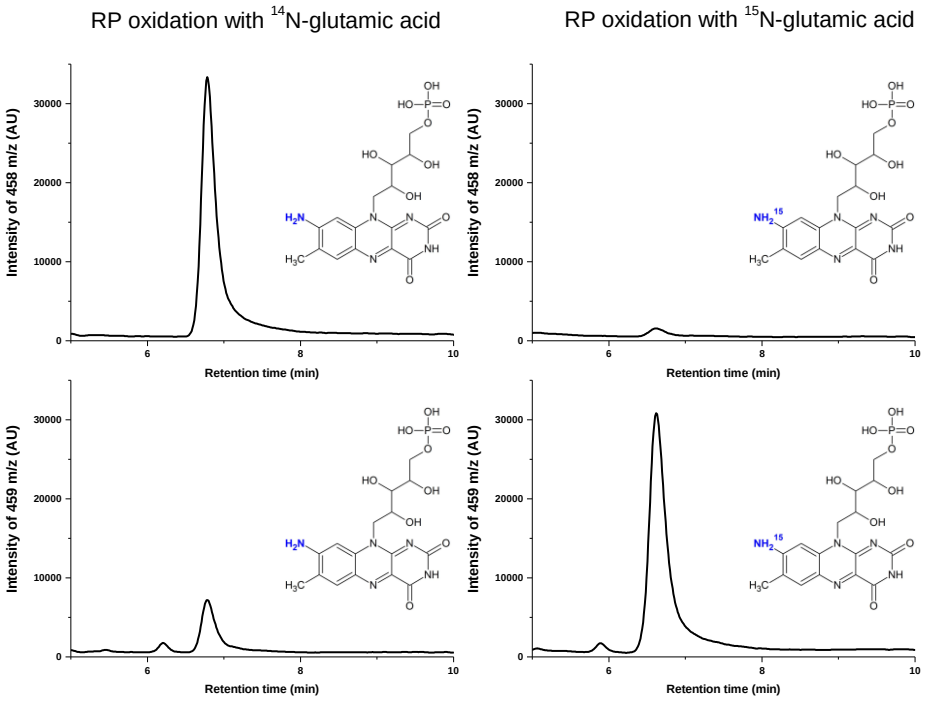

Figure 26: Glutamic acid is the amine donor for the RosB catalysed AFP synthesis. The RosB assay was performed in 500 mM PBS (pH=8) with 20 µM CaCl2, 233 µM RP, 1 mM thiamine and 2.5 mM ^{15}N(γ)-glutamic acid for 20 h at 39 °C. The control was done with 2.5 mM ^{14}N(γ)-glutamic acid. The samples were separated via HPLC (Method – Kinetex Biphenyl column, Injection volume=10 µL) and analysed with Single ion monitoring (SIM) at 70 V for the $\frac{m}{z}$ values 458 and 459. Left column: $\frac{m}{z}$ values of the control; a strong signal can be seen for 458 $\frac{m}{z}$. Right column: $\frac{m}{z}$ values of the assay with ^{15}N(γ)-glutamic acid; a strong signal can only be seen for 459 $\frac{m}{z}$.

On the one hand, the RP oxidation with ^{14}N(γ)-glutamic acid shows a strong signal for 458 $\frac{m}{z}$ and a weak one for 459 $\frac{m}{z}$. On the other hand, the RP oxidation with ^{15}N(γ)-glutamic acid shows only a signal for 459 $\frac{m}{z}$. The weak 459 $\frac{m}{z}$ signal with ^{14}N(γ)-glutamic acid, is most likely caused by natural occurring ^{13}C. This result verifies the previous assumption; the mass shift occurs only with the isotope labelled glutamic acid and hence the γ-amine residue of glutamic acid is the donor in the RosB catalysed reaction.

3.5.2. Role of thiamine

As shown in the cofactor screen experiment (chapter 3.4), thiamine derivatives seem to be needed to promote the RP oxidation by RosB. Figure 27 illustrates the flavin amounts as peak areas of RosB assays in 100 mM BTP solution (pH=8.8) with 20 μM $CaCl_2$, 100 μM RP, 5 mM

glutamic acid, 39 μM RosB and 10 mM thiamine (Th) or 10 mM thiamin diphosphate (ThPP) for 3 h at 39 °C. The control was the assay without any thiamine derivative.

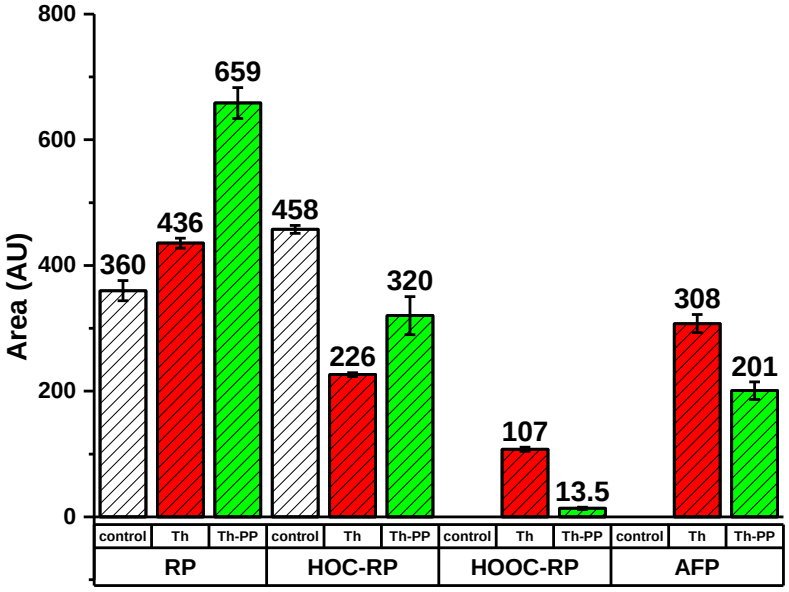

Figure 27: The influence of thiamine and thiamine diphosphate on the RosB assay is shown. The RosB assay was done in 100 mM BTP solution (pH=8.8) with 20 µM $CaCl_2$, 100 µM RP, 5 mM glutamic acid, 39 µM RosB and 10 mM thiamine (Th) or thiamin diphosphate (ThPP) for 3 h at 39 °C. The control was the assay without any thiamine derivative. The samples were measured as triplicates and analysed via HPLC (see chapter 2.6.5, Kinetex column, 10 µL injection volume). HOOC-RP and AFP are only formed in the presence of thiamine or thiamine diphosphate. The shown areas are the peak areas recorded at 480 nm and depicted as the sum of a triplicate with the standard deviation.

If thiamine is not present, the oxidation stops at HOC-RP. This suggests strongly, that thiamine is essential for the oxidation of HOC-RP to HOOC-RP and formation of AFP. The control without any thiamine has a RP peak area of 360 AU (65 % consumed), the assay with thiamine a RP peak area of 435 AU (42 % consumed) and the assay with ThPP a RP peak area of 659 AU (36 % consumed). As expected, the HOC-RP yield is reduced, due to the proceeding reaction, yet the yield for thiamine is 29 % less compared to ThPP. However, the HOOC-RP yield of the assay with thiamine is 7.5 fold higher compared to the ThPP one. Likewise, the AFP yield of the assay with thiamine is 53 % higher compared to the assay with ThPP.

Based on this data, a thiamine concentration dependent experiment was conducted in the same set-up (see Figure 28). No HOOC-RP is formed in three hours without thiamine. The RP signal fluctuates from 360 AU to 337 AU, 397 AU, 362 AU and 232 AU for an unknown reason. The HOC-RP yield decreases as expected (458 AU, 460 AU, 410 AU, 335 AU, 217 and AU with rising thiamine concentration: 0 M, 10 μM, 100 μM, 1 mM and 10 mM). The HOOC-

RP yield increased with rising thiamine concentrations from 0 AU to 17.1 AU, 26.9 AU, 111 AU and 301 AU, respectively. This shows clearly a participation of thiamine, yet the K_m is quite high (in the range of mM).

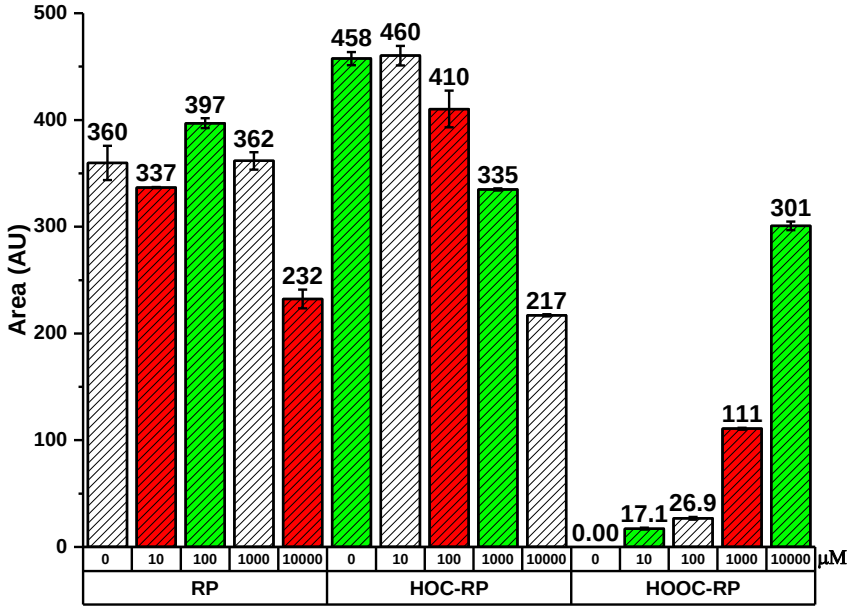

Figure 28: The influence of the thiamine concentration on the HOOC-RP yield is shown. The RosB assay was done in 100 mM BTP solution (pH=8.8) with 20 µM $CaCl_2$, 100 µM RP, 5 mM glutamic acid, 39 µM RosB and 10 µM,100 µM, 1 mM and 10 mM thiamine for 3 h at 39 °C. The samples were measured as triplicates and analysed via HPLC (see chapter 2.6.5, Kinetex column, 10 µL injection volume). HOOC-RP is only formed in the presence of thiamine. The HOOC-RP yield increases with rising thiamine concentration.

This data leads to the conclusion that thiamine and ThPP are potent cofactors to aid the oxidation of HOC-RP, but thiamine is superior. HOOC-RP formation accelerates the overall rate, though AFP formation decreases it, which can be concluded from the RP consumption. However, these concentrations are not physiological.

3.5.3. Role of oxygen

If every oxidation step is analysed, it can be seen that the formation of HOC-RP and AFP releases two electron pairs in each case and the formation of HOOC-RP releases one electron pair which is in need of an electron acceptor. Therefore the role of oxygen in the AFP synthesis was analysed regarding its necessity and possible attacking site.

To understand the oxygen participation in the RosB mechanism, the RosB assay was performed as described in the method - Oxygen dependency assay. Briefly, the assay was first incubated aerobically, and then oxygen was removed in a nitrogen tent. Depending on the

aimed flavin intermediate, thiamine (for HOOC-RP) or thiamine and glutamic acid (for AFP) were added anaerobically and further incubated. In the case of HOC-RP, RosB was only present in the anaerobic step. Figure 29 shows the RosB assays which were navigated with the absence/presence of the cofactors to yield HOC-RP (first lane), HOOC-RP (second lane) or AFP (third lane).

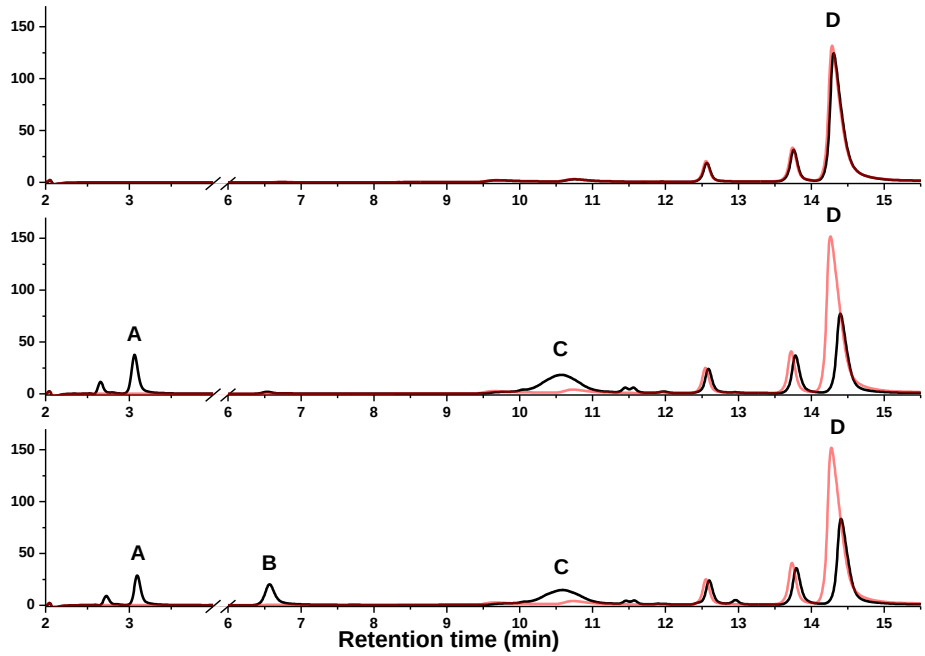

Figure 29: The oxygen participation in the AFP synthesis is shown. The RosB assays (black chromatograms) were performed in 100 mM PBS (pH=8) with 266 µM RP, 20 µM $CaCl_2$ and 125 µM RosB. The reaction mixtures were incubated for 2h at 39 °C (aerobically) and afterwards incubated for 3 h on ice (anaerobically). Necessary supplements were added and further incubated at 39 °C for 3 h. Red chromatograms are negative controls with water instead of protein. Top chromatogram: oxygen-free RosB added as supplement (no initial RosB), second lane= RosB and thiamine added as supplement and third lane: RosB, thiamine and glutamic acid added as supplement (see Method - Oxygen dependency assay for more details). The samples were analysed via HPLC Method – Kinetex Biphenyl column, injection volume=10 µL). A=HOOC-RP, B=AFP, C=HOC-RP and D=RP. The chromatograms were recorded at 480 nm. Oxygen is only required in HOC-RP oxidation step.

The black chromatograms illustrate the assay and the red one the negative control without any RosB. On the one hand, the top chromatogram shows no anaerobic oxidation to HOC-RP with or without any RosB. It is only formed in the presence of oxygen (signal C, chromatogram two and three). On the other hand, the second and third ones show the anaerobic oxidations to HOOC-RP (signal A) and AFP (signal B), respectively. This indicates that oxygen is only required in the initial oxidation step.

Additionally, we wanted to know if oxygen attacks the methyl group. For this reason, we flushed a 500 μL assay batch for 15 min on ice with $^{18}O_2$, $^{16}O_2$ and as a negative control with He. Note that the RosB assay was performed without any glutamic acid, in order to stop the

oxidation at HOOC-RP. Figure 30 shows the HOOC-RP signal with a neutral loss of 214.1 (NL 214.1). Furthermore, the production spectra of m/z 487 (C1), 489, 491 and 493 (C2a-c) are illustrated.

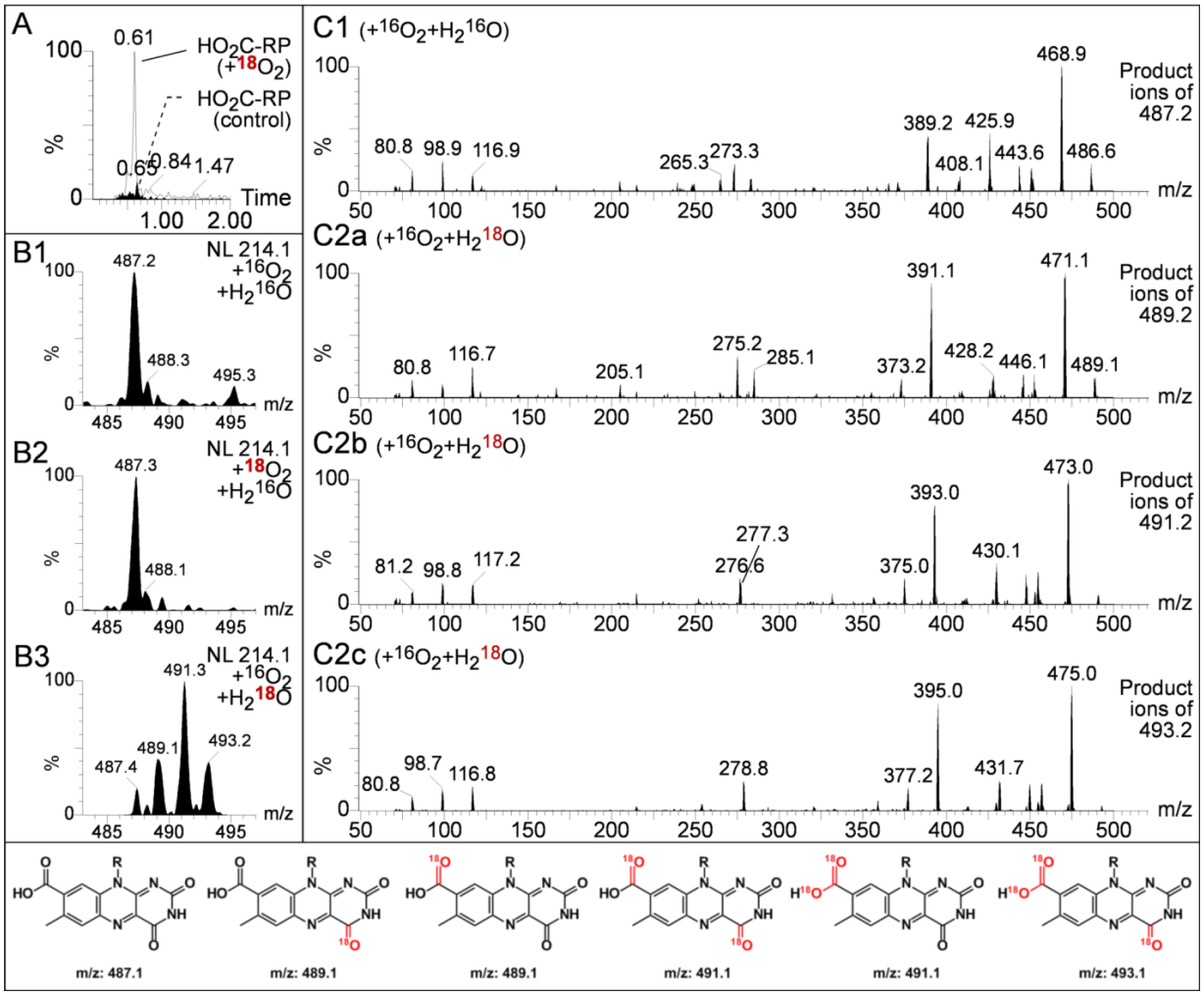

Figure 30: Oxygen attacks RP, but hydrolysis is faster than the oxidation. Left column: The RosB assay was flushed for 15 min on ice (1 bubble/sec) with $^{16}O_2$ (B1), labelled $^{18}O_2$ (B2) or helium (A=control). The neutral loss of 214.1 (-phosphoryibit) is illustrated. Additionally, the assay was performed in $H_2{}^{18}O$/ $H_2{}^{16}O$ (ratio 7:3) with $^{16}O_2$ flushed (B3). The oxidation to HOOC-RP (retention time=0.61 min) does not take place without oxygen (see control in A). In the presence of isotope labelled water the HOOC-RP masses are shifted with its main signal at 491 m/z due to hydrolysis (see possible marked HOOC-RP at bottom). Right column: Production spectra (C) were measured from sample B1 (C1) or m/z 489, 491 and 493 from sample B3 (C2a-c) with a collision energy of 20 eV. The fragments in C1 correspond to m/z 469, $[M+H - H2O]^+$, m/z 451, $[M+H - 2\ H_2O]^+$, m/z 389, $[M+H - H_3PO_4]^+$, and m/z 273, [M+H – phosphoribit]$^+$, which can be only the lower left structure in which R = H. These fragments shift by 2, 4, and 6 u due to incorporation of 1, 2, and 3 ^{18}O-atoms in C2a, C2b, and C2c, respectively. The assumed isotope shift cannot be detected with $^{18}O_2$, due to much faster hydrolysis reaction. The assay was performed in BTP buffered solution (pH=8.8) with 100 µM RP, 20 µM $CaCl_2$, 39 µM RosB and 10 mM thiamine for 90 min at 39 °C. The samples were analysed via UPLC Method - ACQUITY UPLC® BEH C_{18} 1.7 µm column (Injection volume=10 µL). The shown areas are the peak areas recorded at 480 nm and depicted as the sum of a triplicate with the standard deviation.[45]

The data shows, that the control (He flush) shows no oxidation (A) and the flushes with oxygen show the formation of HOOC-RP (B1-2), as expected. Unfortunately, no mass shift

could be observed with $^{18}O_2$. Therefore, the optimised RosB assay was performed in $H_2{}^{18}O$ (B3). Indeed, H^{18}OC-RP, H^{18}OOC-RP and H^{18}O^{18}OC-RP can only be detected in the presence of $H_2{}^{18}O$ with $\frac{m}{z}$ values of 473, 489 and 491, respectively. This suggests that water attacks the methyl group, while oxygen is simultaneous reduced at C4.[29,53] However, the fragmentation pattern of HOC-RP recorded at 50 eV (see Figure 31) opposes a C4 attack by oxygen. The fragment with m/z 172 (lines 1-2) (for RP, control) and 186 (lines 3-4) (HOC-RP) does not contain the ring with the C4 anymore, which is besides C8α the only possible target for hydrolysis[54]. Yet, no shift can be observed in the presence of $H_2{}^{18}O$ (line 2 and 4). This strongly suggests that the oxidation to HOC-RP takes only place under an electrophilic attack of O_2 and excludes the attack of water at the methyl group.

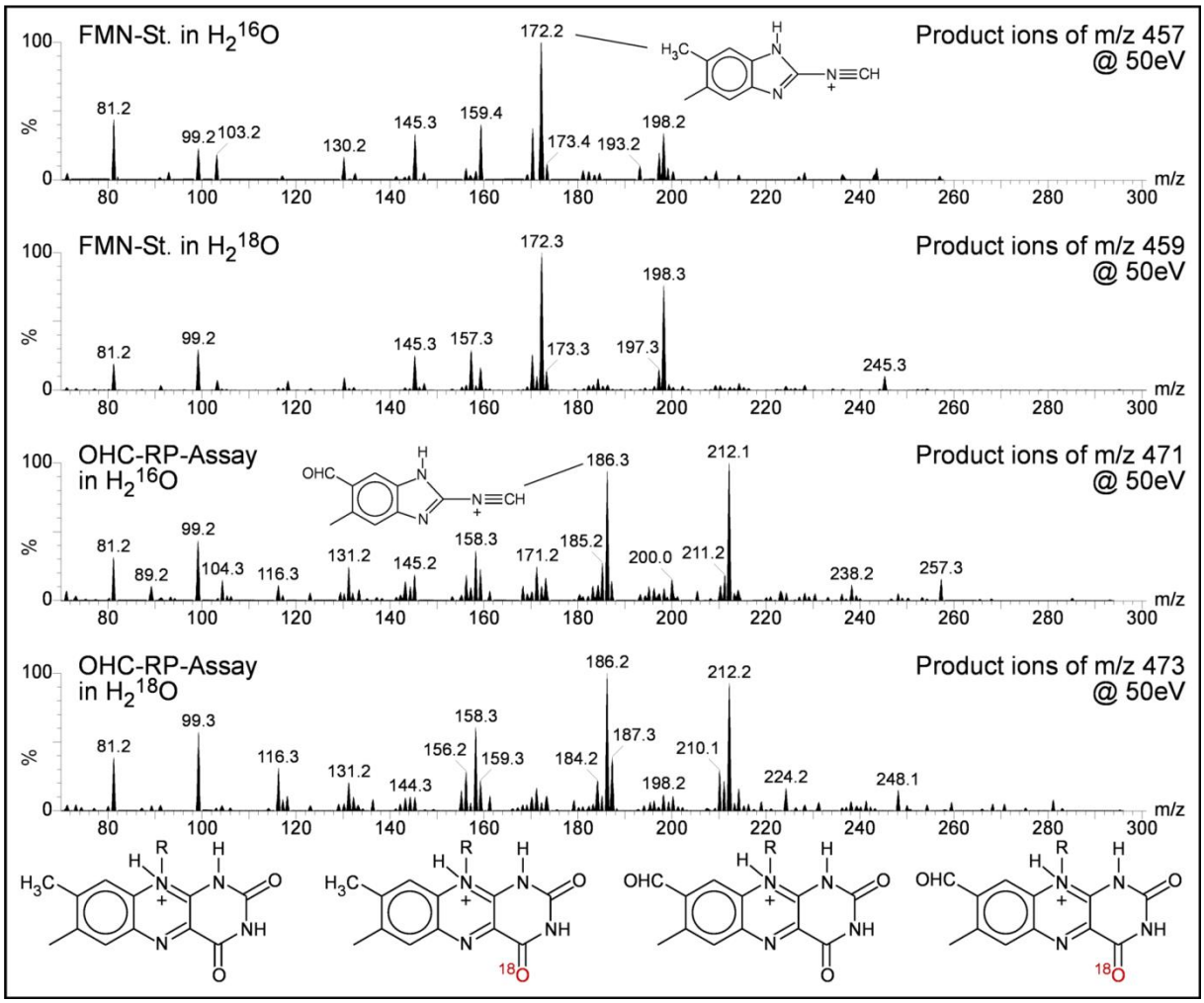

Figure 31: Water does not attack C8α forming the aldehyde moiety. The product spectra of a RP standard (RP-St.) and HOC-RP recorded at 50 eV are shown. The samples were incubated in $H_2{}^{18}O$ and $H_2{}^{16}O$. The fragment assigned to m/z 172.2 and 186.6 do not shift in the presence of $H_2{}^{18}O$ (see third panel). The shown fragment does not contain the C4 anymore (see red labelled oxygen), therefore the only possible target for hydrolysis would be C8α. This indicates that water does not attack C8α in the first oxidation step of RosB catalysis. The same RosB assay was used and analysed as described in Figure 30.

To confirm this observation another experiment was performed. Literature suggests that oxygen is reduced to hydrogen peroxide at the isoalloxazine ring system. Hydrogen peroxide does not occur with an attack at C8α (for more details see Figure 48). A highly sensitive verification reaction is the oxidation of dihydroresorufin (AmplexRed™) to resorufin, in the presence of horse radish peroxidase. To verify H_2O_2 formation the RosB assay was incubated with 100 μM RP for 12 h at 39 °C (see method - Dihydroresorufin for details). Afterwards, 50 μM dihydroresorufin and 2 U horse radish peroxidase were added to the assay and were let incubate for another 30 min at room temperature. The samples were analysed via HPLC (method-Method – Kinetex Biphenyl column) and the results are depicted in Figure 32.

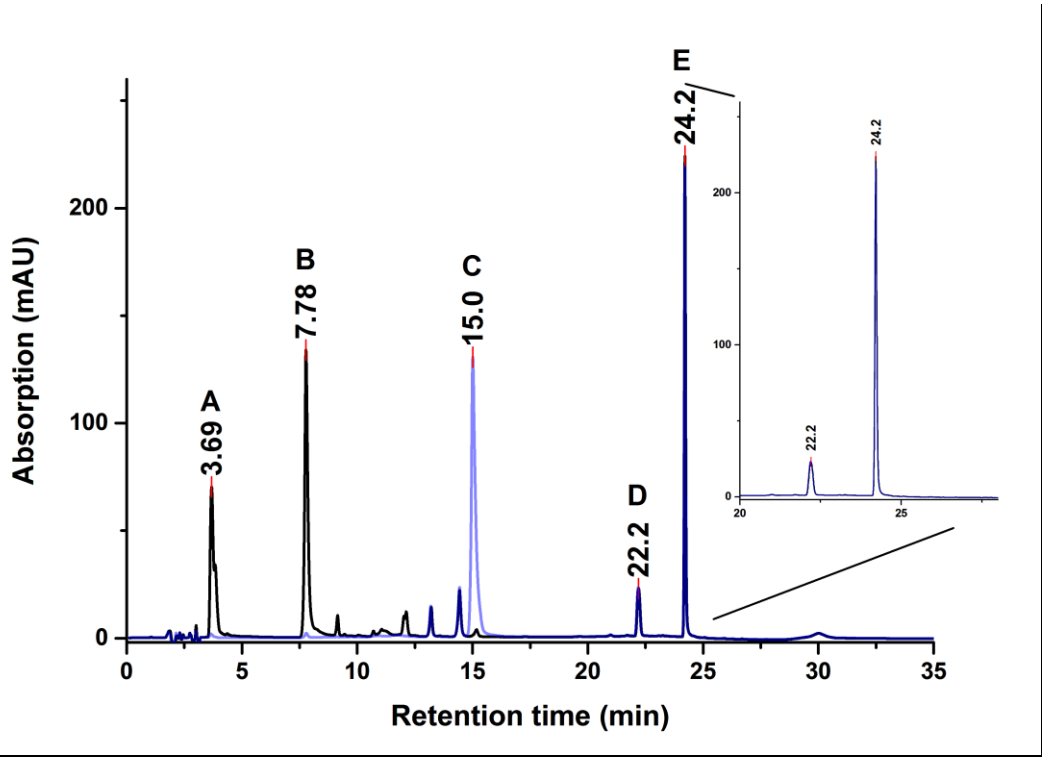

Figure 32: H_2O_2 is not formed during the RosB catalysed oxidation of RP. The RosB assay was performed in 100 mM BTP buffered solution (pH=7) with 100 µM RP, 20 µM, 10 mM thiamine and 39 µM RosB for 12 h at 39 °C. Afterwards, 50 µM dihydroresorufin and 2 U horse radish peroxidase were added and further incubated for 30 min at RT. The samples were analysed via HPLC Method – Kinetex Biphenyl column (Injection volume=10 µL). The black chromatogram shows the assay and the blue one the negative control without RosB recorded at 480 nm. Signal A: HOOC-RP, signal B: AFP, signal C: RP, signal D: dihydroresorufin (reduced) and signal E: resorfuin (oxidized). RP was not oxidized to HOOC-RP or AFP without any RosB. Nevertheless, dihydroresorufin was not oxidized indicating that no hydrogen peroxide was present.

The black chromatogram is exemplary an assay analysis and the blue one is exemplary the control without any RosB. Signals A, B and C are the typical flavin signals HOOC-RP, AFP and RP, respectively. Signals D and E are derived from (dihydro)resorfuin, though signal D is only present in the reduced state of dihydroresorufin (see 2.8.1 for more details). Dihydroresorufin can detect pmol concentration of hydrogen peroxide in 100 μL, yet no significant oxidation of

dihydroresorufin was found in a triplicate experiment. Simultaneous incubation of the RosB reaction and dihyroresorufin led to inhibition of RosB.

In summary, it was shown that oxygen is only required for the first oxidation step forming HOC-RP. Furthermore, oxygen does attack the methyl group, leading to no hydrogen peroxide formation. The hydrolysis appears to be faster than the oxidation to HOOC-RP, which makes it impossible to detect isotope labelled $H^{18}OOC$-RP with $^{18}O_2$.

3.5.4. Role of nicotinamide adenine dinucleotide

As described in the previous chapters, the oxidation to HOOC-RP and AFP takes place even in the absence of oxygen. Additionally, the addition of NAD^+ seemed to increase the AFP yield. For this reason, a quantitative analysis of NAD^+ and $NADP^+$ was done. Figure 33 depicts the flavin yields as peak areas of the RosB assay in 100 mM BTP solution (pH=8.8), 20 μM $CaCl_2$, 100 μM RP, 5 mM glutamic acid, 39 μM RosB, 10 mM thiamine and 5 mM NAD^+ or 5 mM $NADP^+$ for 3 h at 39 °C.

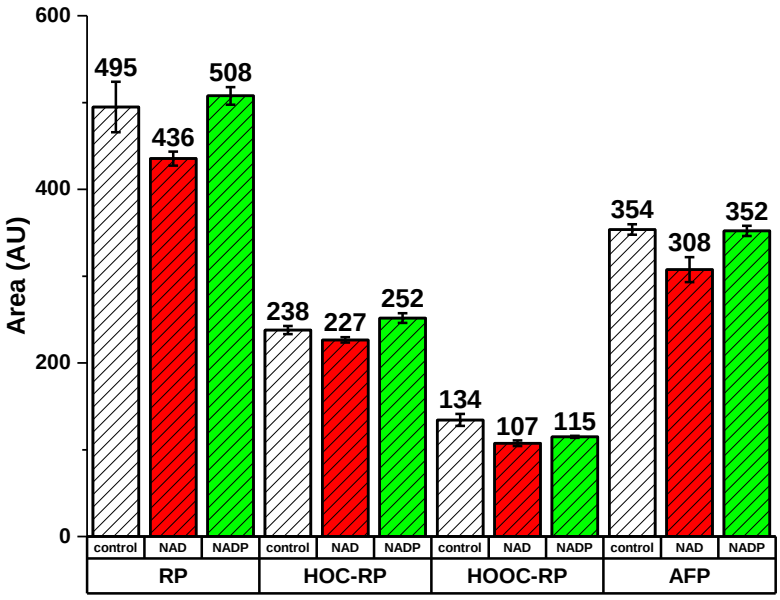

Figure 33: The influence of $NAD(P)^+$ is shown. The RosB assay was done in 100 mM BTP solution (pH=8.8) with 20 µM $CaCl_2$, 100 µM RP, 5 mM glutamic acid, 39 µM RosB, 10 mM thiamine and 5 mM NAD^+ or 5 mM $NADP^+$ for 3 h at 39 °C. The control was the assay with water instead of NAD derivatives. The samples were measured as triplicates and analysed via HPLC (see chapter 2.6.5, Kinetex column, 10 µL injection volume). $NAD(P)^+$ do not show any positive effect under these conditions. The shown areas are the peak areas recorded at 480 nm and depicted as the sum of a triplicate with the standard deviation.

The control assay without any NAD derivative gave an RP area of 495 AU and the assay with NAD^+ and $NADP^+$ areas of 436 AU and 508 AU. The consumption of RP with NAD^+ seems slightly decreased compared to the control and not significantly altered in the case of $NADP^+$. Furthermore, the yields of HOC-RP were 238 AU, 227 AU and 252 AU, respectively, which is a decrease of 4 % (NAD^+) and increase of 6 % ($NADP^+$) in HOC-RP yield. The peak areas of HOOC-RP of the control assay, NAD^+ and $NADP^+$ one are 134 AU, 107 AU and 115 AU, respectively. This results in a yield decrease of 22 % (NAD^+) and 14 % ($NADP^+$). Finally, the areas of AFP are 354 AU, 308 AU and 352 AU, which is only a yield decrease of 13 % in the case of NAD^+. The data is difficult to interpret and in contrast to previous results it does not confirm a positive effect of NAD^+. Other possible electron acceptors in this set-up are RP itself and oxygen. If the reduction of RP or oxygen is kinetically favoured, an effect of $NAD(P)^+$ can be hardly seen.

To eliminate oxygen as oxidation source, another experiment was performed. In this set-up RosB and RP were pre-incubated for 2 h at 39 °C to yield only HOC-RP (same component concentrations as above). Afterwards, the assay was flushed with nitrogen on ice for 10 min and supplied with thiamine and NAD^+ or $NADP^+$. Figure 34 illustrates the flavin yields as peak areas of the RosB assays.

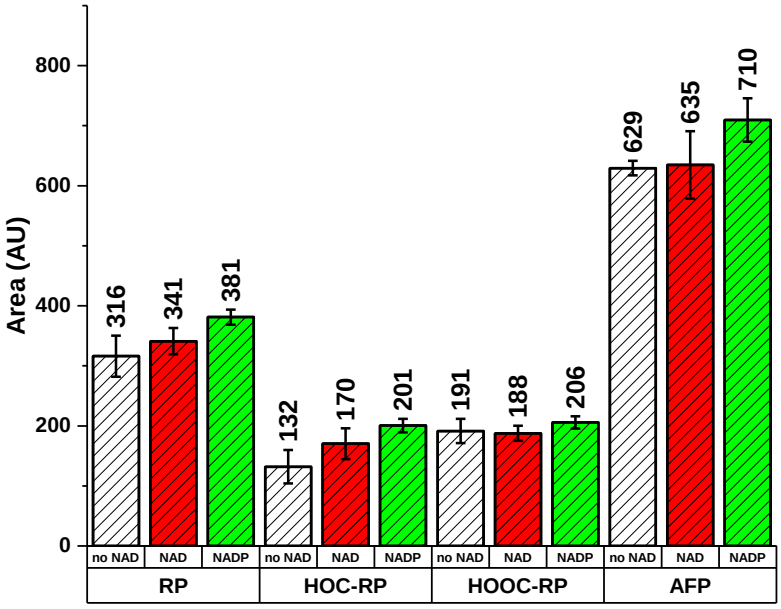

Figure 34: The influence of $NAD(P)^+$ is shown. The RosB assay was pre-incubated in 100 mM BTP solution (pH=8.8) with 20 µM $CaCl_2$, 100 µM RP, 5 mM glutamic acid and 39 µM RosB, for 2 h at 39 °C. The assay was flushed with nitrogen for 10 minutes and fused under nitrogen atmosphere with 10 mM thiamine and 5 mM nicotinamide adenine dinucleotide (NAD^+) or 5 mM nicotinamide adenine dinucleotide phosphate ($NADP^+$). The assay was further incubated for another 3 h at 39 °C. The control was the assay with water instead of NAD^+ derivatives. $NAD(P)^+$ do not show any significant positive effect under these conditions. The shown areas are the peak areas recorded at 480 nm and depicted as the sum of a triplicate with the standard deviation.

The RP peak areas of the control assay, the NAD^+ and the $NADP^+$ one are 316 AU, 341 AU and 381 AU, respectively. Due to the relatively high error bars, the results for the $NADP^+$ experiment are only interpretable (20 % higher than the control). Furthermore, the HOC-RP peak areas are 132, 170 and 201 which results in an increase of 22 % and 52 %. Besides that, the peak areas of HOOC-RP are in the same range with values of 191 AU, 188 AU and 206 AU, respectively. Interestingly, the AFP peak areas are 629 AU, 635 AU and 710 AU which is only an increase of 13 % for $NADP^+$. However it seems, that in the case of $NADP^+$ the removal of O_2 increases the AFP yield. Although the previous positive effect of NAD^+ was not reproducible. The results suggest that none of the NAD derivatives have a significant impact on the AFP yield or RP consumption.

3.6. Protein crystallization of RosB

The difficult RosB reaction let to the assumption that the structure had to have some rare features. A comparison of the primary structures (see Figure 35) revealed, that RosB´s N-terminus shows weak similarity to the flavodoxin superfamily of NAD(P)H:RP dependent reductases and the flavodoxin signature (green boxes) is conserved as well. However, the C-terminal end shows no match with any known sequence (green brackets). Neither the Walker loop nor the Rossmann loop was found.

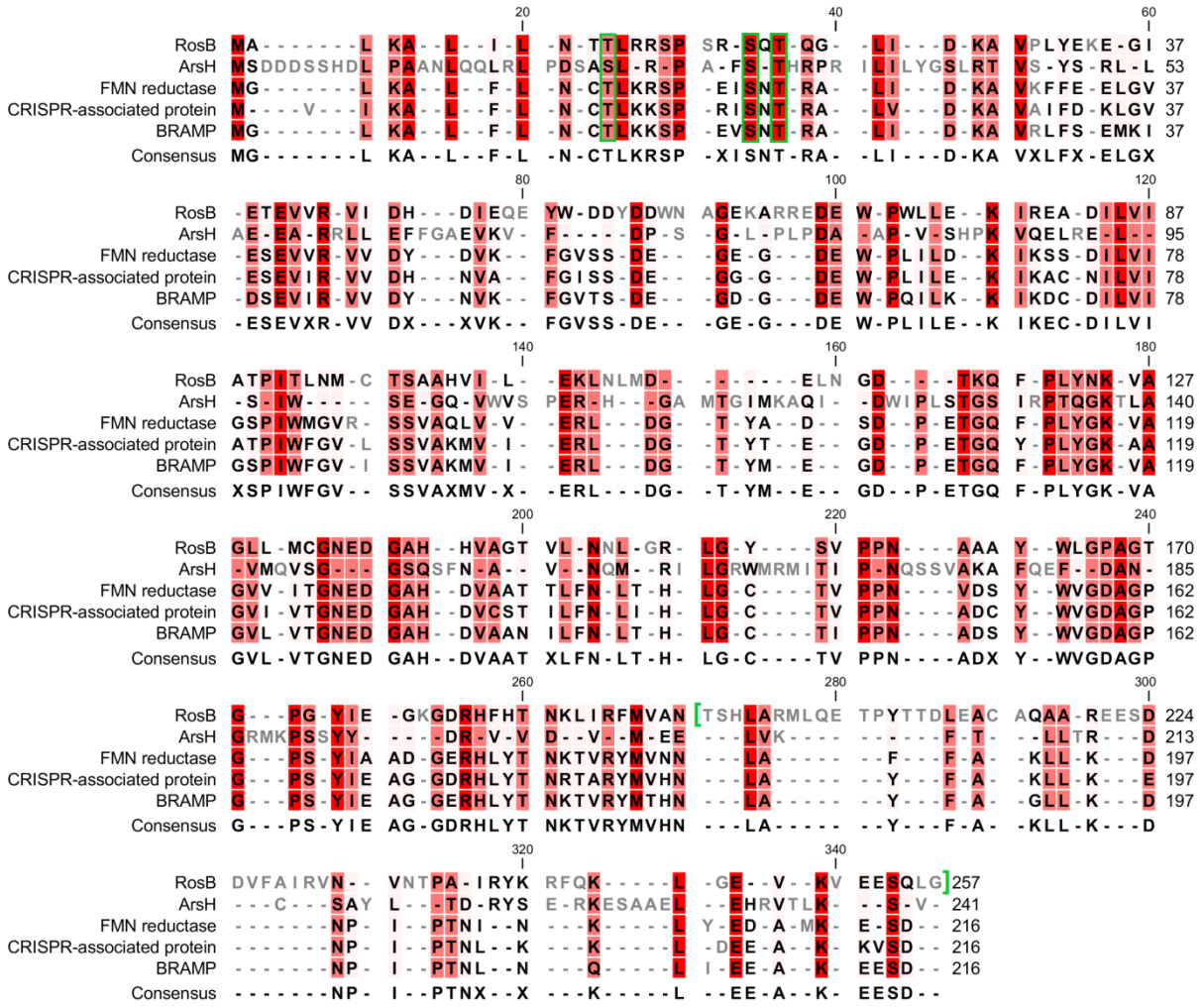

Figure 35: The primary sequence of RosB is shown in comparison to different flavodoxin-like proteins. The N-terminus shows weak similarities to the flavodoxin superfamily of NAD(P)H: RP dependent reductases. The C-terminus shows no similarity to any known sequence (green brackets). The flavodoxin signature sequence Thr 11, Ser 19 and Thr21 is conserved in RosB (green boxes). ArsH = arsenical resistance protein from *Sinorhizobium meliloti*, AEH78015.1; FMN reductase (hypothetical) from *Methanolobus tindarius*, WP_023844905; CRISPR-associated (hypothetical) protein from *Methanosarcina barkeri*, accession number WP_011307054; BRAMP (hypothetical) protein from *Methanosarcina mazei*, WP_048040133.[45]

This made us aim for resolving the crystal structure of RosB. In a collaboration with U. Ermler, U. Demmer and S. Brünle (all MPI, Frankfurt) we successfully obtained the RosB crystals with AFP loaded (Figure 36a) and HOC-RP loaded (Figure 36b). AFP and RP are not distinguishable concerning their electron densities, yet the orange coloured crystals indicate the presence of AFP and not RP. Crystallization experiments with thiamine were also done, however without any success. To get a better understanding of the reaction mechanism, the overall structure was analysed and single point mutations generated to gain a better understanding of the active site of RosB (Master thesis A. Vanselow[55])

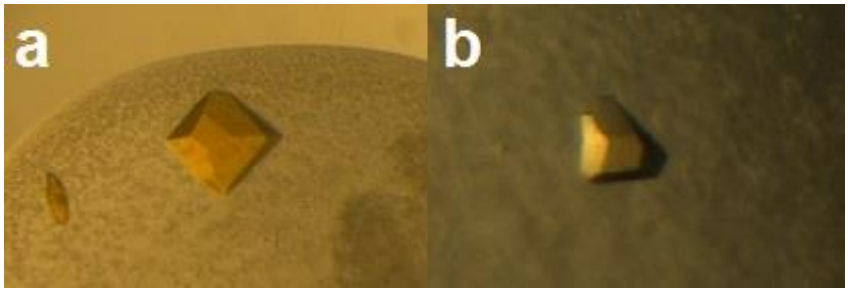

Figure 36: RosB crystals are shown, which are loaded with different flavins. a: RosB crystal loaded with AFP (orange), crystallization conditions: 0.3 M sodium formate, 0.1 M potassium chloride, 17 % (v/v) PEG 3350. b: RosB crystal loaded with HOC-RP, crystallization conditions: 0.3 M sodium formate, 25 % (v/v) Silver Bullet 49, 17 % (v/v) PEG 3350.

3.6.1. The overall structure of RosB

RosB has flavodoxin-like architecture and crystallises as a dimer of dimers in a 222 symmetry. Subunits A (brown)/B (yellow) and C (blue)/D (green) form a dimer of dimers in which each subunit contains one AFP implicating four active sites (Figure 37a). Each subunit has a three layered αβ fold with two α-helices in the front, three ones in the back and five β-sheets in the centre. There are three special linkers (linker1-3). Linker 1 has an additional small α-helix, linker 2 is an extended loop and linker 3 is as well an extended loop containing an α-helical segment (Figure 37b). The C-terminal arm (gray) consists of an α-helix and a β-sheet. The β-sheet interacts with another C-terminal β-sheet (A(B) and C(D) interact with each other). Note that the interaction takes place in moderate proximity to the active sites (flavin carbons in gray).

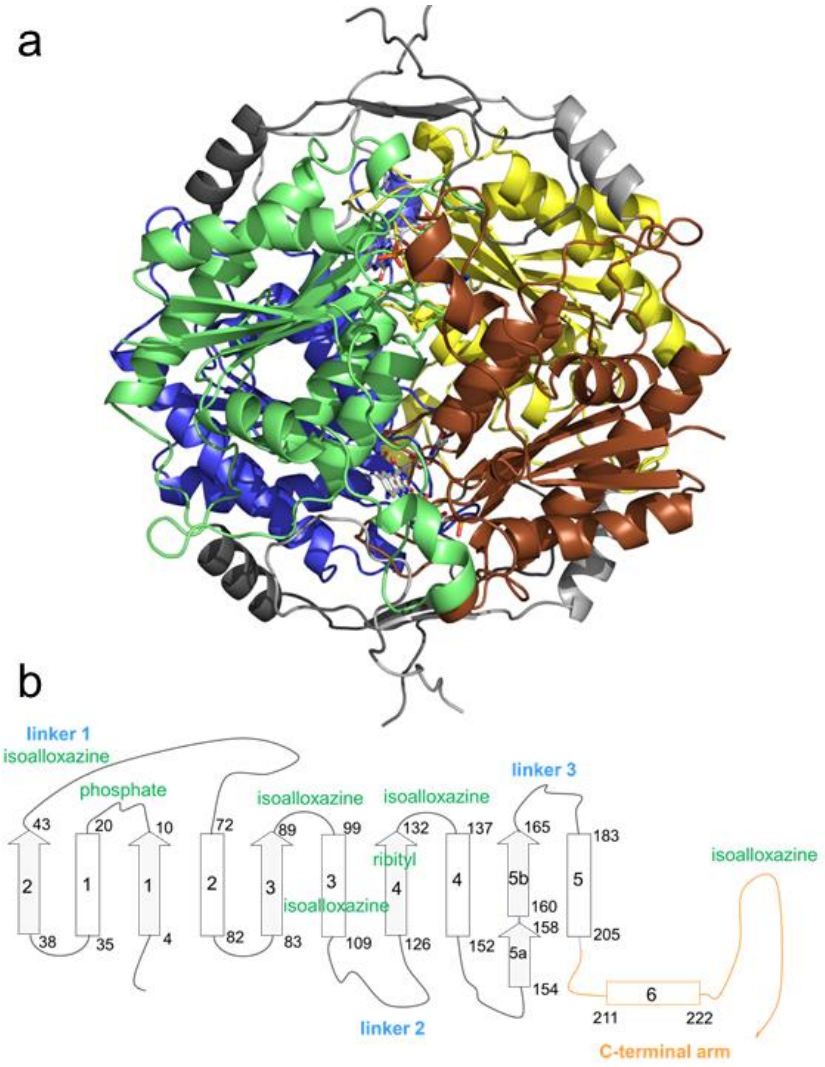

Figure 37a: The structure of the RosB tetramer is shown. Four tightly associated subunits form as a dimer of dimers (A (brown)/B (yellow) and C (blue)/D (green)) the active RosB protein. The unique C-terminal arms are shown in gray and parts of the arm of A(B) and C(D) interact with each other forming two-stranded β-sheet close to the active sites. b: The secondary structure scheme of RosB. Three layers of the flavodoxin-like fold are formed by α-helices (boxes) 1 and 5 (front), by β-strands (arpanels) 2, 1, 3, 4 and 5a (central) and by α-helices 4, 5 and 6 (back).[45]

A DALI analysis[56] identified the ArsH = arsenical resistance protein from *Sinorhizobium meliloti* (pdb code: 2Q62) to be the closest relative with regard to the quaternary structure, yet the sequence identity is only 14 % (Figure 38). ArsH (red) shows the same flavodoxin fold and similar extended linkers except linker 1, which does not have the α-helix upgrade. Additionally, the C-terminal extension of about 50 amino acids is completely absent. ArsH uses RP putatively as a cofactor in a redox process and not as a substrate. [4444]

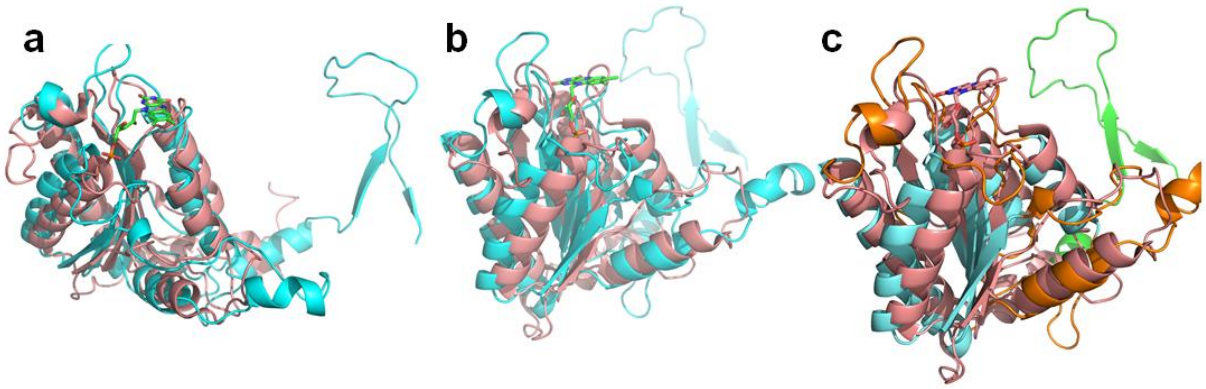

Figure 38: RosB fold (blue) is overlaid with the rank 1 hit (red) of a DALI search in two orientations (a-b). Rank 1 hit: H_2O_2-forming NADPH:RP oxidoreductase ArsH from *Sinorhizobium meliloti* (14% residue identity; see Figure 35). c: RosB is distinguished from all other flavodoxin type proteins by a C-terminal extension of about 50 amino acids (green) and three specialized linkers (orange) connecting secondary structure elements.[45]

A closer look at the active site disclosed the participation of all four subunits, which was hitherto not published for any other protein (Figure 39). Following description refers to subunit A; the flavin is located on top of the β-sheet tips. The first linker of subunit D is in contact with the RP phosphate moiety. Furthermore, the α-helical residues D212-221 (D_1) wraps around the flavin binding site and the loop-forming residues B225-253 (C-terminal arm B) is in contact to the isoalloxazine ring system. The α-helix D_2 (residues 99-109) and D_3 (residues 139-151) protrudes to the RP binding site as well. The serpentine-like shaped C_1 with a short α-helical segment participates into the active site architecture as well.

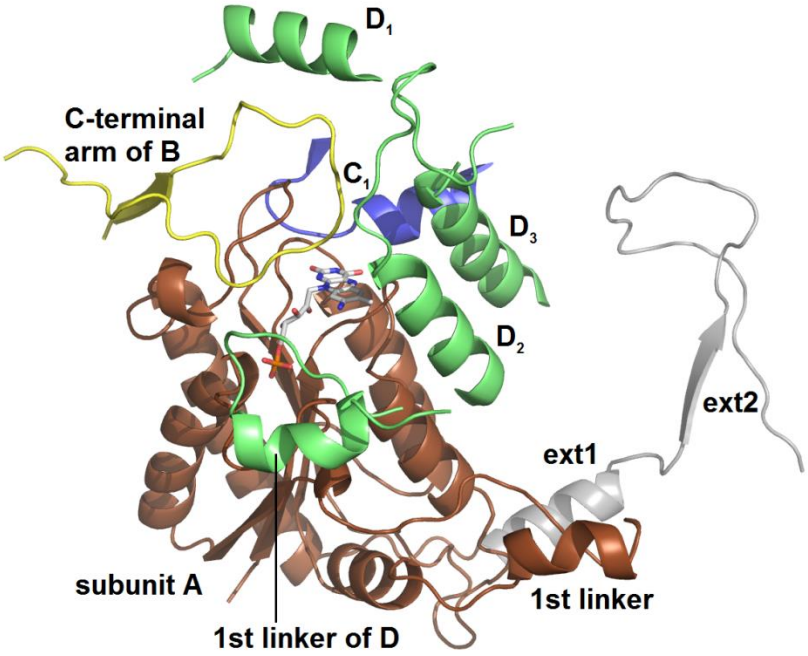

Figure 39: The active site of subunit A of RosB is illustrated. The C-terminal extension of A is grey coloured and is composed of an α-helix formed by amino acid residues A212-221 (ext1) and a hairpin-like loop formed by residues A225-253 (ext2). All four subunits contribute to every active site. The first linker of subunit A ("1st linker", residues A45-70) contains a small α-helical segment and is part of the active site of subunit D (not shown). Accordingly, the corresponding α-helical segment of subunit D ("1st linker of D") takes part into the RP binding site of subunit A. The α-helical residues D212-221 (D_1) of subunit D wraparound of the active site of subunit A (brown), whereas the loop-forming residues B225-253 (C-terminal arm B) is in contact to the flavin (carbon in grey) of subunit A. The α-helix D_2 of subunit D (residues 99-109) is in contact with RP of subunit A and α-helix D139-151 (D_3) contacts RP as well. The linker C_1 has a serpentine line-like course with a short α-helical segment (C1) and is part of the RP binding site of subunit A, too.[45]

Another interesting fact is the short edge-to-edge distance of the flavins from subunit A(B) and C(D) (Figure 40). Within 12.5 Å a transient exchange of electrons is possible. This could be an explanation how the further oxidation of HOC-RP and glutamate can take place without any NAD^+. While one flavin becomes oxidized the adjacent one is reduced. Afterwards, the reduced flavin can be re-oxidized with O_2 or released to give space for an oxidized flavin.

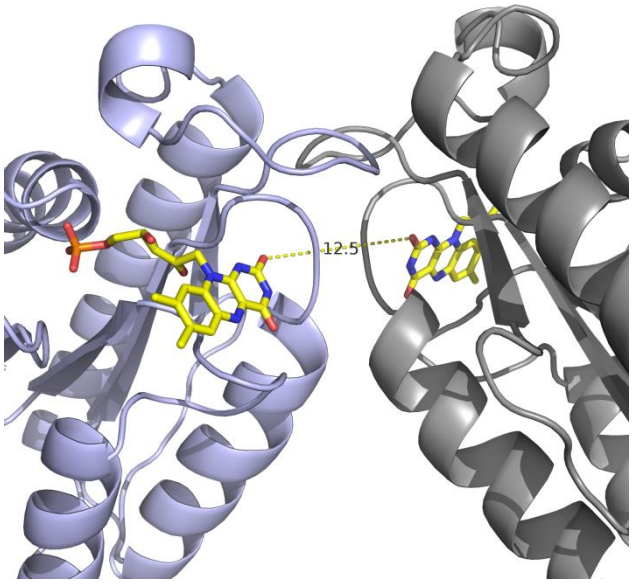

Figure 40: The subunit A and C of RosB are shown. Their flavins (yellow carbons) have only an edge to edge distance of 12.5 Å, which allows a transient exchange of electrons. This would allow the reduction of one flavin, while the other one becomes oxidized during catalysis. Afterwards, a re-oxidation with molecular oxygen can take place.[45]

AFP is deeply buried inside of RosB with an anion hole built up by the AFP isoalloxazine ring itself and by the residues LeuD109, TyrD53, LeuA12, ArgA13, ThrA92, GluD105 and ArgB242 (Figure 41). This cavity is capable of binding negatively charged molecules like glutamate, water, O_2 or even thiamine, because the entries (indicated with arrows) have a diameter of 7 Å. However, thiamine can only bind with a previous conformational change.

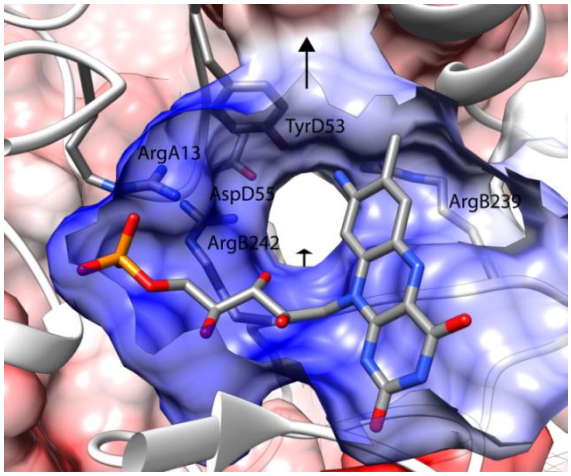

Figure 41: The anion hole in which negatively charged molecules like glutamate, hydroxyl or molecular oxygen can be stabilized. The hole is built up by the isoalloxazine ring system of AFP itself and by the residues LeuD109, TyrD53, LeuA12, ArgA13, ThrA92, GluD105 and ArgB242 (not all amino acids shown). The arrow indicates the entries into the hole with a diameter of 7 Å, which makes it even possible to let thiamine enter. However, thiamine does not fit without major conformational changes.[45]

The anion hole differs slightly between bound HOC-RP and AFP (see Figure 42). ArgB239 is slightly rotated in order to leave space for a water molecule, which is in perfect position to generate HOOC-RP from HOC-RP (see Figure 42b). The aldehyde group of HOC-RP bridges via water molecules (the red dots implicate water molecules) to ArgA13, ArgB239 and ArgB242. LeuD109, TyrD53, ArgB242 undergo minor displacements. Additionally, the encircled pair in panel A is in van der Waals contact to C8α. It is either two water molecules or O_2. The presence of O_2 would support an attack at C8α.

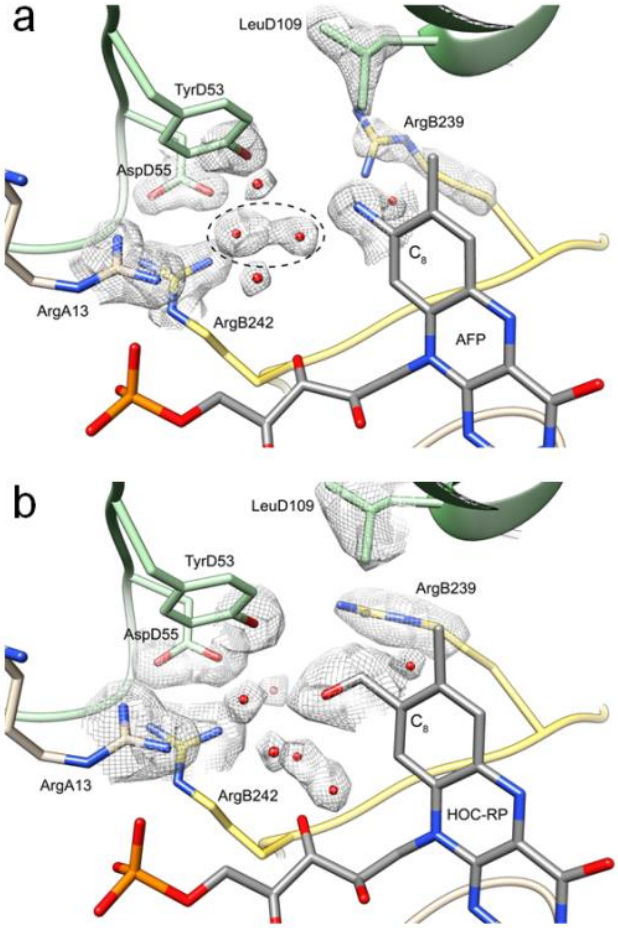

Figure 42: The RosB structures around the C8α of the flavin are shown. a) RosB loaded with AFP. The red dots indicate water molecules. The encircled pair can also be O_2. b) RosB loaded with HOC-RP. The aldehyde moiety (C8α) is distinguishable from the amine group. ArgB239 is slightly rotated in order to leave space for a water molecule, which is in perfect position to generate HOOC-RP from HOC-RP. LeuD109, TyrD53, ArgB242 undergo minor displacements. The 2Fo-Fc electron densities are drawn at a contour level of 1.0 σ.[45]

In summary, RosB is a matchless tetrameric dimer of dimers, whereas each subunit shows a flavodoxin-like fold. It contains three specialized linkers and a so far unique C-terminal arm. All four subunits protrude to each active site. The edge-to-edge distance of two adjacent flavins is 12.5 Å, so that a transient exchange of electrons is possible. The flavin is deeply

buried and supports the formation of an anion hole, which can stabilize partial negative charged cofactors like glutamate, water or oxygen.

3.6.2. Mutagenesis studies

The described structural features of RosB (chapter 3.6.1) are based on *in silico* results. To examine the active site in more detail, the residues which were the closest ones to the bound flavin were selected. Alanine mutants were generated, because the methyl residue is non-bulky and chemically inert. The generated mutated proteins are summarized in Table 11. Table 12 summarized their activity in a RosB assay as triplicates.[55] The RosB wild type is abbreviated to wt in this chapter.

Table 11: The mutated RosB enzymes, their location and their effect on RosB activity are summarized.[55]

name	localization	effect
Leu93Ala	*re*-side C7α methyl of RP	no effect
Glu105Ala	*re*-side C7α methyl of RP	no substrate binding
Leu109Ala	C7α methyl of RP	activity reduction
Tyr53Ala	C8 α methyl of RP	activity reduction
Asn94Ala	O=C4 of RP	no substrate binding
Arg151Ala	*si*-side isoalloxazine ring	no substrate binding
Tyr240Ala	*re*-side isoalloxazine ring	no substrate binding
Thr11Ala	P-loop	no substrate binding
Gln20Ala	P-loop	no effect
Thr21Ala	P-loop	activity reduction
Arg13Ala	flavin/P-loop	activity reduction, no AFP formation
Ser19Ala	flavin/P-loop	no substrate binding
Asp55Ala	flavin binding	no substrate binding
Lys241Ala	flavin binding	no effect
Arg242Ala	flavin binding	activity reduction

Table 12: The activities of the mutated RosB enzymes are shown. % refers to the activity in relation to the wt activity. A = Ala.[55]

Active mutants	RosB activity in μM(AFP)/mg(RosB)/min/L	Inactive Mutants	RosB activity in μM(AFP)/mg(RosB)/min
wt	7.0 ± 1.1 (100 %)	**Tyr53A**	0.1 ± 0.0 (1 %)
Lys241A	7.4 ± 1.5 (106 %)	**Thr11A**	0 (0 %)
Leu93A	6.4 ± 0.3 (91 %)	**Arg13A**	0 (0 %)
Gln20A	5.6 ± 0.2 (80 %)	**Ser19A**	0 (0 %)
Arg242A	2.6 ± 0.0 (37 %)	**Asp55A**	0 (0 %)
Leu109A	2.4 ± 0.3 (34 %)	**Glu105A**	0 (0 %)
Arg151A	0.8 ± 0.1 (11 %)	**Tyr240A**	0 (0 %)
Thr21A	0.7 ± 0.2 (10 %)		
Asn94A	0.5 ± 0.5 (7 %)		

The data shows that RosB with the mutated residues Leu93A, Gln20A and Lys241A (A=Ala) do not have any significant impact on the activity. The mutated RosBs eluted with bound AFP (as the wt) showed a remaining activity of >80% compared to wt. The mutated residues Thr11A, Ser19A, Asp55A, Glu105A and Tyr240A caused a loss of RosB activity (<0.1 % of wt).

Besides that, no bound flavins could be detected in the HPLC (data not shown). Thr11 and Ser19 are conserved elements of the flavodoxin signature and known to be important for flavin binding (see Figure 44a). Asp55 and Glu105 are part of the mentioned anion hole and it seems that the hydrophobic methyl group of alanine disturbs a sensitive balance of surface charge, which inhibits flavin binding. Tyr240 position is crucial for flavin binding. It is positioned on the re-side of the isoalloxazine ring system and is in van der Waals distance to undergo π-π stacking with the isoalloxazine one (see Figure 43). This would also explain the absorption maximum shift of bound AFP, which is described in chapter 3.2.1. Additionally, the phenyl group is kept in place by hydrogen-bonds to GluA135 and ArgD151 (not shown). The importance of the hydrogen-bond of Arg151 could be shown in RosB Arg151A. The activity dropped to 0.8 ± 0.1 (11 %) and no flavin was bound to the protein.

RosB Arg13A showed no AFP formation, although HOOC-RP was formed (major fraction of bound flavin to the eluted protein). This indicates its importance in glutamate binding (see Figure 43). Tyr53 is in close proximity to C8α and participates in the stabilisation of water

bridges as shown in Figure 42. Yet, another important feature can be derived from its position, which is illustrated in Figure 45.

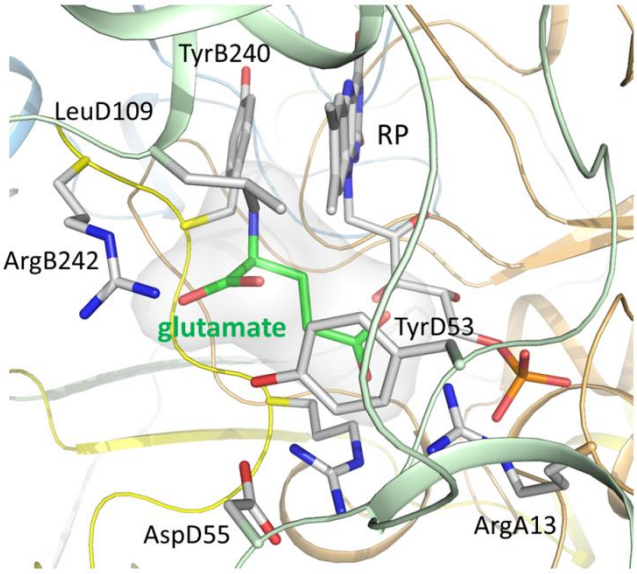

Figure 43: An active site model of RosB with glutamate is illustrated. Glutamate clearly fits into the solvent-occupied pocket adjacent to the C8 formyl. The pocket is generated by the isoalloxazine ring of AFP and by the shown amino acid residues which not only leave space for H_2O and O_2 but also for glutamate. Subunit A (brown), subunit B (yellow) and subunit D (green).[45]

If the surface charge contributions of Tyr53 and Leu109 are removed, the entries into the RosB active site are united and the diameter dramatically increased. This probably changes the surface charge distribution and solvent accessibility. This assumption is also reflected in the remaining activity of RosB Leu109A (2.4 ± 0.3; 34 %wt). Leu109 is the only residue being in van der Waals contact with C8α. However, both do not participate in flavin binding. RosB Thr21A shows also an activity reduction of 0.7 ± 0.2 (10 %) but still a flavin binding capacity.

RosB AsnA94 had a remaining activity of 0.5 ± 0.5 (7 %) and builds most likely a H-bridge to the C4 of the flavin. RosB Arg242A has residual activity of 2.6 ± 0.0 (37 %) and flavins were bound to it after purification as well. Figure 44 summarizes the mutated residues as picture. Panel a shows the residues which are crucial for flavin binding, because a mutation to alanine made RosB incapable of it. Panel b illustrates the residues which led RosB to a reduced/absent activity after mutation to alanine. Yet they were still able to bind flavins.

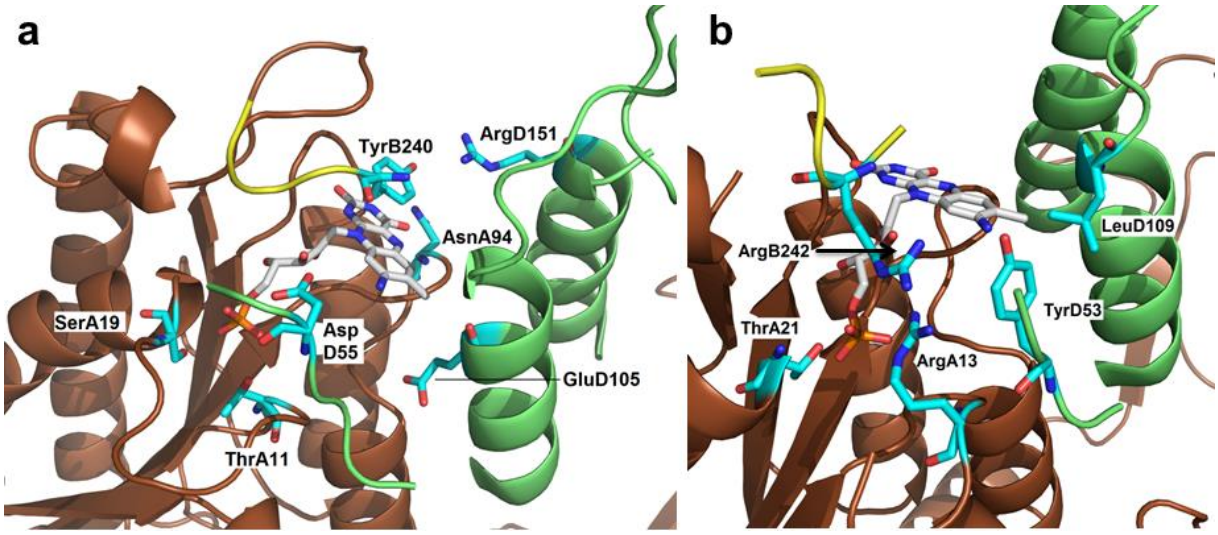

Figure 44: The mutated residues are shown (carbons in turquoise). All mutations were single mutations and transformed to alanine. a) The summary of mutants which showed no substrate binding. b) The summary of mutants which had a reduced activity but still showed flavin binding capacities. RosB Arg13A showed a lack of AFP formation and accumulation of HOOC-RP, which indicates the importance in binding glutamate; the amine donor. Subunit A=brown), subunit B=yellow and subunit D=green.

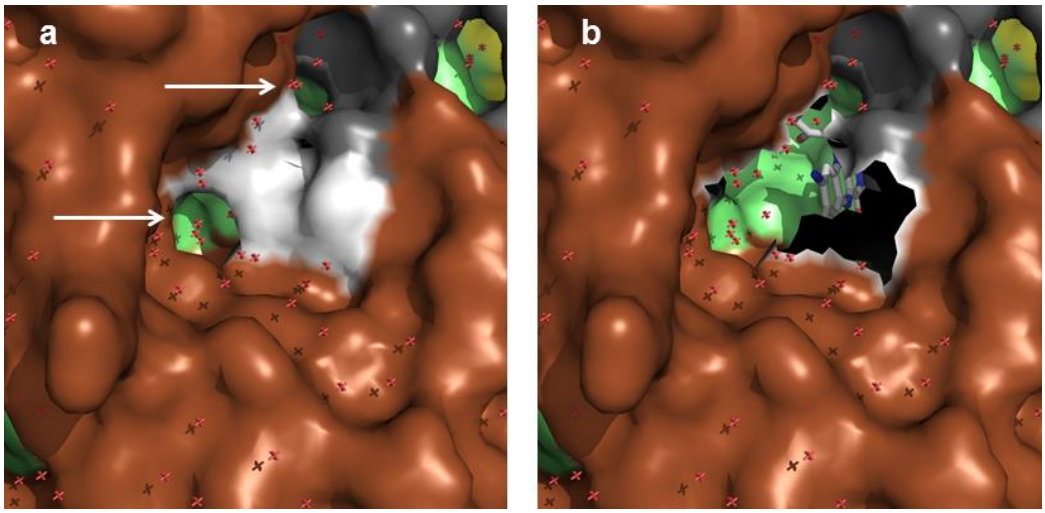

Figure 45: a) The entries leading towards the anion hole (indicated with arrows) are shown from outside. The flavin from subunit D is in focus. b) The surface charge of the "gatekeepers" Leu109 and Tyr53 are manually removed to show their importance in the control of the entry size. The surface charge is calculated with pymol (default setup). Subunit D=brown, subunit A= green and Leu109 and Tyr53 are grey coloured. AFP (carbons in grey) is exposed without the gatekeepers Leu109 and Tyr53.

3.6.3. The updated roseoflavin biosynthesis

RosB is part of the roseoflavin biosynthesis as shown in Figure 46. RibC (RP biosynthesis) phosphorylates the precursor RF yielding the RosB substrate RP. Subsequently, RosB oxidizes RP to HOC-RP with O_2. Thiamine aids the following oxidation to HOOC-RP. Glutamate is the amine donor and substitutes the carboxylic residue forming CO_2, α-ketoglutarate and AFP. AFP is not accepted as a substrate by RosA, therefore an unknown phosphatase is assigned to hydrolyse the phosphate. RosA methylates AF twice forming MAF and finally RoF. The electron acceptors X and A^+ remain unidentified.

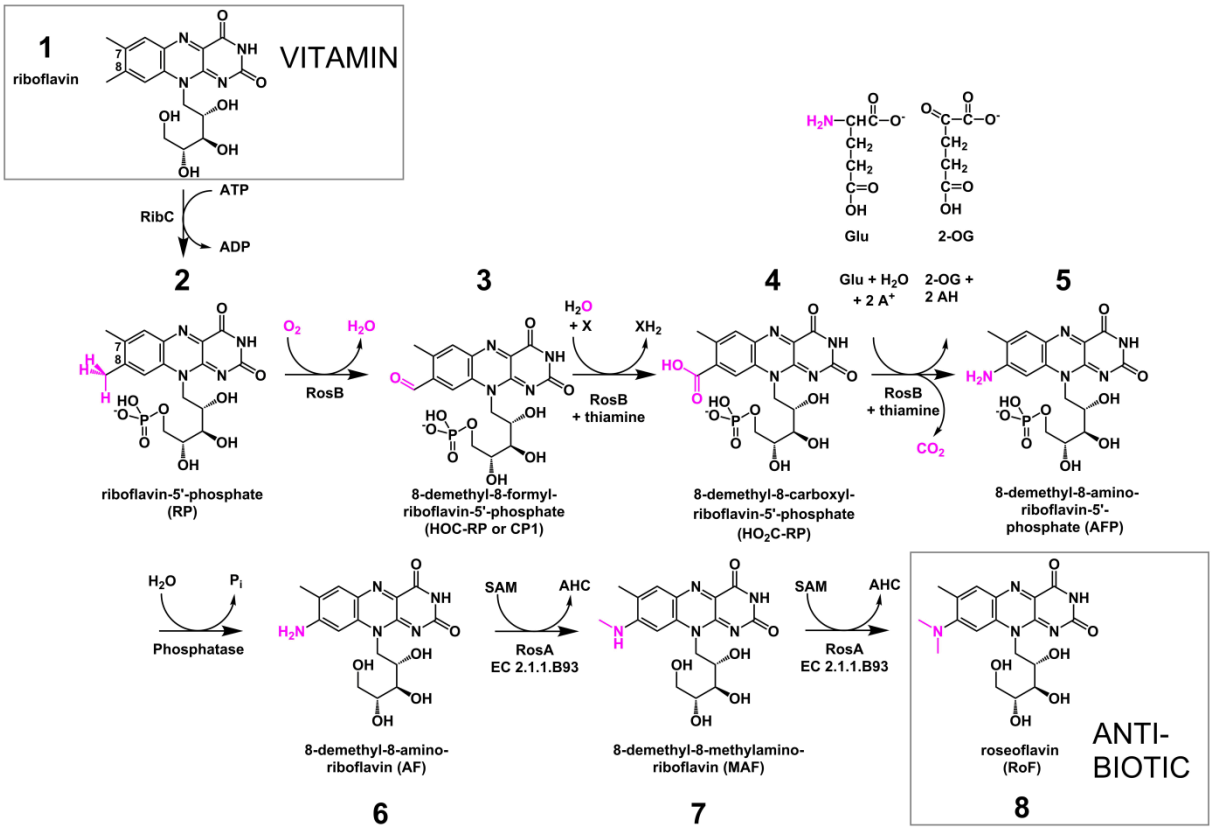

Figure 46: The updated roseoflavin biosynthesis is illustrated. RF (**1**) is phosphorylated by RibC under consumption of one ATP. The newly formed RP (**2**) is taken up by RosB and oxidized in the presence of O_2 to HOC-RP (**3**). Thiamine is needed to promote the oxidation yielding HO_2C-RP (**4**). After glutamate has bound to RosB, the carboxylic residue becomes cleaved off and replaced by an amine group leaving CO_2 and α-ketoglutarate (2-OG). RosA does not accept the RosB product AFP (**5**), therefore a yet unknown phosphatase has to hydrolyse the unwanted phosphate group. RosA methylates AF (**6**) twice with the cosubstrates S-adenosyl methionine (SAM) generating adenosyl cysteine and roseoflavin (**8**).[58]

3.7. Disruption of *rosB* in *Streptomyces davawensis*

The gene *BN159_7989* (*rosB*) was found with the altered Gust method (see chapter 2.4.7).[17] The phenotype of the *rosB* deletion strain was its lack of RoF in the supernatant. To validate these results the following experiment was performed. Figure 47 shows the *S. d* mutant where *rosB* is replaced by an Apra cassette. On one hand the agar of the wt is stained red, due to RoF secretion. On the other hand the mutant lacks *rosB* and is not able to produce RoF. A PCR reaction with the primers fp_S. davawensis_rosB_outofgene and rp_S. davawensis_rosB_outofgene (PCR program: DGTGR) was performed. The primers flank the *rosB* gene, though *rosB* (864 bp) and the Apra cassette (1180 bp) differ in size. The shown PCR gel shows clearly a shift to roughly 1200 bp for the mutants four (B), seven (C) and eight (D). Finally, the *S. davawensis* mutants were successfully grown in TSB medium +Apra, which *S. davawensis* wt is not capable of.

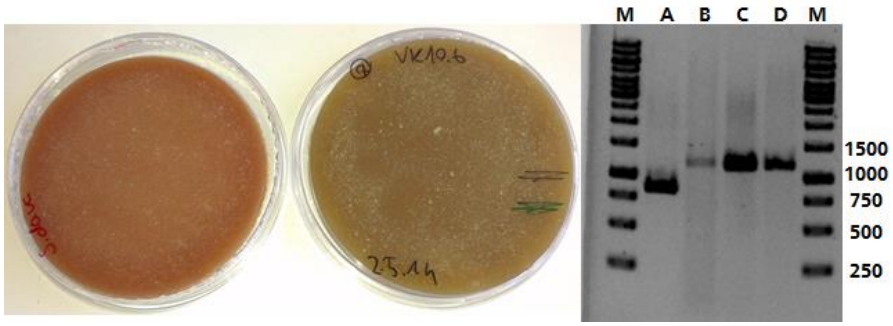

Figure 47: *S. davawensis wt* (left) and *S. davawensis rosB::apra* (mid) were grown on MS agar plates for seven days at 30 °C. The wt plate shows a red stain, which is caused by roseoflavin production, whereas the mutant does not. The PCR gel (right) shows the PCR reaction (PCR program DGTGR) with for/rev primer "S. davawensis_rosB_outofgene" using the genomic DNA of *S. davawensis* wt (A) and *S. davawensis rosB::apra* clones (B, C, D) as template. The theoretical size of rosB is 864 bp and the size of the Apra cassette is 1180 bp. All three mutants show the right size.

4. Discussion

RosB catalyses a complex reaction and is one of the enzymes which is active in the RoF biosynthetic pathway in *S. davawensis*. It has been shown that a single enzyme is able to catalyse the conversion of RP to AFP. A putative reaction mechanism based on the data of this work is shown in Figure 48. The reaction with RP takes only place in neutral/basic solutions (see Figure 13); a proton is abstracted at C8α (1). The C8 methyl group has the most acidic protons as mentioned before and H-NMR spectroscopy analysis in D_2O showed a deuteration of it even without any enzyme (indicating that the proton is activated).[12] Furthermore, the positively charged amino acid residues within the binding pocket of RosB (AsnA134, GluA135 and AspA136) stabilises and favours the transient delocalization of a negative charged flavin intermediate (see Figure 48,2). The formally reduced intermediate (2) is then attacked electrophilically by oxygen at C8α. The peroxide intermediate (**3**) is then hydrolysed forming a hydroxyl and HOC-RP (**4**). Some flavoproteins are known which catalyse a reaction involving an attack at position C4' [29,31] which would form hydrogen peroxide instead of hydroxyl and formally a hydride. Another route would be an attack at N5 forming a hydrogen peroxide aswell.[59] However both reaction pathways can be ruled out in the case of RosB. Firstly, the crystal structure data revealed moderate space in the proximity at C8α, though no space is available at C4' due to the π-π stacking between TyrB240 and the isoalloxazine ring system. Secondly, H_2O_2 could not have been detected, which is consistent with results from another lab.[60] Thirdly, $H_2{}^{18}O$ does not hydrolyse $H^{16}OC$-RP, but $H^{16}O^{16}OC$-RP. Yet, isotope labelled ^{18}O was only found at O4, which can be derived from the fragmentation pattern (Figure 31). This indicates that water does not attack C8α but O_2. A repetition of the $^{18}O_2$ experiment with only RP and RosB yielding HOC-RP can provide further evidence.

Chapter 3.5.2 clearly disclosed the necessity of thiamine over thiamin diphosphate for the following oxidation. The newly formed formyl group becomes protonated by a water molecule yielding 6. The formal reduced intermediate is then attacked at the formyl carbon by a hydroxyl group forming 7. 7 undergoes a disproportionation which gives a semiquinone like intermediate (8). The enolic moiety shifts another electron pair into the isoalloxazine ring system yielding the reduced HOOC-RPH_2 (9). An electron acceptor A^+ oxidizes HOOC-RPH_2 to HOOC-RP (10).

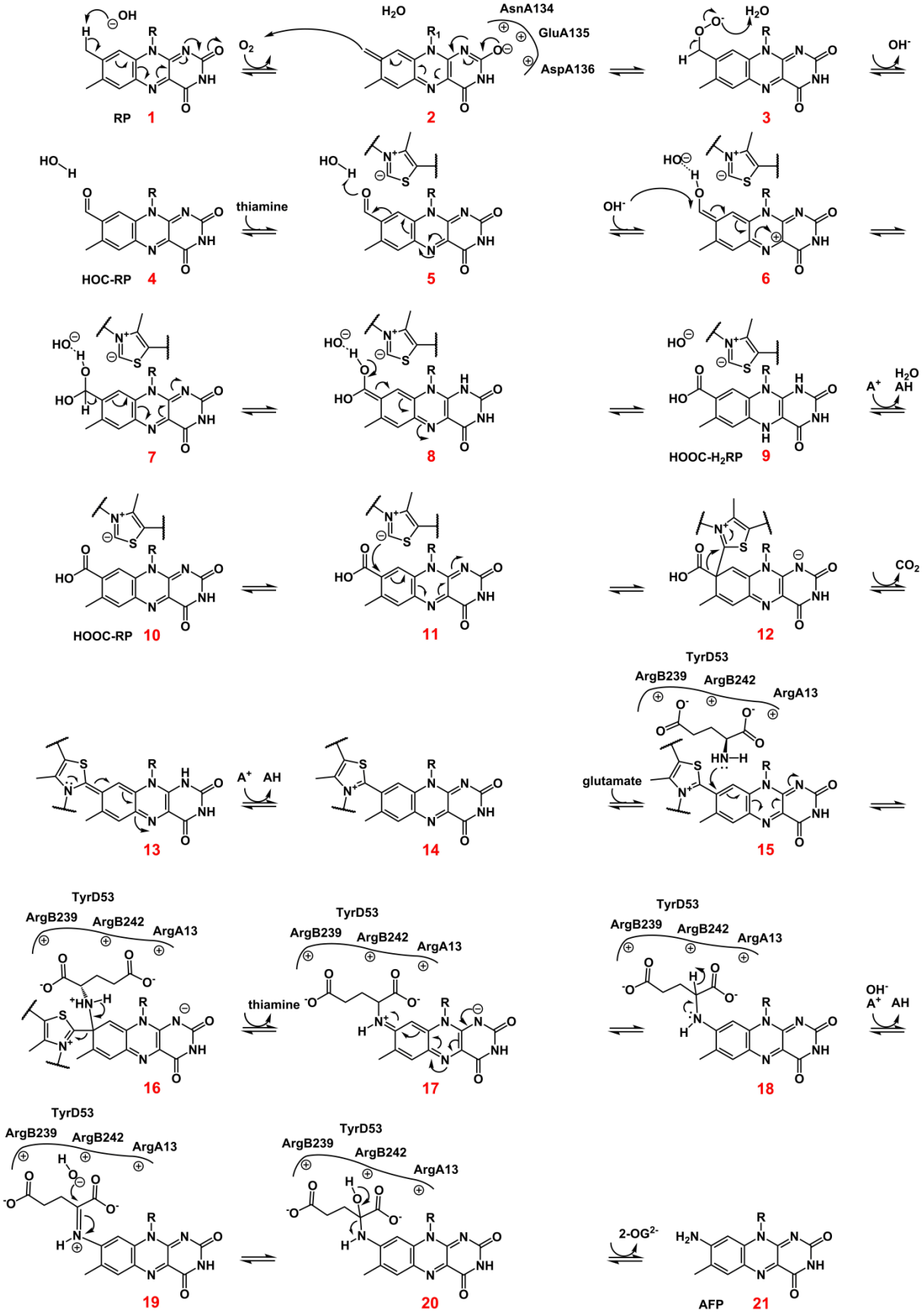

Figure 48: The proposed AFP synthase (RosB) mechanism is shown. RP is oxidized with O_2, yielding HOC-RP. Thiamine and a hydroxyl are needed to form HOOC-RP. Glutamate, another hydroxyl and an electron acceptor (A^+) is needed to yield the product AFP.

Initial experiments suggested that NAD(P)$^+$ seemed to be a promising candidate for A$^+$. Although further investigations were contradictory; aerobically no effect could be observed and anaerobically it was negligible (see Figure 34). In general NAD(P)$^+$ is known to aid several enzymes, such as DNA ligase, oxidoreductase, enzymes of the Sir2p family, deacetylases and as well regulation of energy metabolism[61]. However, these enzymes are truly NAD$^+$-dependent and do not function without it. The oxidation of RP to AFP continues without NAD(P)$^+$ and is therefore not necessary. Another possible explanation for the electron acceptor is the transfer of electrons from one flavin to another one. Objects such as electrons can overcome a potential barrier (e.g. wall or protein chain), because the probability to exist in the barrier or beyond is according to the solved Schrödinger equation unequal 0 and decays exponentially with distance (considered from a quantum mechanical perspective). Such "tunneling effects" are acknowledged in proteins and are believed to take place in the range of $<$14 Å[62,63]. Figure 40 shows that the edge-to-distances (12.5 Å) are sufficient to allow electron transfers within RosB. The reduced neighboured flavin can subsequently be re-oxidized by O_2.

The thiamine carbene attacks C8 (11) and one electron pair is again delocalized in the isoalloxazine ring system as shown in 12. CO_2 is removed under reductive cleavage yielding a thiamin semiquinone intermediate (13). The intermediate is again re-oxidized by A$^+$ forming 14. Glutamate binds to RosB and is held in place by the previous described anion hole ArgB239, ArgB242 and ArgA13 and TyrD53. The high hydrophobicity and positive charge of the anion hole does not only stabilise negatively charged species, but also increases the reduction potential of RP, which aids the reaction[12]. The λ-amine group of glutamate attacks at C8 (β position in relation to thiamine), which is derived from the classical pyruvate decarboxylase mechanism (15). The intermediate 16 cleaves off thiamine through an imine formation (17). The imine is then oxidized by A$^+$ forming 18. A hydroxyl group attacks the imine as shown in 19 and finally AFP and α-ketoglutarate are yielded after a proton re-arrangement (20).

Thiamine is a cofactor, which stays as a prosthetic group at the active site of the assisted enzyme.[64] It is known to help enzymes, such as pyruvate decarboxylase, dehydrogenases and transketolases[64]. However, the reaction pattern is always the same; thiamine binds to the enzyme and the carbanione is formed, which then attacks a keto group in β-position in relation to a carboxylic acid. The acid is cleaved off and the thiamine substrate complex is hydrolysed giving the regenerated thiamine carbanione and the substrate minus CO_2. Unfortunately, it was not possible to crystallize thiamine with RosB, enthuse we could not further investigate the role of thiamine. This leaves the question: How does thiamine participate in the RosB reaction? Besides that, why does HOC-RP oxidation take only place in

the presence of thiamine, which does not fit the classical reaction pattern? The observation made in Figure 28 clearly points out, that thiamine increases HOOC-RP formation. This might indicate that the protonation at 5 is performed by a neutral thiamine providing the ylid thiamine and the protonated HOC-RP. However, autoxidation occurs without thiamine at longer incubation time as shown in Figure 23 (black chromatogram). This indicates that HOOC-RP formation can take place without thiamine. The structural data is self-contradictory. The active site does not provide space for thiamine and more improbable for thiamine and glutamate without a conformational change. Besides that, the needed thiamine concentrations are in the mM range, however measured concentration for thiamine and thiamine diphosphate in bacterial cells are in the nM range.[65]

The SEC elution profile shown in Figure 17 strongly suggests that RosB with bound AFP has a different conformation than flavin-free RosB, due to the different elution times. Significant conformational changes are further supported by the result of RosB Tyr21A. The alanine residue does not seem to influence flavin binding and it is not in the close proximity of the isoalloxazine ring system, yet the activity is almost fully abolished (10 % of wt activity). To have an impact it is either part of a docking station for a cofactor or it is brought in distance through a conformational change.

The entries formed by Leu109 and Tyr53 have a diameter of 7 Å, which are big enough for thiamine to enter the active site. Furthermore, thiamine as cofactor shows higher AFP yields than its biologically active analogue thiamin diphosphate. This raises doubts for thiamine to be the true cofactor. It is possible that thiamine is a close derivative of the true cofactor; a thiazole containing compound or another compound which is also able to form a carbanion. The hidden cofactor might be the unknown co-eluted substance with a $\frac{m}{z}$ value of 323.2 having a possible mass loss of 44 u (-CO_2) ($\frac{m}{z}$=279.2 Figure 11). Thiamine-formyl$^+$ has a theoretical $\frac{m}{z}$ value of 309 and does not match. Binding studies with electron paramagnetic resonance spectroscopy (EPR) or isothermal titration calometry (ITC) can be an approach to answer the question, whether thiamine binds to RosB or not. These techniques can also determine, whether NAD(P)$^+$ binds to RosB or not. Additionally, a fragmentation pattern analysis of 323 via MS-MS could identify/disprove the possible thiamine analogue or the electron acceptor.

Another arguable step is the decarboxylation step itself:

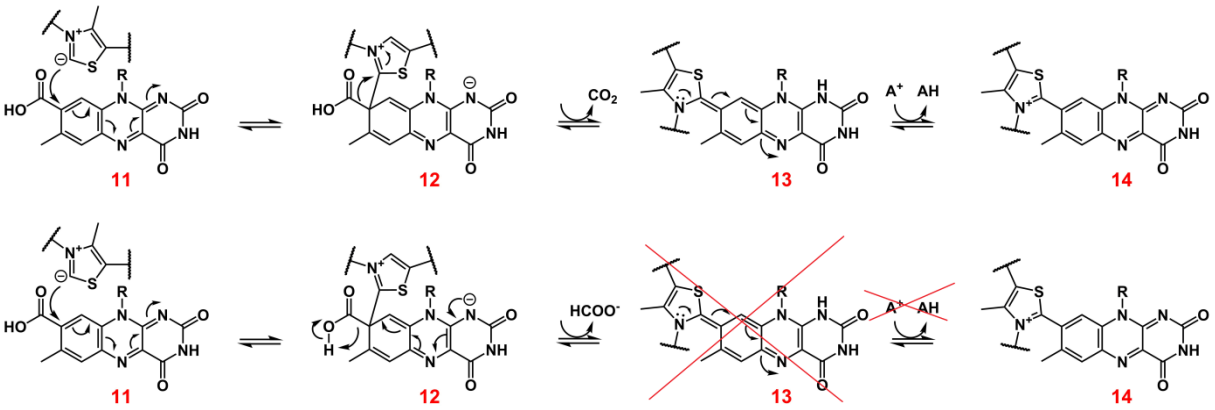

Figure 49: Two possible reaction processes: A reductive cleavage removing CO_2 (top panel) and the cleavage of formic acid (bottom panel). Top panel: The thiamine carbanione attacks HOOC-RP at C8 cleaving off CO_2, which reduces the isoalloxazine to a semiquinone. An electron acceptor (A^+) reoxidizes it. Bottom panel: The thiamine carbanione attacks HOOC-RP at C8 cleaving off formic acid. 13 and A^+ are not needed in this step.

The reductive cleavage is the classical approach for a thiamine catalysed reaction. Cleaving off a formic acid would reduce the reaction by one step and make A^+ unnecessary. The formic acid formulation is assisted by the work of Jhulki et al.[60] They detected NADH formation in a coupled RosB assay using formate dehydrogenase. However the assay was performed without thiamin and therefore the yield was only 25 % after 6 hours. A GC analysis of the gas atmosphere of a sealed RosB assay might shed light on the question.

^{15}N(γ)-glutamic acid experiments showed, that glutamate is clearly the N-donor. Although one questions still remains; does glutamate attack directly, or does it regenerate a residue of the active site? The closest lysine residue (Lys241) was mutated to alanine, though it showed no effect on the RosB activity. Matrix-Assisted-Laser-Desorption-Ionization (MALDI) or Electron-Spray-Ionization (ESI) combined with Time-Of-Flight (TOF) or Fourier-Transform-Ion-Cyclotron-Resonance (FT-ICR) could be a promising analysis method to observe a possible mass shift in RosB $\frac{m}{z}$ values with the ^{15}N(γ)-glutamic acid experiment.

The proposed mechanism summarizes the RosB reaction mechanism leaving only a few question marks. RosB itself has a comparable low activity (activity of 0.44 $\frac{nmol}{min \times mg(Protein)} \pm$ 0.01 (n=6)), which is even lower than the one of RosA[66] . The reason for that could be a yet immature roseoflavin biosynthesis or for safety reasons. RosA the third enzyme in Rof biosynthesis has a higher binding affinity to its product Rof than its substrate AF[16,66]. It is postulated that RosA interacts with an exporter, which than secretes RosA. This can also apply

for RosB; RosB is purified with bound AFP, which indicates a high binding affinity. This points to a possible "idle state" *in vivo* until the elusive AFP phosphatase picks AFP up. Afterwards, the AFP phosphatase proceeds to RosA delivering the substrate AF. This RoF cascade can also have accelerating properties, like it was shown for the citrate synthase and malate dehydrogenase complex,[67] and could explain the observed rates. The *S. davawensis* was shown to be resistant to its secondary metabolite roseoflavin[24], its RP riboswitch contains a mutation, which makes RoF not bind to it. Although this might not be the case for HOC-, HOOC- and/or AF-P and the influence on other *S. davawensis* flavoproteins is not known. An optimized kinetic rate could therefore be sacrificed, in order to prevent any leakage from the RoF cascade, which could inhibit other flavoproteins. Besides that, the oxidation from RP to AFP is a multi-step reaction, which is per se time-consuming. The question of a resistance mechanism can be answered by finding a mutated RosB, which is able to catalyse the AFP formation and simultaneously has a significant lower AFP binding affinity.

RosB catalyses not only a unique reaction, but has also a unique fold. It is the first known enzyme which evolved from a flavodoxin using RP as a cofactor to an upgraded flavodoxin using RP as a substrate[45]. Flavodoxins bury their flavin deeply inside, which is also the case for RosB. However, enzymes which use RP as a substrate, like FAD synthetases, consume specifically the reduced RPH_2 and not RP.[68] RosB accepts only the oxidized RP and the product AFP is also kept from any reduction as can be assumed from the colouring orange cell pellet (Figure 9). The C-terminal extension is 50 amino acids long and shows no similarity with any known sequence. Even a BLASTP with only the C-terminus gives no alignment (data not shown). This suggests that this feature is elementary for the new function. RosB Arg151A and RosBArg242A substantiate that hypothesis.

5. Conclusion and Outlook

The key enzyme of roseoflavin biosynthesis RosB was characterised. It uses RP as a substrate, O_2 and glutamic acid as cosubstrates and thiamine as a cofactor. The intermediate HOOC-RP and the product AFP were identified and it was shown that the intermediates can be selectively produced depending on the presence/absence of the cofactors. The role of glutamic acid was unravelled and the participation of molecular oxygen described. Thiamine most likely aids the oxidation from HOC-RP to HOOC-RP and it catalyses the decarboxylation of HOOC-RP, yet further evidence is needed to assign thiamine a complete new role besides assisting the decarboxylation reaction. An electron acceptor was not found, although the intramolecular distance from one flavin to another is short enough to allow an electron transfer through tunneling effects, which reduces RP to RPH_2 or RP to a semiquinone RP. The reduced flavin is then dissociated and can be re-oxidized elsewhere. The crystal structure of RosB was resolved with bound AFP (1.7 Å) and HOC-RP (2.0 Å). It revealed an αβ flavodoxin fold with loop extensions and a C-terminal arm which showed to have an important function. All four subunits participate in active site formation, which is also a new phenomenon for flavodoxins. The active site has two entries with a diameter of 7 Å each. An anion hole is in the proximity of C8α of the flavin and gives room for O_2, glutamic acid or water. Thiamine would only fit with a conformational change.

Nevertheless, the RoF biosynthesis is still incomplete. The elusive phosphatase might be found by screening the *S. davawensis* crude extract with a coupled assay of AFP, SAM and RosA. If a fraction contains an active phosphatase it will supply AF for RosA, which will then form roseoflavin. This shifts the absorption maximum from 479 nm (AF) to 503 nm (roseoflavin) and can easily be monitored by UV-VIS spectroscopy. A RosB mutant library could yield interesting mutants which produce only HOC-RP, HOOC-RP, accept new substrates like cresol (starting compound for organic synthesis) or synthesize 8-substituted RP derivatives. These derivatives can be used in pharmaceutical applications or localization experiments, because RP is a fluorophore. If antibiotic potency is linked to the redox potential difference between RP and 8-demethyl-8-X-RP than HOC-RP would be a better choice, because it has an even lower redox potential than RP (RP= -190 mV, HOC-RP(open)= -90 mV)[69]. However, the redox potential is only important for the inhibition of flavoproteins and not for binding to the RP riboswitch.

6. Acknowledgement

First of all, I would like to thank M. Mack for this project, his guidance and the freedom I experienced to be creative during my thesis. Secondly, I want to thank J. Schwarz for her help in the early stage of my PhD. Besides that, I want to thank S. Großhennig, the other PhD students, and the technical assistants; especially K. Schlosser and C. Koch. Furthermore, I want to thank our collaboration partners from the MPI Frankfurt and R. Sandhoff from the DKFZ for a very successful teamwork. Finally, I want to thank my family, friends and my girlfriend for their support and distraction during my free-time.

7. References

1 Hardisson, C. & Manzanal, M. B. Ultrastructural studies of sporulation in Streptomyces. *Journal of Bacteriology* **127**, 1443-1454 (1976).

2 Kieser, T., Bibb, M. J., Buttner, M. J., Chater, K. F. & Hopwood, D. A. *Practical streptomyces genetics*. (John Innes Foundation, 2000).

3 Jankowitsch, F. *et al.* Genome sequence of the bacterium *Streptomyces davawensis* JCM 4913 and heterologous production of the unique antibiotic roseoflavin. *Journal of Bacteriology* **194**, 6818-6827 (2012).

4 Gust, B., Challis, G. L., Fowler, K., Kieser, T. & Chater, K. F. PCR-targeted Streptomyces gene replacement identifies a protein domain needed for biosynthesis of the sesquiterpene soil odor geosmin. *Proc Natl Acad Sci U S A* **100**, 1541-1546 (2003).

5 Schrempf, H. *et al.* (NY: Springer, New York,, 2007).

6 O. Welsh, L. Vera-Cabrera & Salinas-Carmona, M. C. Mycetoma. *Clinical Dermatology* **25**, 195-202 (2007).

7 Otani, S. *et al.* Roseoflavin, a new antimicrobial pigment from *Streptomyces*. *The Journal of Antibiotics* **27**, 88-89, doi:http://doi.org/10.7164/antibiotics.27.88 (1974).

8 Euler, H. V. *et al.* Synthese des Lactoflavins (Vitamin B2) und anderer Flavine. *Helvetica Chemia Acta*, doi:http://10.1002/hlca.19350180170 (1935).

9 Sa, N., Rawat, R., Thornburg, C., Walker, K. D. & Roje, S. Identification and characterization of the missing phosphatase on the riboflavin biosynthesis pathway in Arabidopsis thaliana. *The Plant Journal* **88**, 705-716, doi:http://10.1111/tpj.13291 (2016).

10 Mandal, M. & Breaker, R. R. Gene regulation by riboswitches. *Nat Rev Mol Cell Biol* **5**, 451-463 (2004).

11 Fraaije, M. W. & Mattevi, A. Flavoenzymes: diverse catalysts with recurrent features. *Trends in Biochemical Sciences* **25**, 126-132, doi:http://10.1016/S0968-0004(99)01533-9.

12 Weber, S. & Schleicher, E. *Flavins and Flavoproteins*. (Human Press, 2014).

13 Lim, S. H., Choi, J. S. & Park, E. Y. Microbial production of riboflavin using riboflavin overproducers,Ashbya gossypii, Bacillus subtilis, andCandida famate: An overview. *Biotechnology and Bioprocess Engineering* **6**, 75-88, doi:http://10.1007/bf02931951 (2001).

14 Matsui, K., Juri, N., Kubo, Y. & Kasai, S. Formation of roseoflavin from guanine through riboflavin. *Journal of Biochemistry (Tokyo)* **86**, 167-175 (1979).

15 Juri, N. *et al.* Formation of roseoflavin from 8-amino- and 8-methylamino-8-demethyl-D-riboflavin. *Journal of Biochemistry (Tokyo)* **101**, 705-711 (1987).

16 Jankowitsch, F. *et al.* A novel *N,N*-8-amino-8-demethyl-D-riboflavin Dimethyltransferase (RosA) catalyzing the two terminal steps of roseoflavin biosynthesis in *Streptomyces davawensis*. *Journal of Biological Chemistry* **286**, 38275-38285 (2011).

17 Schwarz, J. *Aufklärung der Biosynthese des Antibiotikums Roseoflavin aus dem Bakterium Streptomyces davawensis* Ph.D. thesis, Applied Science University Mannheim, (2014).

18 Abbas, C. A. & Sibirny, A. A. Genetic Control of Biosynthesis and Transport of Riboflavin and Flavin Nucleotides and Construction of Robust Biotechnological Producers. *Microbiology and Molecular Biology Reviews : MMBR* **75**, 321-360, doi:http://10.1128/MMBR.00030-10 (2011).

19 Pedrolli, D. B. *et al.* The antibiotics roseoflavin and 8-demethyl-8-amino-riboflavin from *Streptomyces davawensis* are metabolized by human flavokinase and human FAD synthetase. *Biochemical Pharmacology* **82**, 1853-1859 (2011).
20 Lee, E. R., Blount, K. F. & Breaker, R. R. Roseoflavin is a natural antibacterial compound that binds to FMN riboswitches and regulates gene expression. *RNA Biology* **6**, 187-194 (2009).
21 Mansjo, M. & Johansson, J. The riboflavin analog roseoflavin targets an FMN-riboswitch and blocks *Listeria monocytogenes* growth, but also stimulates virulence gene-expression and infection. *RNA Biology* **8**, 674-680 (2011).
22 Serganov, A., Huang, L. & Patel, D. J. Coenzyme recognition and gene regulation by a flavin mononucleotide riboswitch. *Nature* **458**, 233-237, doi:10.1038/nature07642 (2009).
23 Ott, E., Stolz, J., Lehmann, M. & Mack, M. The RFN riboswitch of *Bacillus subtilis* is a target for the antibiotic roseoflavin produced by *Streptomyces davawensis*. *RNA Biology* **6**, 276-280 (2009).
24 Pedrolli, D. B. *et al.* A highly specialized flavin mononucleotide riboswitch responds differently to similar ligands and confers roseoflavin resistance to *Streptomyces davawensis*. *Nucleic Acids Res* **40**, 8662-8673 (2012).
25 Otani, S., Kasai, S. & Matsui, K. in *Methods in Enzymology* Vol. Volume 66 (ed Lemuel D. Wright Donald B. McCormick) 235-241 (Academic Press, 1980).
26 Pedrolli, D. B. *et al.* in *Flavins and Flavoproteins: Methods and Protocols* (eds Stefan Weber & Erik Schleicher) 41-63 (Springer New York, 2014).
27 Northrop-Clewes, C. A. & Thurnham, D. I. The Discovery and Characterization of Riboflavin. *Annals of Nutrition and Metabolism* **61**, 224-230 (2012).
28 Macheroux, P., Kappes, B. & Ealick, S. E. Flavogenomics – a genomic and structural view of flavin-dependent proteins. *FEBS Journal* **278**, 2625-2634, doi:http://10.1111/j.1742-4658.2011.08202.x (2011).
29 Massey, V. The reactivity of oxygen with flavoproteins. *International Congress Series* **1233**, 3-11, doi:http://dx.doi.org/10.1016/S0531-5131(02)00519-8 (2002).
30 Yeh, E., Blasiak, L. C., Koglin, A., Drennan, C. L. & Walsh, C. T. Chlorination by a Long-Lived Intermediate in the Mechanism of Flavin-Dependent Halogenases. *Biochemistry* **46**, 1284-1292, doi:http://10.1021/bi0621213 (2007).
31 Poole, L. B. Flavin-Dependent Alkyl Hydroperoxide Reductase from Salmonella typhimurium. 2. Cystine Disulfides Involved in Catalysis of Peroxide Reduction. *Biochemistry* **35**, 65-75, doi:http://10.1021/bi951888k (1996).
32 Fraikin, G. Y., Strakhovskaya, M. G. & Rubin, A. B. Biological photoreceptors of light-dependent regulatory processes. *Biochemistry (00062979)* **78**, 1238-1253, doi:http://10.1134/S0006297913110047 (2013).
33 Fraaije, M. W., van den Heuvel, R. H. H., van Berkel, W. J. H. & Mattevi, A. Covalent Flavinylation Is Essential for Efficient Redox Catalysis in Vanillyl-alcohol Oxidase. *Journal of Biological Chemistry* **274**, 35514-35520 (1999).
34 Tóth-Petróczy, Á. & Tawfik, D. S. The robustness and innovability of protein folds. *Current Opinion in Structural Biology* **26**, 131-138, doi:http://dx.doi.org/10.1016/j.sbi.2014.06.007 (2014).
35 Knight, E. & Hardy, R. W. F. Isolation and Characteristics of Flavodoxin from Nitrogen-fixing Clostridium pasteurianum* *The Journal of Biological Chemistry* **241**, 2752-2756 (1966).
36 Watenpaugh, K. D., Sieker, L. C. & Jensen, L. H. Flavins and Flavoproteins **405** (1976).

37 Saraste, M., Sibbald, P. R. & Wittinghofer, A. The P-loop — a common motif in ATP- and GTP-binding proteins. *Trends in Biochemical Sciences* **15**, 430-434, doi:http://dx.doi.org/10.1016/0968-0004(90)90281-F (1990).
38 Sambrook, J. & W., R. D. *Molecular cloning : a laboratory manual.*, Vol. 1 (Cold Spring Harbor Laboratory, 2001).
39 Laboratory, E.-E. M. B. *Protein Expression E.coli Expression-Seleno-Methionine Labeling of Protein in E.coli*, <https://www.embl.de/pepcore/pepcore_services/protein_expression/ecoli/seleno/> (2016).
40 Hobbs, G., Frazer, C. M., Gardner, D. C. J., Cullum, J. A. & Oliver, S. G. Dispersed growth of Streptomyces in liquid culture. *Applied Microbiology and Biotechnology* **31**, 272-277, doi:http://10.1007/BF00258408 (1989).
41 Sosio, M. *et al.* Artificial chromosomes for antibiotic-producing actinomycetes. *Nature Biotechnology* **18**, 343-345 (2000).
42 Simon, R., Priefer, U. & Puhler, A. A Broad Host Range Mobilization System for In Vivo Genetic Engineering: Transposon Mutagenesis in Gram Negative Bacteria. *Nature Biotechnology* **1**, 784-791 (1983).
43 Laemmli, U. K. Cleavage of Structural Proteins during the Assembly of the Head of Bacteriophage T4. *Nature* **227**, 680-685 (1970).
44 Bradford, M. M. A rapid and sensitive method for the quantitation of microgram quantities of protein utilizing the principle of protein-dye binding. *Analytical Biochemistry* **72**, 248-254, doi:http://dx.doi.org/10.1016/0003-2697(76)90527-3 (1976).
45 Konjik, V. *et al.* The crystal structure of RosB gives new insights into the reaction mechanism of this first known member of a new family of flavodoxin-like enzymes. *Angewandte Chemie International Edition* **accepted**, doi:10.1002/anie.201610292 (2016).
46 Kanehisa, M. *COMPOUND: C00018* <http://www.genome.jp/dbget-bin/www_bget?C00018> (1995).
47 Kanehisa, M. *COMPOUND: C00647*, <http://www.genome.jp/dbget-bin/www_bget?C00647> (1995).
48 Kanehisa, M. *COMPOUND: C00003*, <http://www.genome.jp/dbget-bin/www_bget?cpd:C00003> (1995).
49 Kanehisa, M. *COMPOUND: C00006*, <http://www.genome.jp/dbget-bin/www_bget?cpd:C00006> (1995).
50 Kanehisa, M. *COMPOUND: C00194*, <http://www.genome.jp/dbget-bin/www_bget?C00194> (1995).
51 Kanehisa, M. *COMPOUND: C00378*, <http://www.genome.jp/dbget-bin/www_bget?C00378> (1995).
52 Kanehisa, M. *COMPOUND: C00068*, <http://www.genome.jp/dbget-bin/www_bget?C00068> (1995).
53 Abad, E., Zenn, R. K. & Kästner, J. Reaction Mechanism of Monoamine Oxidase from QM/MM Calculations. *The Journal of Physical Chemistry B* **117**, 14238-14246, doi:http://10.1021/jp4061522 (2013).
54 Hazekawa, I., Nishina, Y., Sato, K., Shichiri, M. & Miura, R. A Raman Study on the C(4)=O Stretching Mode of Flavins in Flavoenzymes: Hydrogen Bonding at the C(4)=O Moiety. *Journal of Biochemistry* **121**, 1147-1154 (1997).
55 Vanselow, A. *Active site amino acid residues in RosB – the key enzyme of roseoflavin biosynthesis* M.sc. thesis, Hochschule Mannheim, (2016).
56 Holm, L. & Rosenstrï¿½m, P. i. Dali server: conservation mapping in 3D. *Nucleic Acids Research* **38**, W545-W549, doi:10.1093/nar/gkq366 (2010).

57 Ye, J., Yang, H. C., Rosen, B. P. & Bhattacharjee, H. Crystal structure of the flavoprotein ArsH from Sinorhizobium meliloti. *FEBS Letters* **581**, 3996-4000, doi:http://10.1016/j.febslet.2007.07.039 (2007).
58 Schwarz, J., Konjik, V., Jankowitsch, F., Sandhoff, R. & Mack, M. Identification of the Key Enzyme of Roseoflavin Biosynthesis. *Angewandte Chemie International Edition* **55**, 6103-6106, doi:http://10.1002/anie.201600581 (2016).
59 Liu, H.-w., Lin, C.-I. & McCarty, R. M. Name Reactions in Biological Chemistry. *Angewandte Chemie*, n/a-n/a, doi:10.1002/ange.201603291 (2016).
60 Jhulki, I., Chanani, P. K., Abdelwahed, S. H. & Begley, T. P. A Remarkable Oxidative Cascade That Replaces the Riboflavin C8 Methyl with an Amino Group during Roseoflavin Biosynthesis. *Journal of the American Chemical Society* **138**, 8324-8327, doi:http://10.1021/jacs.6b02469 (2016).
61 Lin, S.-J. & Guarente, L. Nicotinamide adenine dinucleotide, a metabolic regulator of transcription, longevity and disease. *Current Opinion in Cell Biology* **15**, 241-246, doi:http://10.1016/s0955-0674(03)00006-1 (2003).
62 Page, C. C., Moser, C. C. & Dutton, P. L. Mechanism for electron transfer within and between proteins. *Curr Opin Chem Biol* **7**, 551-556, doi:http://dx.doi.org/10.1016/j.cbpa.2003.08.005 (2003).
63 Moser, C. C., Keske, J. M., Warncke, K., Farid, R. S. & Dutton, P. L. Nature of biological electron transfer. *Nature* **355**, 796-802 (1992).
64 Kluger, R. & Tittmann, K. Thiamin Diphosphate Catalysis: Enzymic and Nonenzymic Covalent Intermediates. *Chem. Rev.* **108**, 1797–1833, doi:http://10.1021/cr068444m (2008).
65 Makarchikov, A. F. *et al.* Thiamine triphosphate and thiamine triphosphataseactivities: from bacteria to mammals. *Cellular and Molecular Life Sciences CMLS* **60**, 1477-1488, doi:10.1007/s00018-003-3098-4 (2003).
66 Tongsook, C. *et al.* Structural and kinetic studies on RosA, the enzyme catalysing the methylation of 8-demethyl-8-amino-d-riboflavin to the antibiotic roseoflavin. *FEBS Journal* **283**, 1531-1549, doi:http://10.1111/febs.13690 (2016).
67 Jung, T. *Untersuchungen zur Komplexbildung von Enzymen des Citratzyklus in Bacillus subtilis und Escherichia coli* PhD rer. nat. thesis, Karlsruher Institut für Technologie (KIT), (2016).
68 Kearney, E. B., Goldenberg, J., Lipsick, J. & Perl, M. Flavokinase and FAD synthetase from Bacillus subtilis specific for reduced flavins. *Journal of Biological Chemistry* **254**, 9551-9557 (1979).
69 Singer, P. T. & Edmondson, E. D. 8a-Substituted Flavins of Biological Importance. *FEBS Letters* **42**, 1-14 (1974).

8. Appendix

8.1. Oligonucleotides used in this study

Bramp_rev_BamHI+Stop

5'-AATAGGATCCTCAGCCGAGTTGGCTCTCCT-3'

Bramppetfor

5'-TTAATCATATGGCTCTCAAGGCTCTCAT-3'

iFD7989fw

5'-AAGTCGAACCAGTCGCTACGGGAAGGAACGAGAAGAATGATTCCGGGGATCCGTCGACC-3'

iFD7989rv

5'-CGGGCGCCAAAAAGCGCCCGGCTTTCGCTCTCGGGTTCATGTAGGCTGGAGCTGCTTC-3'

fp_S. davawensis_rosB_outofgene

5'-GCTACGGGAAGGAACGAGAA-3'

rp_S. davawensis_rosB_outofgene

5'-CGAAATCCCTTGAACAGAACC-3'

8.2. Plasmids

pIJ790	λ RED Plasmid, *cat* (Clm^R), P*araBAD,* temperature sensitive replication	Schwartz *et al..,*2015
pESAC13	*E. coli-Streptomyces* Artificial Chromosome pPAC-S1 derivative with *oriT* of the RK2 Replikon, Kan^R	Sosio *et al..,* 2,000
pET24a(+)	*E. coli* expression plasmid, $Kana^R$	Merck KGaA, Darmstadt
pET24a(*rosB)*	pET24a derivative with gene *BN159_7989*	this work
pET24a($rosB^{TAA}$)	pET24a derivative with gene *BN159_7989*	this work

pRare2-pACYC184-derived	coding tRNAs for (AGA, AGG, AUA, CUA, GGA, CCC, and CGG)	Merck, Darmstadt

8.3. Strains and their genotypes

Escherichia coli DH5α *PR9406*	F^-,φ80d*/lacZ*ΔM15*, recA*1*, endA*1*, gyrA*96*, thi*$^-$*, hsdR*17 (r_K^- m_K^+), *supE*44*, relA*1*, deoR*, Δ(*lac*ZYA-*arg*F) U169	Hanahan, 1983
Escherichia coli DH10b *rosB*$^-$	disruption of *rosB* *BN159_7989*::Apra^R	this work
Escherichia coli Top10	F^- *mcrA D*(*mrr-hsdRMS-mcrBC*) 80*lacZ* M15 *lacX74 recA1* *araD139* (*ara-leu*)*7697 galU galK* *rpsL*(Str^R) *endA1* λ^-	Invitrogen, Carlsbad USA
Escherichia coli Rosetta 2 (DE3) pLysSRARE	F^- *ompT, hsdS*B(r_B^- m_B^-) *gal dcm* λ(DE3) [*lacI lacUV5*-T7 gene 1 *ind1* *sam7 nin5*]) pLysSRARE (Cam^R)	Merck KGaA, Darmstadt
Streptomyces wt *davawensis 7989*	with *BN159_7989*::ApraR	this work
Escherichia coli *BL834*	F^- *ompT gal dcm lon hsdS*$_B$($r_B^-m_B^-$) λ(DE3 [*lacI lacUV5-T7p07 ind1 sam7 nin5*]) [*malB*$^+$]$_{K\text{-}12}$(λ^S)	Macheroux, Graz Austria

8.4. List of abbreviations

AFP	8-demethyl-8-aminoriboflavin-5’-phosphate
Apra	apramycin
BTP	1,3-bis(tris(hydroxymethyl)methylamino)propane
Carb	carbenicillin
Cm	chloramphenicol
CB12	coenzyme B12
CV	column volume
DAD	diode array detector
DTT	1,4-dithio-D-threitol
FLD	fluorescence light detector
HOC-RP	8-demethyl-8-formyl-5’-phosphate
HOOC-RP	8-demethyl-8-carboxyl-5’-phosphate
IEP	isoelectric point
IPTG	isopropyl β-D-1-thiogalactopyranoside
Kana	kanamycin
LB	lysogeny broth
M9	minimal 9 mineral medium
MAF	8-demethyl-8-methylamino-riboflavin
Molecular weight cut-off	MWCO
MS	mass spectrometry
MS medium	mannitol starch medium
PBS	phosphate buffered saline
PLP	pyridoxal 5'-phosphate
PMP	pyridoxamin 5'-phosphate

RF	riboflavin
RP	riboflavin-5`-phosphat
RT	room temperature
S. cinnabarinus	*Streptomyces cinnabarinus*
S. davawensis	*Streptomyces davawensis*
TCA	trichloroacetic acid
Th	thiamine
ThPP	thiamine diphosphate
TSB	tryptic soy broth
UPLC	ultra pressure liquid chromatography
wt	wild type
YS	yeast-starch
YT	yeast tryptone

9. Table of Figures